Immunotherapy of Endometrial Cancers with mRNA-based Vaccine

Dissertation

zur Erlangung des akademischen Grades

Doctor rerum naturalium

(*Dr. rer. nat.*)

eingereicht am 21.10.2024

Fachbereich Chemie der

Fakultät für Mathematik, Informatik und Naturwissenschaften

der Universität Hamburg

vorgelegt von

Moritz Freyberg, M. Sc.

geboren in Mainburg

Hamburg

Oktober 2024

Dissertationsgutachter / dissertation reviewers:

1. Gutachterin / first reviewer**: Prof. Dr. Zoya Ignatova**, Institute of Biochemistry and Molecular Biology, Universität Hamburg

2. Gutachter / second reviewer: **Prof. Dr. Daniel N. Wilson**, Institute of Biochemistry and Molecular Biology, Universität Hamburg

Prüfungskommission/ examination comitte: **Prof. Dr. Zoya Ignatova**
Prof. Dr. Wolfram Brune
Prof. Dr. Chris Meier

Datum der Disputation/ date of doctoral disputation: **13.12.2024**

Datum der Freigabe der Dissertation zur Veröffentlichung: **21.10.2026**

Die vorgelegte Dissertation wurde von Oktober 2020 bis Oktober 2024 am Institut für Biochemie und Molekularbiologie am Fachbereich Chemie der Fakultät für Mathematik, Informatik und Naturwissenschaften an der Universität Hamburg unter Anleitung von Prof. Dr. Zoya Ignatova angefertigt.

The submitted dissertation was conducted from October 2020 until October 2024 at the Institute of Biochemistry and Molecular Biology at the Department of Chemistry of the Faculty of Mathematics, Informatics, and Natural Sciences at the University of Hamburg under the supervision of Prof. Dr. Zoya Ignatova.

Table of Contents

List of Abbreviations V

Abstract 1

Zusammenfassung 3

1. Introduction 5

1.1 Immune cells and function of the adaptive immune response 5

1.2 Adaptive immune system and cancer 8

1.3 Basics and challenges of cancer immunotherapy 9

1.4 Checkpoint inhibitor and cell therapy in cancer immunotherapy 11

1.5 mRNA-based vaccine in cancer immunotherapy 12

1.6 mRNA design for cancer immunotherapy vaccines 14

1.6.1 Impact of nucleotide modifications on immunogenicity and translation efficiency of exogenous mRNAs 16

1.6.2 Impact of modified nucleotides on translational elongation and termination 17

1.8 Circulating versus *ex vivo* mRNA-based vaccine 20

1.9 Endometrial cancer 22

2. Aim of thesis 24

3. Results 25

3.1 5'UTR of alpha-globin and termination with dual stop codon improve the expression of the mRNA design for *ex vivo* vaccine 25

3.2 LNPs are not suitable to deliver mRNA in moDCs for *ex vivo* vaccine setup 29

3.3 Lipofactamine efficiently delivers of *ex vivo* mRNA vaccine to moDCs 32

3.4 m1Ψ modification differently affects expression yields and maturation of moDCs 34

3.5 Optimized mRNA vaccine does not provoke innate immunogenicity 36

3.7 Antigen-encoding mRNA is processed to epitopes presented on the cell surface 38

3.8 Selection of target antigens in endometrial cancer 40

3.9 Optimized mRNA encoding candidate antigens activate T cells 43

4. Discussion 46

5. Conclusion 52

6. Material and Methods 53

7.References 62

8. Supplementary Information 90

8.1 DNA template sequences 90

8.2 5’ UTR sequences and properties..... 92
9. List of the hazardous substances used by GHS..... 93
10. Acknowledgments 96
EIDESSTATTLICHE VERSICHERUNG..... 97

List of Abbreviations

5moU	5-methoxy-uridine
A	Adenine
aa	Amino acid
ACT	Adaptive cell therapy
APCs	Antigen-presenting cells
BCR	B cell receptor
BMI	Body mass index
bp	Base pair
C	Cytosine
CAF	Cancer-associated fibroblast
CAR	Chimeric antigen receptor
CD	Cluster of differentiation
CDS	Coding sequence
CTA	Cancer/testis antigen
DNA	Desoxy ribonucleic acid
DC	Dendritic cell
dsRNA	Double-stranded ribonucleic acid
EC	Endometrial cancer
eRF	Eukaryotic release factor
FLuc	Firefly luciferase
G	Guanine
HCN	High copy number
HC	Hypermutated carcinomas
ICI	Immune checkpoint inhibitors
IFN	Interferon
IRES	Internal ribosome entry site
IL	Interleukine
LCN	Low copy number

LNP	Lipid nanoparticle
m	Methyl
MHC	Major histocompatibility complex
moDCs	Monocyte-derived dendritic cells
mRNA	Messenger ribonucleic acid
m1Ψ	N1-methyl-pseudouridine
PAMP	Pathogen-associated molecular patterns
PBMC	Peripheral Blood Mononuclear Cell
POLE	Polymerase epsilon
RLuc	Renila luciferase
RLR	RIG-I-like receptor
rt mRNA	Readthrough mRNA
sd mRNA	Self-designed mRNA
ssRNA	Single-stranded ribonucleic acid
TAA	Tumor-associate antigen
TCR	T cell receptor
TLRs	Toll-like receptors
TME	Tumor microenvironment
t-RNA	Transfer ribonucleic acid
TSA	Tumor-specifc antigens
U	Uracil
UTR	Untranslated region
VDJ	Variable-diversity-joining
Ψ	Pseudouridine

Abstract

Endometrial cancer ranks amongst the most prevalent gynecological cancers in developed countries, with rising rates of both incidence and mortality. Despite the availability of established conventional treatments, e.g. surgery, chemotherapy, and radiotherapy, challenges, including chemoresistance and relapse, still pose a significant problem for tumor treatment, particularly at advanced stages of the disease. Consequently, cancer immunotherapy, which leverages the immune system to combat malignant cells, has garnered considerable attention as a potential therapy for endometrial cancer. In this study, we focus on generating an *ex vivo* mRNA-based vaccine for the treatment of endometrial cancer. *Ex vivo* mRNA vaccines have been developed and show promising results in clinical trials for cancers, such as melanoma, prostate, and lung, however, their application for endometrial cancer treatment remains unexplored. *Ex vivo* vaccine mRNAs, encoding for an antigen expressed by the tumor, are delivered to antigen-presenting cells *in vitro*, facilitating the expression and processing of antigens. Consequently, this enables CD8+ T cells to recognize and eliminate transformed cells.

Expression of the antigen in antigen-presenting cells is crucial for the vaccine efficacy and is influenced by the design of the mRNA. We therefore optimized different parts of mRNA, with a particular focus on the 5'UTR and the stop codon. Our findings indicate that incorporating the 5'UTR of alpha-globin into the mRNA construct leads to the highest translation in antigen-presenting cells, compared to other highly expressing 5'UTRs. Similar to pseudouridine, 5-methoxy-urdine, and N1-methyl-pseudouridine enhanced readthrough in a manner dependent on the stop codon identity. For N1-methyl-pseudouridine, the utilization of two consecutive UAA stop codons maximized protein levels by minimizing the readthrough, thereby also preventing the generation of unwanted neoepitopes that could lead to adverse effects or compromise efficacy. Lipid nanoparticles have emerged as an efficient delivery system for mRNA *in vivo*; however, our results indicate their inefficiency for delivering mRNA to antigen-presenting cells *in vitro* and are thus unsuitable for *ex vivo* vaccines. We demonstrate that for *ex vivo* vaccines, fully modified mRNA is beneficial, as it displayed the highest translation yields and did not activate the innate immune response. In addition, high maturation levels of antigen-presenting cells could be achieved by a cocktail of maturation factors. Our optimized mRNA displayed efficient translation and induced epitope presentation on the cell surface. Utilizing the Human protein atlas database, we identified four tumor antigens *CT83*, *CEP55*, *MAGE A4*, and *FAP* as viable targets for mRNA-based immunotherapy of endometrial cancers. While *CT83*, *CEP55*, and *MAGE A4* expression is restricted to tumor cells, *FAP* is also present in cells of the tumor microenvironment, thus allowing for the targeting of the tumor

and its microenvironment, simultaneously. Co-culture of CD8+T cells and antigen-presenting cells transfected with our optimized mRNA encoding for the respective antigens led to T cell activation and proliferation further confirming the suitability of our mRNA for an *ex vivo* vaccine approach. Together these results emphasize the importance of mRNA design for vaccine efficacy and establish the foundation for the development of an *ex vivo* mRNA-based vaccine for treating endometrium cancer.

Zusammenfassung

Endometrium Krebs ist in Industrieländer die am häufigsten diagnostizierten Krebsart des weiblich Geschlechtstrakts, mit immer mehr ansteigenden Fallzahlen und Todesfällen. Obwohl klassische Behandlungsmethoden wie operatives entfernen des Tumors, Chemotherapie oder Strahlentherapie für Endometrium Krebs gute etabliert sind, kann eine Heilung nicht immer erzielt werden. Komplikation wie Resistenzentwicklung, starke Nebenwirkungen oder Rückfälle stellen immer noch ein großes Problem für die Behandlung dar, vor allem in den fortgeschrittenen Stadien der Krankheit. Krebsimmunotherapie, welche das Immunsystem nutzt, um den Tumor zu bekämpfen, hat deshalb in den letzten Jahren großes Interesse als Behandlungsmethode für Endometrium Krebs geweckt. Unser Ziel in dieser Arbeit ist es einen mRNA zu entwickeln, welche sich als *ex Vivo* Impfstoff gegen Endometrium Krebs einsetzen lässt. Für ex *Vivo* Impfstoffe werden mRNAs, welche für Antigen codieren das vom Tumor expremiert wird, in Antigen präsentierenden Zellen eingeschleußt, wo diese Proteine exprimiert und für die Aktivierung von T-Zellen prozessiert werden. Nach Aktivierung können CD8+ T-Zellen bösartige Zellen erkennen und diese vom Organismus eliminieren. Obwohl bereits einige zirkulierende Impfstoffe gegen Tumore der Haut, Prostata oder Lunge entwickelt wurden, und in klinischen Studien vielversprechende Resultate gezeigt haben gibt es bis dato noch keinen *ex Vivo* Impfstoff für endometriale Tumore.

Das Expressionslevel von Antigenen ist ein entscheidender Faktor für die Effektivität des Impfstoffes und ist abhängig von dem Design der mRNA. Unser Ziel war es deshalb eine optimierte Impfstoff mRNA zu entwickeln mit besonderem Fokus auf die 5'UTR und dem Stopcodon. Es stellt sich heraus, dass die 5'UTR der Alpha-Globin mRNA zur höchsten Proteinexpression in Antigen-präsentierenden Zellen im Vergleich zu andern 5'UTRs führte. In dieser Arbeit zeigte sich, dass die Modifizierungen mit N1-Methyl-Pseudourdin oder 5-Methoxy-Uridin ähnlich wie Pseudourdin zu erhöhten Readthrough Raten führte. Das Verwenden von zwei aufeinanderfolgenden UAA Stopcodon bei N1-Methyl-Pseudourdin Modifizierung erhöht nicht nur die Proteinlevel, sondern erhöht auch die Terminierungseffizenz, was die Bildung von Neoepitopen, welche möglichen Nebenwirkungen verursachen und die Wirkung beeinflussen können, minimiert. Während Lipid Nano Partikel ein effizientes Mittel sind mRNA Impfstoffe zu den gewünschten Zellen *in vivo* zu bringen, zeigten wir, dass sie für *in vitro* nicht geignet sind. Wir zeigen, dass für einen *ex Vivo* Impfstoff modfizierte mRNA verwendet werden sollte, da diese besser translatiert wurde, nicht dass angeborene Immunesystem aktivierte, und die Reifung der Antigen-präsentierenden Zellen mithilfe einer Mischung von Signalfaktoren erreicht werden konnte. Unsere generiert mRNA

wurde effizient translatiert und führt zu einer Präsenz von Epitopen and er Zelloberfläche. Mithilfe des Human Protein Atlas wurden in dieser Arbeit vier Tumorantigene *CT83*, *CEP55*, *MAGEA4* und *FAP,* welche sich für mRNA basierte Krebstherapie in Endometrium Krebs eigenen identifieziert. Während *CT83*, *CEP55* und *MAGE A4* nur in den eiglichen Tumorzellen präsent sind, kommt *FAP* auch in den Zellen der Tumormikroumgebung für. Dies erlaubt sowohl den Tumor als auch die Umgebung gleichzeitig zu bekämpfen. Nach Aufnahme unsere optimierten für die ausgewählten Antigene codierende mRNA durch Antigen-präsentierenden Zellen und anschließender Co-Kultivierung mit CD8+ T-Zellen kommt es zur Aktivierung und Proliferation der T-Zellen. Dies zeigt das unser mRNA als ex vivo Impfstoff für Endometrium Krebs verwendet werden kann. Alles in allem zeigt diese Arbeit die Wichtigkeit des mRNA Design auf und legt den Grundstein für ein *ex vivo* Impfstoff zur Behandlung von Endometrium Krebs.

1. Introduction

1.1 Immune cells and function of the adaptive immune response

The immune system in vertebrates consists of two branches, the innate immune response, and the adaptive immune response. The innate immune response is the first line of defense, responsible for fast detection and elimination of pathogens from the organism by recognizing common molecular features of pathogens (1). In contrast, the adaptive immune response has evolved as a more tailored immune response that recognizes pathogen-specific antigens and provides protection against subsequent infection with the same microorganism (2). The adaptive immunity utilizes two cell types as key regulators of the immune response, the antibody-producing B lymphocytes, involved in the humoral immune response, and the T lymphocytes, which mediate the cellular immune response (3). Both undergo extensive somatic gene recombination driven by RAG1 and RAG2 during their developmental stages (4). This recombination allows them to recognize a diverse repertoire of antigens through their respective receptors.

B lymphocytes originate from hemopoietic stem cells in the bone marrow where they undergo distinct developmental stages acquiring their antigen specificity (5). In the early stages, B cells are subjected to the rearrangement of heavy- and light-chain immunoglobulin gene clusters (VDJ recombination) directed by RAG1 and RAG2, ultimately leading to the expression of the B cell receptor (BCR) on the cell surface (6). These immature B lymphocytes then undergo two selection rounds to ensure functionality while avoiding autoimmunity. During positive selection, BCRs are presented with unspecific ligands. If these are not provoking a sufficient BCR signal, these B cells are subjected to apoptosis (7). A subsequent round of negative selection where B lymphocytes are presented with self-antigens ensures that these B cells do not lead to an autoimmune response (8). Only if both rounds are passed, B lymphocytes migrate from the bone marrow to the spleen, where they remain dormant until activation (9). After encountering an antigen, B cells can be activated independently of T cells leading to proliferation and antibody production (10). However, the vast majority of B cells depend on interactions with T cells to be activated. After the internalization of the antigens and crosslinking with the immunoglobin receptor, B cells interact with CD4+ T cells, previously primed for this epitope, leading to B cell activation and differentiation into plasma- or memory cells responsible for antibody production (11).

T cells, on the other hand, can be separated into two functional classes depending on their interaction with major histocompatibility complex (MHC) molecules, which bind and present

short peptide fragments. Helper T cells that express CD4 co-receptors, which will interact with MHC class II, and cytotoxic T cells that express CD8 molecules, and can bind to MHC class I (12). MHC molecules thereby help the immune system recognize foreign molecules by cross-presenting them to immune cells (13). They are highly polygenic and polymorphic making it hard for pathogens to by-pass immune detection as binding preferences of MHC receptors to specific peptides vary greatly between individuals (13) Both populations of T cells originate from the thymus; where they differentiate from lymphoid progenitor cells (thymocytes) (14). Similar to B cells, T cells undergo VDJ rearrangement in the early stage of development leading to the development of the T cell receptor (TCR), allowing them to recognize a broad spectrum of antigens (4). At this stage, T cells express both CD4 and CD8 before they undergo two rounds of selection: positive selection where the required TCR functionality is tested, and a round of negative selection where cells are eliminated that display autoreactivity (15). Cells that pass both rounds of selection will mature to either CD4+ or CD8+ T cells depending on the affinity for either MHC I (CD8) or MHC II (CD4) during the positive selection (15).

In contrast to B cells, T cells cannot internalize antigens themselves and are dependent on antigen-presenting cells (APCs) to become active (3). APCs include monocytes, Langerhans cells, and dendritic cells (DCs), all capable of acquiring antigens through endocytosis, phagocytosis, micropinocytosis, and proteolysis, subsequently presenting them to T cells (16). In contrast to all other nucleated cells, APCs do not only express MHC I but also MHC II, allowing them to interact with both CD4+ and CD8+ lymphocytes (10). Depending on the mechanism of which antigens were acquired, they bind to the two different MHC molecules (Fig. 1.1) (17). Antigens that are internalized from the extracellular space are trafficked to the endolysosomal compartment where they undergo proteolysis to epitopes (9-11 aa long peptides), with compatible epitopes binding to the grove of MHC II (16). MHC II molecules are mainly located in the endolysosomal compartment of immature APCs (18,19). Detection of pathogen-associated molecular patterns (PAMPs) through distinct pattern recognition receptors (PRRs) leads to their maturation and translocation of MHC II to the cell surface, allowing corresponding CD4+ T cells to recognize these epitopes (20–22). In contrast, MHC I molecules bind and present intracellular epitopes to CD8+ T cells; the epitopes are generated by proteolysis mainly through the ubiquitin-proteasome pathway (23). MHC I molecules reside predominantly in the ER lumen of immature APCs (24). Similar, to MHC II maturation of APCs triggered by PAMPs, MHC I molecules get trafficked to the plasma membrane after maturation (22).

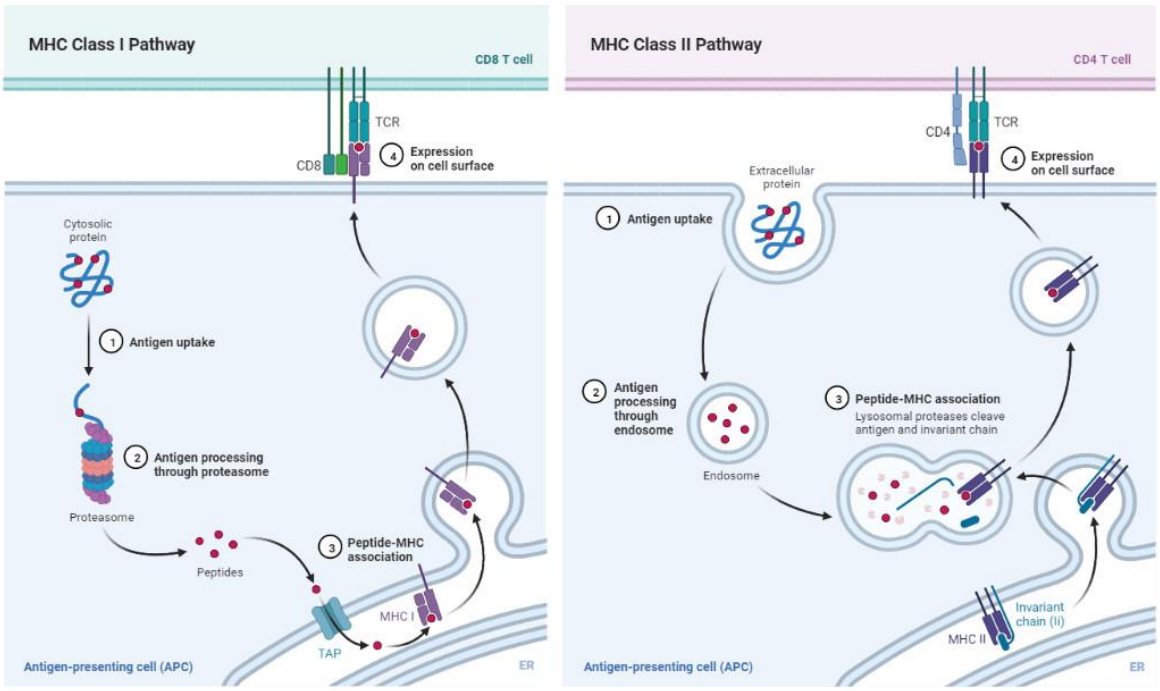


Figure 1.1 MHC II, I antigen processing and presentation. Endogenous proteins are degraded into epitopes through the proteasome. After trafficking to the ER lumen, they bind to compatible MHC I molecules and are translocated to the cell surface where the can activate CD8+ T cells. Extracellular antigens are processed in the endolysosomal compartment allowing bind to MHC II molecules. MHC II/epitope complexes can activate CD4+ T cells when being expressed on the cell surface. Figure adapted from (25).

APCs ultimately migrate to the lymph nodes where they can activate T cells by forming the so-called immunological synapse after the TCR and associated co-factors recognize the epitope/MHC complex, which causes activation and clonal expansion of T cells (26). Activated CD4+ T cells release cytokines, such as interleukin-2 (IL-2), interferon-γ (IFN-γ), or interleukin-4- 4 (IL-4) to regulate and activate the immune reaction, e.g. production of antibodies by B cells (27). Activated CD8+ cells, in contrast, circulate throughout the organism to detect cells that have the corresponding epitope bound to the MHC I molecule in an effort to eliminate infected or transformed cells from the organism (28). Once, the interaction between the TCR and the target host cell's MHC I receptor is established the cytotoxins perforin and granzymes are released leading to the apoptosis of the target cell (3).

1.2 Adaptive immune system and cancer

Innate and adaptive immunity play an essential role for both, allowing the organism to combat pathogens and also safeguard it from potentially malignant cells. Elimination of pathogens reduces the risk of virus- and inflammation-induced tumorigenesis, while expression of novel antigens by potential malignant cells allows for their detection and elimination from the organism, both reflecting the tumor-suppressing properties of the immune system (29). Similar to an infection with a pathogen, antigens that are released by the malignant cells can be internalized by APCs and cross-presented to T cells leading to the elimination of these cells (30). This process, known as immunosurveillance, has been identified as a key mediator for tumor cell surveillance (31–33). For example, mice with RAG2 gene knockout and consequential immunodeficiency are more susceptible to age-related neoplasia and MCA carcinogen-induced sarcomas (31). Immunosurveillance consists of three distinct phases summarized under the term immunoediting: elimination, equilibrium, and escape (Fig. 1.2). In the elimination phase cells of the adaptive and innate immune system collectively detect and eliminate malignant cells before they manifest as clinically detectable tumors (34). However, if tumor cells can't be eliminated from the organism completely, i.e. development of immune-resistant malignant cells, the tumor enters the equilibrium phase. Here CD8+ and CD4+ T cells, combined with the release of cytokines such as interleukin-12 (IL-12) and IFN-γ, restrict the outgrowth of the tumor. This prevents the formation of a substantial tumor mass by keeping transformed cells dormant (34,35). However, genetic instability of malignant cells and continuous selection pressure by immune cells can selectively favor tumor cells that are capable of escaping detection and elimination by the immune system due to low immunogenicity (36). Malignant cells can acquire lower immunogenicity through several mechanisms. This includes increased expression of the programmed cell death protein 1 ligand (PD-L1), downregulated IFN-γ release by T cells, or loss of antigen cross-presentation (37–39). Once the tumor enters this escape phase, tumor cells proliferate uncontrollably, resulting in a clinically detectable tumor (40). Restoring functional immunosurveillance after tumor cells enter the escape phase has been a major focus in recent years, serving as a potential alternative to conventional chemotherapy/radiotherapy (41–43).

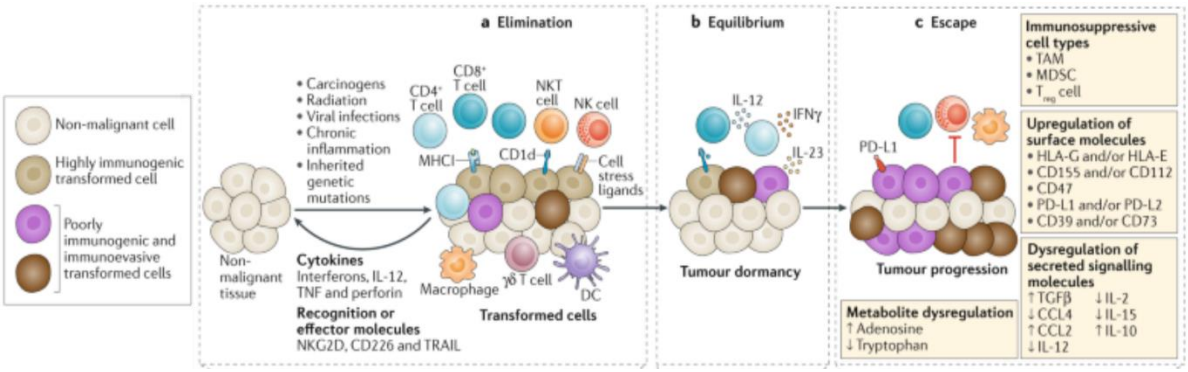


Figure 1.2 The three phases of immunoediting. In the elimination phase, immune cells can recognize and kill malignant cells before they become clinically apparent. During the equilibrium phase, the immune cells constrain the net outgrow. In the escape phase, tumor cells have acquired immune evasive/immune suppressive features causing an uncontrollable outgrowth. Figure adapted from (44)

1.3 Basics and challenges of cancer immunotherapy

Cancer currently ranks as the second leading cause of death worldwide and it's predicted to become first by the year 2060 (45). Thus, improving the landscape of current care through the development of novel and more effective treatments is essential.

In recent years, immunotherapy has emerged as one of the most promising approaches for treating various forms of cancer, significantly improving the standard of care for a variety of cancers, such as melanoma, bladder, and lung (46–48). Cancer immunotherapy leverages the patient's own immune system to recognize and combat tumor cells (49). It takes advantage of genetic and epigenetic alterations in tumor cells that give rise to novel antigens, so-called neoantigens, which are detected by the immune system as mentioned in the previous chapter (Chapter 1.2) (50). These neoantigens enable immune cells to recognize and eliminate neoplastic cells, however, cancer cells can develop mechanisms to escape immune detection as mentioned earlier (Chapter 1.2). Cancer immunotherapy restores the capability of immune cells to detect malignant cells by specifically stimulating the immune system to overcome resistant mechanisms, ultimately leading to the elimination of cells expressing neoantigens (50). Immunosuppressive mechanisms include the interference with T cell signaling (51–53), resistance to apoptosis (54,55), secretion of immunosuppressive cytokines (56,57), or the formation of a physical barrier preventing the recruitment and activation of immune cells (58). These resistance mechanisms are often facilitated by the tumor microenvironment (TME) and still pose a significant challenge to the field of cancer immunotherapy. The TME is comprised

of a heterogeneous accumulation of infiltrating and resident host cells, the extracellular matrix (ECM), as well as secreted factors such as cytokines (Fig 1.3) (59). Immune cells are recruited to the TME through the release of cytokines and chemokines. Cells, such as macrophages, dendritic cells, or monocytes contribute to immune evasion by secreting inflammatory cytokines and preventing neoplastic cell recognition, thereby aiding tumor progression (60). Macrophages constitute the majority of immune cells found in TME (61). While they serve a critical role for pathogen phagocytosis and antigen-presentation (M1 macrophages), they can also have immunosuppressive functions, important for wound healing (M2 macrophages) (62,63). Due to hypoxia and secretion of cytokines, M2 macrophages are the prevalent type of macrophages residing in the TME, thereby aiding tumor growth (59,64). The abundance of T lymphocytes in the TME is commonly presumed to be an indicator for tumor progression, classifying tumors into immune-responsive “hot” tumors and immune-evasive “cold” tumors (65). However, recent data suggests that the ratio and phenotype of the TME-residing T cells more accurately reflects immune responsiveness. The presence of immune-stimulating type 1 helper and CD8+ T cells in the TME is associated with stronger immune responsiveness and lower cancer cell proliferation, whereas elevated levels of regulatory and type 2 helper T cells contribute to tumor progression (66–71). In “cold” tumors, the release of cytokines, such as IRF2, CXCL9, or CXCL10, is suppressed, impairing the infiltration of immune-responsive T cells to the core of the tumor (72–74). Infiltration of T cells is additionally reduced by stromal components, mainly consisting of the ECM and fibroblasts (75,76).

Particularly, Cancer-associated fibroblasts (CAFs) play a significant role in impairing lymphocyte infiltration, representing a pivotal component of the ECM, which forms a physical barrier blocking access to the center (77,78). Consequently, CAFs are the most important matrix component of the TME (79). In normal tissue, fibroblasts are usually dormant, only activated upon environmental cues such as wound healing (80). CAFs in contrast, display high proliferation and migration rates and are capable of remodeling the ECM (81). Furthermore, they contribute to tumorigenesis through remodeling metabolic pathways, secretion of cytokines, growth factors, and chemokines (82–84). Secretion of exosomes by CAFs has been additionally observed to play a significant role in tumor progression and oncogenesis (85–88). In endometrial cancer specifically, CAFs can aid tumor progression through activation of the IL-6/STAT-3/c-Myc pathways and the loss of the regulative microRNA miR-148b from the secreted exosomes, further emphasizing the crucial role CAFs play in the TME and cancer progression (88,89).

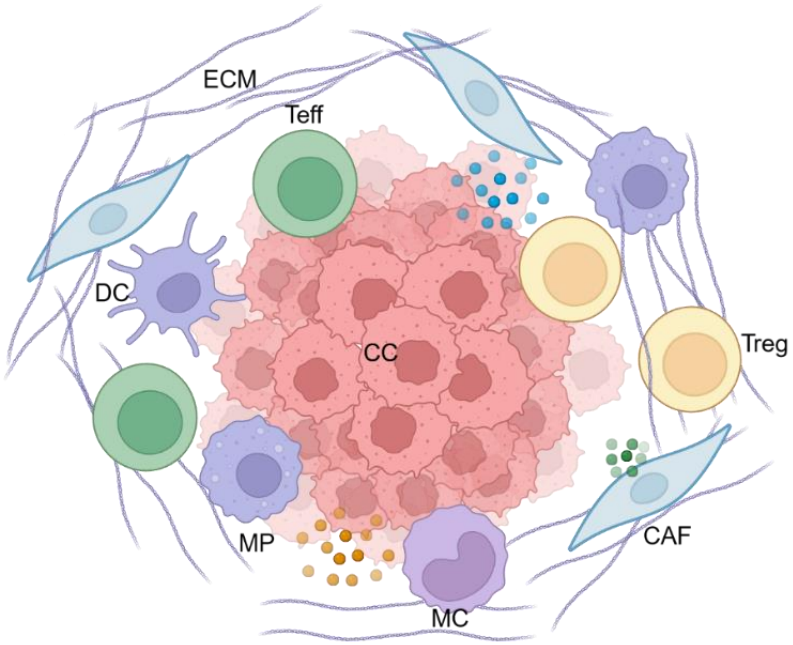


Figure 1.3 Schematic representation of the TME. The TME consists of several different cell types, the extracellular matrix and secreted factor. CAF= cancer-associated fibroblasts, DC= dendritic cells, Treg= regulatory T cell, Teff= effector T cell, CC= cancer cell, MC= monocyte, MP= macrophage. Figure made with Biorender.

1.4 Checkpoint inhibitor and cell therapy in cancer immunotherapy

To overcome immunosuppressive mechanisms of tumor cells, a variety of different strategies are adopted in cancer immunotherapy, including immune checkpoint inhibitors (ICIs), adaptive cell therapy (ACT), and tumor-specific vaccines. These all rely on the patient's own immune system to recognize and eliminate tumor cells (90,91).

ICIs are monoclonal antibodies that bind to co-inhibitory receptors. Typically these receptors are only expressed by immune cells facilitating the negative regulation of the T cell-mediated immune responses, thereby protecting the organism from autoimmune diseases (92,93). However, the expression of those inhibitory receptors by cancer cells exploits this negative feedback loop inducing tumor tolerance or T cell exhaustion (92). ICIs inhibit the receptor-mediated silencing of T lymphocytes by tumor cells promoting an immune response to the malignant cells (94). In particular, ICIs targeting the cytotoxic T-lymphocyte antigen-4 (CTLA-4), programmed cell death-1 (PD-1), and its ligand PD-L1 have demonstrated high efficacy for treating a variety of different cancer types and have been clinically approved for patients (95–98). For example, endometrial cancer (EC) is suggested to be characterized by an

immunosuppressive tumor environment, therefore cancer immunotherapy for EC to date has primarily focused on immune checkpoint inhibitors, e.g. PD-1/PD-L1 antibodies (99–101). Currently, three inhibitors are approved by the FDA for clinical treatment of advanced endometrial cancer (102). Nevertheless, despite these promising results intrinsic resistance of certain cancer types facilitated by low anti-tumor T cell generation, infiltration, or aberrations in immune effector signaling pathways remain a significant challenge for employing ICIs for cancer treatment (93,103,104). These challenges must be overcome for ICIs to be established as a broadly used therapeutic approach.

ACT utilizes the patient's T lymphoblasts by modifying them *in vitro*. Peripheral blood T cells are isolated from the patient and engineered through viral transduction to express a chimeric antigen receptors (CARs) (105). These T cells, so-called CAR-T cells, are capable of recognizing neoantigens on cancerous cells, independently of MHC involvement (106). This enables them to eliminate cancerous cells with immune evasion mechanisms involving the MHC receptor or malignant cells that lack neoantigens that generate epitopes and are instead only expressed on the cell surface (106). CAR-T cell therapy has shown encouraging results, particularly for hematological malignancies, leading to the approval of several CAR-T cell therapies for clinical use (107–110). However, similar to ICIs, there are still multiple limitations preventing CAR-T cells to be utilized as a common therapeutic approach. This includes poor CAR-T cell expansion, infiltration, and in particular, “off-target” effects due to low antigen specificity, potentially leading to lethal toxicity (111–114).

1.5 mRNA-based vaccine in cancer immunotherapy

Besides ICIs and ACT, mRNA-based vaccines have emerged as a promising tool for cancer immunotherapy. The feasibility of using an effective mRNA vaccine on a large scale has been demonstrated during the COVID-19 pandemic. Both BioNTech/Pfizer and Moderna developed effective mRNA-based vaccines, protecting from SARS-CoV-2 with limited adverse effects, thus, paving the way for mRNA vaccines as a future key therapy to combat tumors (115). To elicit an immune response, the mRNA vaccine has to be delivered to APCs, which translate the mRNA into the antigen of interest (116). As described in a previous chapter (Chapter 1.1), the antigen is processed to epitopes and binds to MHC molecules, before being subsequently trafficked to the cell surface, capable of stimulating B- and T cells (116) (Fig. 1.4)

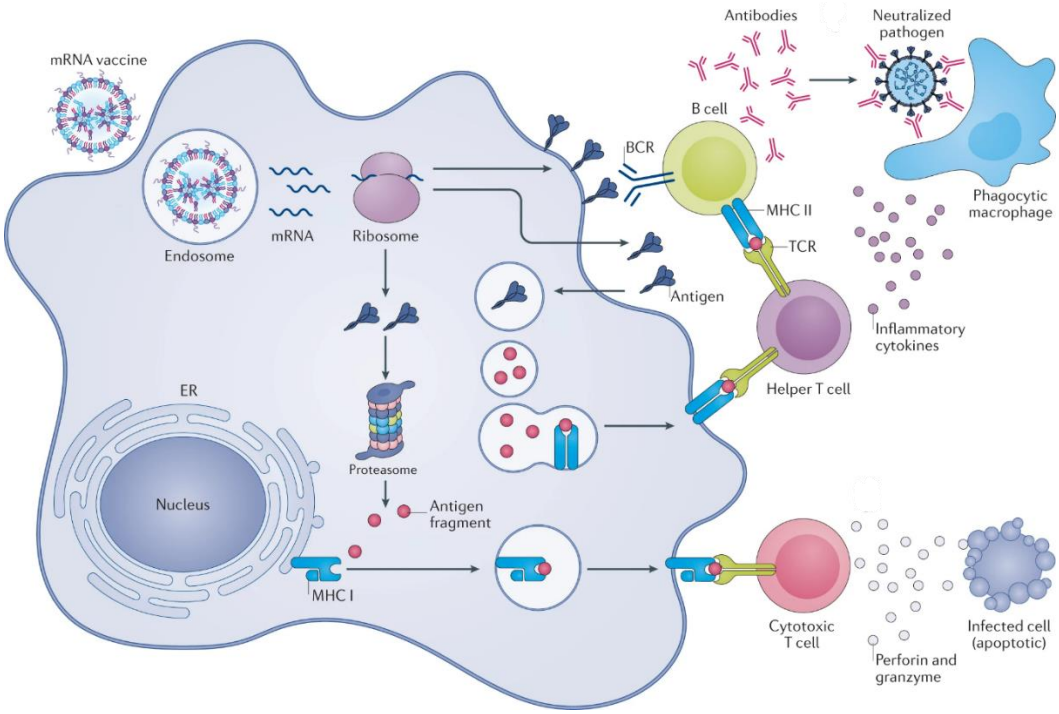


Figure 1.4 Basic principal of mRNA-based vaccine. The encapsulated mRNA is internalized and translated by APCs. The produced antigens are processed into epitopes (antigen fragments). Compatible epitopes bind MHC molecules and are trafficked to the cell surface where they can activate B- and T cells facilitating the elimination of infected cells and the neutralization of pathogens. Figure adapted from (116).

The groundwork for mRNA vaccines was laid more than three decades ago when Martinon and colleagues successfully induced virus-specific cytotoxic T lymphocytes by injecting mice with liposome-encapsulated mRNA (117). However, mRNA-based vaccines were not considered feasible for another decade due to limitations such as mRNA instability, inefficient *in vivo* delivery, and strong innate immunity activation (118). Starting in the early 2000s, this perception changed when numerous technological innovations and extensive research were able to demonstrate that mRNA-based vaccines could be a viable option for treating diseases. Capping and tailing of the mRNA, as well as efficient purification techniques improved mRNA stability (119–121). Lipid nanoparticles (LNPs) enabled researchers to more efficiently deliver the mRNA *in vivo* (122–124). Additionally, modification of nucleotides, in particular uridines, significantly reduced the innate immunogenicity and allowed for efficient translation of the mRNA, which will be extensively discussed in a later chapter (125,126).

mRNA vaccines demonstrate several key advantages in comparison to traditional vaccines, i.e. pathogen-, subunit-, or DNA-based vaccines. (i) Improved safety as they do not pose the risk of being incorporated in the host's genome and are not per se infectious (127). (ii)

Improved efficacy: introduction of modifications enables the mRNA to be more stable and highly translatable (126,128), LNPs facilitate efficient uptake into the cytoplasm of target cells (123), and anti-vector immunity is omitted allowing for repeated administrations (129–132). (iii) mRNA vaccines can be produced rapidly and are comparably inexpensive due to the high yield of the *in vitro* transcription, enabling the fast development of treatments for new pathogens, as demonstrated during the COVID-19 pandemic (133).

1.6 mRNA design for cancer immunotherapy vaccines

Improving the individual structural elements of the mRNA for mRNA-based vaccines has been a main focus of research as this can drastically enhance efficacy. An mRNA consists of a 5'cap, 5'UTR, the CDS, framed by a start and a stop codon, the 3'UTR, and a polyA tail.
The 5'cap consists of a 7-methylguanosin (m7G) unit connected to the first nucleotide of the mRNA by a triphosphate. It protects the mRNA from exonuclease-mediated degradation and simultaneously plays a critical role in pre-mRNA splicing, nuclear export, and translation initiation (134). In higher eukaryotes, the first nucleotide adjacent to the 5'cap can be modified. This modification, the so-called cap 1, is a key element for distinguishing between exogenous and endogenous mRNAs by the innate immune system (135,136). Further modifications at the second nucleotide (cap 2) impact protein expression in a cell type-dependent manner and improve immune evasion (137). Advances in synthetic 5'cap analogs, such as ARCA or Clean cap have further pushed the field of mRNA vaccine forward. These cap analogs enhance translation compared to naturally occurring 5'cap structures (138). This all emphasizes the importance of the 5'cap structure and identity, which should guide the design of an mRNA-based vaccine, aiming to maximize protein expression and avoid an unwanted immune response.
The 5' and 3' UTR are pivotal for regulating mRNA expression. Regulatory elements in the UTRs, such as internal ribosome entry sites (IRES), microRNA binding sites, or structured regions impact mRNA stability, splicing, and efficiency of translation (139–142). In particular, the 5'UTR sequence is proposed to have a significant impact on translation, regulating ribosome load on the mRNA, which in turn affects protein yield (143,144). However, a trade-off between ribosome load and mRNA stability seems to exist (143,144). Thus, maximizing ribosome load might not necessarily lead to the highest protein yield over an extended period of time, as mRNA stability is reduced. For mRNA vaccines, sequences derived from human alpha- and beta-globin have been utilized as UTRs (145,146). However, combinational sequences of UTRs from different genes have shown potential to further improve protein

expression (139,147,148).

In mammalian mRNAs, the polyA tail is approximately 250 nt long and significantly impacts the mRNA stability (149). It protects mRNAs from both 3'exonuclease activity and 5'cap hydrolysis, thus affecting the mRNA lifespan (150,151). Therefore, integration of a polyA tail in the mRNA therapeutic is essential. Commonly, a 120nt-long polyA tail is added to the mRNA, however, a segmented polyA tail might be more beneficial and was used in the COVID-19 vaccine of BioNTech (152). Segmented polyA tails reduce the recombination of plasmid DNA with no effect on mRNA half-life or translation (153,154).

The CDS of the mRNA vaccine encodes for the desired antigen. Optimization of the codons within the CDS, such as removing low-abundance codons enhances protein yield (155,156). However, antigen processing to epitopes is a relatively inefficient process (157–159). To enhance the efficiency several other elements are inserted in the CDS, aiming to improve epitope production and cell surface presentation. For instance, the addition of cytoplasmic and transmembrane domain of the MHC class I trafficking signal (MITD), the MCH class I secretion signal (SEC), and the Tetanus toxoid CD4+ T cell epitope P2 (P2) enhance antigen processing (160,161).

In cancer immunotherapy, mRNA vaccines are utilized to prime T cells for antigens expressed by tumor cells, which the primed T cells recognize and eliminate from the organism (162). Consequently, the targeted antigen should only be expressed at low levels in the healthy tissue to avoid unwanted off-target effects. Suitable targets can be broadly classified into two categories: tumor-specific antigens (TSA) and tumor-associated antigens (TAA). TSAs are solely expressed in tumor cells and can arise from genetic mutations, splicing defects, or altered post-translational modifications (163). While this makes TSA highly suitable for immunotherapy, in particular for personalized treatments, as neoantigens differ from patient to patient, the latter must be first identified by sequencing of the tumor tissue, which increases time and cost (164). Recently, Moderna in collaboration with Merck successfully completed a Phase 2 clinical trial by vaccinating patients with mRNAs encoding patient-specific TSAs against melanoma, thus, demonstrating the feasibility of TSAs as targets for mRNA-based cancer immunotherapy (165).

TAAs on the other hand are proteins that display elevated expression in cancerous tissue, however, they can expressed at lower levels in healthy cells (166). This includes the reactivation of ontogenetically expressed genes, the overexpression of certain proteins in malignant cells, and cancer/testis antigens (CTAs) (163). Expression of CTAs is restricted to tumor cells and testis tissue, making this group of antigens highly interesting as targets for cancer immunotherapy, in particular for gynecological cancers such as breast or endometrial tumors (167)

1.6.1 Impact of nucleotide modifications on immunogenicity and translation efficiency of exogenous mRNAs

Nucleotide modifications significantly impact the efficiency of mRNA-based vaccines. To date, over 140 distinct modifications of the canonical nucleotides adenine, guanine, cytosine, and uracil have been detected in RNAs, mainly in tRNAs and rRNAS (168). These modifications are typically installed post-transcription by dedicated enzymes. Nucleotide modification has a plethora of functions ranging from altering base pairing and modulating secondary structure to regulating translation efficiency, which demonstrates their importance in post-transcriptional control of translation (169–171).

Nucleotide modifications play a key role in the biology of endogenous mRNA, however, they are essential for the correct functionality of exogenously delivered mRNA. The innate immune system recognizes PAMPs through distinct PRRs, these include Toll-like receptors (TLRs) and RIG-I like receptors (RLRs) (172). TLR7 and TLR8 are pivotal for detecting foreign single-stranded RNA (ssRNA), TLR3 recognizes double-stranded RNA (dsRNA), and TLR9 is activated by unmethylated CpG DNA (173–175). Stimulation of these receptors triggers an intercellular signal cascade, inducing the production of type I interferons, inflammatory cytokines, and anti-viral proteins, to combat the infection (173–175).

Unmodified mRNA are potent activators of the above-mentioned PRRs and trigger the innate immune response, thereby reducing the translation efficiency (125,176). Nucleotide modifications of *in vitro* transcribed mRNA are capable of omitting this immune response in two ways. Firstly, nucleotide modifications lower the amount of dsRNA, which is produced as a byproduct during *in vitro* transcription (IVT), increasing ssRNA purity (177). Secondly, modifications inhibit the activation of TLRs. In 2005 Karikó and colleagues were the first to demonstrate that distinct nucleotide modifications, such as pseudouridine (Ψ), can suppress TLR stimulation to varying extents and subsequently omit the activation of the innate immune response (125). Interestingly, Ψ is also capable of reducing RIG-I activation contributing to the reduced immunogenicity (178). The percentage of modified mRNA nucleotides thereby positively correlates with suppressing immunogenicity (125).

Additionally, chemical modifications of uridine furthermore enhance translation efficiency (179). IVT mRNA containing unmodified uridines activates the RNA-activated protein kinase (PKR), which in turn phosphorylates eIF2α inhibiting mRNA translation (180). Modification of uridines inhibits PKR activation restoring efficient mRNA translation.

Previously, Ψ has been commonly utilized for modifying IVT mRNA to increase translation efficiency, however, numerous studies have now demonstrated the improved translation efficiency of N1-methyl-Ψ (m1Ψ) compared to other nucleotide modifications (126,181). This

is due to its capability of increasing the rate of translation initiation and hence ribosome density on the mRNA (126). Therefore, fully m1Ψ-modified mRNA is currently the standard for mRNA-based vaccines such as the COVID-19 mRNA vaccines (182).

1.6.2 Impact of modified nucleotides on translational elongation and termination

Although mRNAs whose uridines are fully replaced with modified uridines have become the standard for mRNA-based therapies, there may be potential drawbacks associated with this strategy regarding translational elongation and termination.

Elongation commences after the formation of the 80s initiation complex in which Met-tRNA$_i^{Met}$ is localized at the peptidyl-site (P-site) of the ribosome, concluding translation initiation (183). The elongation cycle can be distinguished into three distinct phases. First, the codon at vacant aminoacyl-site (A-site) is decoded by a cognate tRNA. This is mediated by the complex of eEF1A/GTP, forming a ternary complex with the cognate tRNA and recruiting it to the A-site (184). Following base-pairing interaction between mRNA and tRNA, GTP is hydrolyzed by eEF1A, eEF1A/GTP are released from the ribosome, and the tRNA is fully accommodated in the A-site (184). In the second phase, a peptide bond is formed, transferring the nascent peptide from the peptidyl-tRNA in the P-site to the amino group of the tRNA at the A-site (aa-tRNA), which rapidly occurs after accommodation of the aa-tRNA, promoted by eIF5A (185). In the last phase, the new peptidyl-tRNA is translocated from the A- to the P-site, leading to eventual releases of the deacylated tRNA from the exit-site (E-site) of the ribosome. This translocation is mediated by eEF2 and allows for a new round of translation to start (186). While elongation is highly orchestrated, nucleotide modifications are proposed to have the capability to modulate this process. They have been reported to impact both speed and fidelity of translation influencing protein production (187–189). Ψ for example, is known to decrease elongation rates and can induce amino-acid misincorporation leading to the formation of unwanted neoantigens (190,191). Therefore, the impact of nucleotide modifications on translation elongation needs to be considered when designing an mRNA-based vaccine.

Termination is the last phase of the translation process (Fig. 1.5). It occurs when a translating ribosome encounters one of the three canonical stop codons (UGA, UAG, or UAA) at the A-site. As these three codons are typically not decoded by canonical tRNAs, no ternary complex is recruited to the vacant A-site for elongation (192). This allows the binding of both eRF1 and eRF3 to the A-site (193,194). eRF1 is responsible for recognizing the stop codon and facilitates the release of the nascent polypeptide chain, which is promoted by eRF3 (195,196). Ultimately, this leads to the splitting of the ribosome and its recycling facilitated by a specific

factor, ABCE1 (197). mRNA and deacylated tRNA are subsequently released 40s subunit to enable the ribosome to participate in multiple rounds of translation (198)

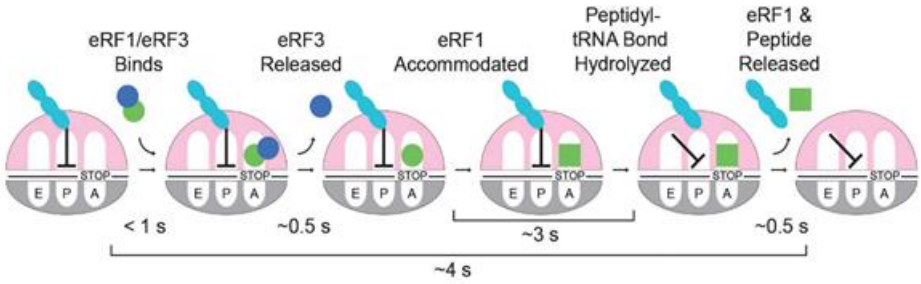


Figure 1.5 Timing and sequence of translation termination. Schematic illustrates the assessment of termination timings using FRET. Time from stop codon encounter to peptide release is ~4s with fast recruitment of eRF1 and eRF3 of <1s but comparatively slow release of the nascent peptide release of eRF3 dissociation (~4s). eRF1 and eRF3 coordinate translation in a highly conserved process ensuring termination fidelity. Adapted from (198)

Although the termination is a very efficient process, in some cases readthrough can occur and is influenced by both stop codon identity, as well as the adjacent nucleotides downstream of the stop codon (199–201). The termination capability differs between stop codons, with UGA being the most and UAA the least susceptible to readthrough with small molecule compounds and suppressor tRNAs (202,203). In addition to the stop codon itself, the nucleotides downstream further modulate termination capability. The most potent modulator is the nucleotide flanking the termination codon at the 3' (the +4 nucleotide). This is due to a stacking interaction of the +4 nucleotide with G626 of the 18s rRNA (204). The interaction is less stable with a pyrimidine than a purine leading to a +4 dependent termination efficiency of URRA≈URRG>URRU>URRU (204,205).

In addition to stop codon identity and downstream nucleotides, recent data further suggest that modification of the uridine in the stop codon affects termination efficiency (206–208). Modifying uridine to Ψ within the stop codons reduces termination capability in a stop codon identity-dependent manner (readthrough susceptibility: UGA>UAG>UAA) (208). The effect of m1Ψ on stop codon readthrough, which is now commonly used in vaccines, however, has not been studied yet.

When utilizing mRNA for therapeutic purposes readthrough of stop codons should be avoided for two primary reasons. Firstly, the readthrough of the stop codon causes a C-terminal extension of the protein. This extension, depending on the amino acid sequence, can render

the protein insoluble and target it for lysosomal degradation (209). This reduces the overall protein yield and subsequently vaccine efficacy. Secondly, stop codon readthrough harbors the possibility of producing unwanted off-target effects through neoantigenes. This occurs when the C-terminal extension of the protein is processed into epitopes that are capable of activating CD8+ T cells, which subsequently induce autoimmunity (210–212). Taking this together, this emphasizes that the sequence of mRNA-based vaccines should be designed to minimize stop codon read-through.

1.7 Delivery of mRNA vaccines

While mRNA can be delivered *in vivo* in its naked form, i.e without an additional carrier, the uptake efficiency by cells is low, and it is highly susceptible to degradation by RNases, both reducing vaccine efficacy (213–215). Therefore, various forms of mRNA delivery *in vivo* have been proposed, with LNPs emerging as the preferred option in recent years (124). LNPs typically consist of four lipids: the ionizable lipid, a phospholipid, cholesterol, and a lipid conjugated with a polyethyleneglycol (PEG) derivative, which are mixed by a laminar flow to encapsulate the mRNA cargo (Fig 1.6 A). The ionizable lipid is essential, as its hydrophilic head group alters charge depending on the pH. Under acidic conditions it is positively charged, which promotes electrostatic interactions with the negatively charged mRNA, thus forming stable LNPs (216). At physiological pH, the charge is neutralized, reducing potential toxicity (217). Phospholipids are integrated into LNPs to promote the fusion of LNPs with cellular and endosomal membranes, thereby enhancing cell uptake (218). Cholesterol plays a pivotal role in LNP stability and promoting cellular uptake (219). Lastly, PEGylated lipids prevent both aggregation of LNPs and lower immunogenicity by reducing the binding of serum proteins, thereby extending circulation time (220)

LNPs are internalized by cells through receptor-mediated endocytosis (Fig 1.6 B). The endogenous Apolipoprotein E (ApoE) binds to the surface of LNPs, facilitating their interaction with the low-density lipoprotein receptor (LDLR) on cells, which subsequently mediates the uptake (221). After internalization, the acidic pH inside the endosomal compartment induces the ionizable lipid to become positively charged, which destabilizes the endosomal membrane and causes the release of the mRNA into the cytoplasm (221). Biodistribution of LNPs is predominantly influenced by LNP size and surface charge (222,223). These characteristics can be modulated through various methods, including altering the molar ratios of lipids, adjusting the N to P ratio during mixing (ratio of positively charged amino groups to negatively charged phosphate groups), and controlling the speed of the laminar flow during the mixing

process (224–226). While LNPs have demonstrated that they are a viable option for mRNA delivery they still face various challenges, such as residual immunogenicity, off-target delivery, or inefficient release of mRNA from the endosomal compartment, all contributing to reduced vaccine efficacy (124,227,228).

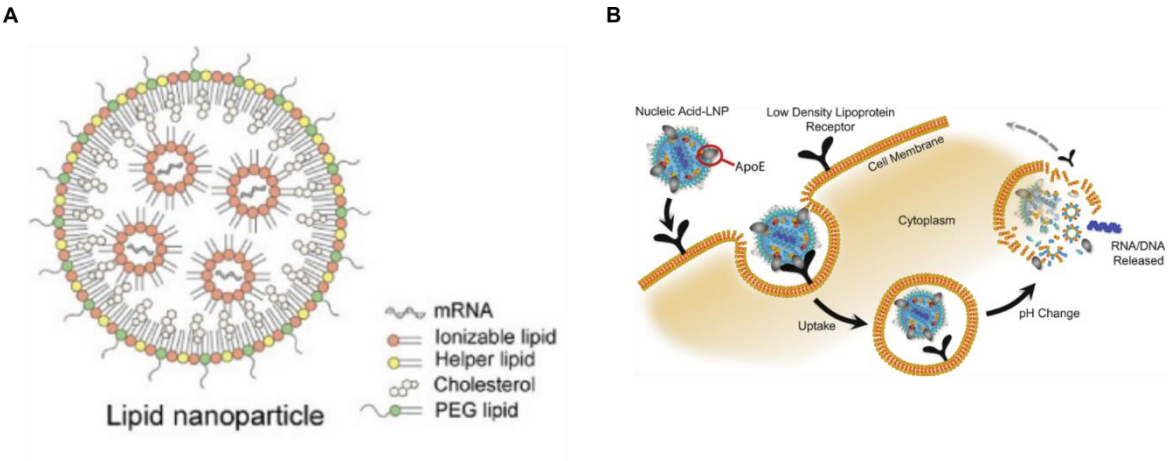


Figure 1.6 Basic principle of cellular uptake of LNP. (**A**) Schematic representation of LNP structure with encapsulated mRNA. Adapted from (229). (**B**) Principle of LNP internalization by cells. ApoE binds to LNP surface facilitating receptor-mediated endocytosis by LDLR. mRNA is released into cytoplasm after endosomal destabilization. Adapted from (230).

1.8 Circulating versus *ex vivo* mRNA-based vaccine

To target TSAs or TAAs expressed by malignant cells, T cells are primed by delivering the antigen-encoding mRNA to APCs mainly dendritic cells. This can be accomplished by utilizing the classic circulating mRNA vaccine approach (Fig. 1.7), which elicits an immune response by directly injecting encapsulated mRNA into the patient (231). Following mRNA internalization by DCs in the spleen, the mRNAs are subsequently translated and processed into epitopes to be presented on the cell surface. This primes the naive T cells for the corresponding antigen, enabling them to recognize and eliminate tumor cells with this target antigen as described in detail in Chapter 1.5 (232).

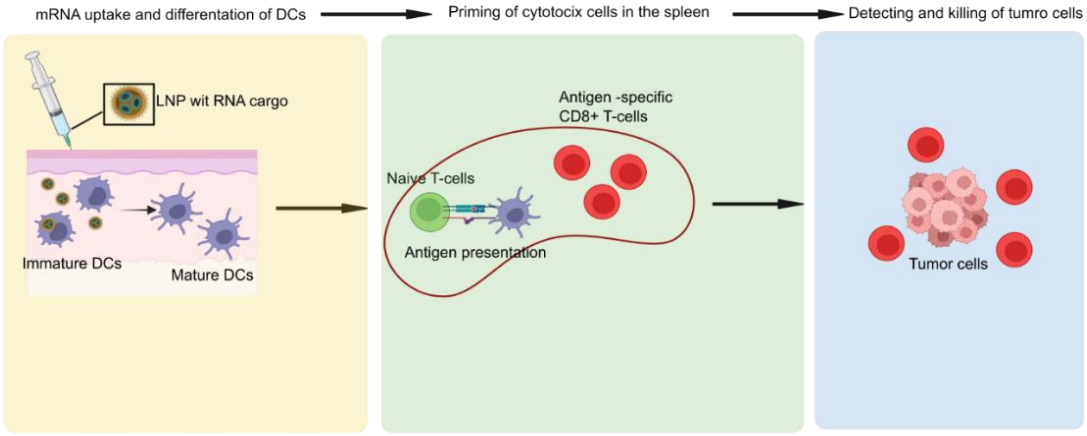


Figure 1.7 Schematic representation of the circulating mRNA vaccine approach. circulating approach consists of three distinct phases: (i) mRNA is internalized by immature DCs after vaccination of the patient. mRNA is translated by the DCs and presented on the cell surface of mature DCs. (ii) Presentation of antigen to naïve T cells by mature DCs in the spleen. (iii) Detection and killing of tumor cells by CD8+ T cells. Figure made with Biorender

However, this approach still faces several challenges. The direct injection of mRNA requires its encapsulation. Choosing the right encapsulation components, e.g. lipids for LNPs, is challenging as they determine the efficiency of delivery to the target side (233). Selection of inadequate components can negatively impact the uptake of mRNA into cells and/or delivery to off-target sides reducing the immune response and ultimately efficient elimination of the tumor (124,234). Recent data suggest that for a robust immune response simultaneous delivery of unmodified mRNA is required (178,235), however, this mRNA is not translated and can lead to unwanted adverse reactions (126,236).

Therefore, research has simultaneously focused on a second potential approach, the *ex vivo* vaccine (Fig. 1.8). Here DCs are isolated from the patient and directly transfected with the mRNA encoding the targeted antigen. Following DCs maturation they are co-cultured with T cells, priming them for the target antigen. These T cells are subsequently reintroduced into the patient after clonal expansion, to recognize and eliminate tumor cells (237). This method demonstrates several advances over circulating mRNA vaccines. The mRNA is delivered *in vitro* to cells, which drastically increases delivery efficiency and eliminates the possibility of off-target delivery (118). Additionally, the priming of T cells *in vitro* provides the opportunity to expand activated T cells increasing the likelihood of generating a sufficient number of T cells capable of targeting and eliminating malignant cells. Collectively, *ex vivo* vaccines are a promising approach for cancer immunotherapy.

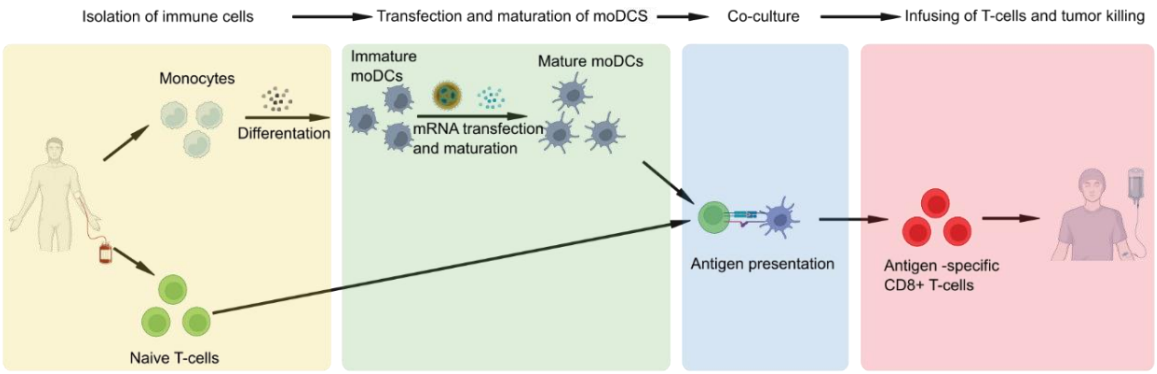


Figure 1.8 Schematic representation of the *ex vivo* mRNA vaccine approach. The *ex vivo* approach consists of four distinct phases: (i) Isolation of immune cells from the patient. (ii) Transfection and maturation of APCs. (iii) Co-culture of APCs and T cells. (iiii) Reintroduction of antigen-specific T cells into the patient after clonal expansiom. Figure with Biorender.

1.9 Endometrial cancer

Endometrial cancer originates from malignant cells in the endometrium. It has emerged as the most prevalent gynecological cancer in developed countries, with a rising rate of both incidence and mortality in recent years (238,239). Amongst women, it is now the sixth most common cancer with 417,000 new diagnoses in 2020 globally, and the 14th leading cause of death with 97,370 disease-related deaths in 2020 (240). Increased prevalence of risk factors, mainly obesity and an aging population, have led to a rise in yearly diagnoses posing a substantial burden on public health (241). EC occurrence is highly associated with excessive body weight, with every 5kg/m^3 increase in BMI elevating the risk of developing EC by 54% (242). With a median age of diagnosis at 61 years, it predominantly affects women in postmenopausal stage and its incidence is closely associated with a woman's current reproductive stage (102,243). Excessive amounts of exogenous and endogenous estrogen associated with obesity, insulin resistance, and post-menopause are recognized as the main risk factors for developing EC, e.g. elevated serum estrogen levels double the risk of EC incidence (102,244,245). While cyclical progesterone and menstrual shedding maintain endometrial health during reproductive years, the production of estrogen stimulates the proliferation of the endometrium. An imbalance towards an elevated amount of estrogen is presumed to be the leading cause of endometrial tumorigenesis (102,244). Based on the histological type, grade, and receptor expression ECs have been historically classified into

two subtypes: type I and type II (246). Approximately 80% of all ECs are classified as type I, typically characterized by endometrioid histology, low tumor grade, slow progression, and a favorable overall survival rate (247). The occurrences of these tumors are associated with prolonged estrogen overexposure and predominantly arise from endometrial hyperplasia (102,248).

In contrast, type II ECs which include serous carcinoma, clear cell carcinoma, and mixed carcinoma exhibit a more aggressive behavior (249). They commonly display non-endometrioid histological characteristics and a high tumor grade, being associated with an unfavorable prognosis (250). In contrast to type I type II, ECs are presumed to originate from endometrial polyps or atrophy rather than prolonged estrogen exposure (251).

Although this dualistic model has been typically applied for the classification of ECs since its establishment in 1983, advances in sequencing and modern array technology have led to the proposal of a new classification system. This system classifies ECs into four groups according to their transcriptomic and proteomic features: Ultra mutated POLE, hypermutated endometrial carcinoma, low-copy number endometrial tumors and high-copy number endometrial tumors (252). Ultra-mutated POLE ECs exhibit a high mutation rate specifically in the esonucleasic POLE domain, few aberrations in copy number, and are generally associated with a favorable prognosis (253). Hypermutated carcinomas (HCs) are characterized by microsatellite instability causing an accumulation of high numbers of mutations and are associated with an intermediate, stage-dependent prognosis (254,255). Low copy number (LCN) endometrial tumors are characterized by a low amount of alterations to copy numbers with only a limited amount of mutations. For this tumor type the prognosis is stage-dependent and ranges from intermediate to excellent (247,256). Lastly, high copy-number (HCN) endometrial tumors display extensive alterations in their somatic copy numbers and limited mutation frequencies. While these tumors represent only 20% of all diagnosed cases, they account for 50-70% of EC-associated mortality (247,257).

EC is primarily diagnosed in the early onset of the disease (258). At this stage treatment primarily involves surgery, removing the uterus and the ovary completely as well as the fallopian tube bilaterally, improving the overall survival to 95% (259,260). For patients with advanced or recurrent EC, the location of metastases and the likelihood of complete cytoreduction determines the feasibility of surgical intervention (102). In the majority of these cases additional adjuvant treatment, predominantly radiotherapy or platinum-based chemotherapy is required (261,262). Despite those interventions, the overall survival rate for advanced-stage EC markedly drops to 50-15% (263). Thus, the development of novel therapies for treating EC is of high interest.

2. Aim of thesis

Cancer immunotherapy has emerged as a promising tool to treat a variety of tumors. This approach leverages the patient's own immune system to target and eliminate cancerous cells, enhancing the capability of immune cells for detection and consequent elimination of malignant cells. The high efficacy, versatility, and minimal side effects of mRNA-based vaccines make them an excellent option for fighting pathogens and for applications in immunotherapy of various tumors. In this thesis, we aimed to generate an *ex vivo* mRNA-based therapeutic (vaccine) capable of targeting endometrial cancer, and in this way to address the need for efficient treatment options at later stages of the disease. We focus on designing and optimizing the mRNA sequence, specifically tailored for *ex vivo* application. We identify four potential antigens as suitable targets in endometrial cancers and verify their expression and ability to activate T cells in an *ex vivo* setup, thus demonstrating the effectiveness of our mRNA vaccine to trigger an immune response. We evaluate mRNA delivery, translation efficiency, and epitope production to assess the effectiveness of our vaccine. By testing the stimulation of the innate immunity, we investigate the safety of our vaccine.

3. Results

3.1 5'UTR of alpha-globin and termination with dual stop codon improve the expression of the mRNA design for *ex vivo* vaccine

The efficacy of mRNA vaccines for cancer immunotherapy depends on multiple factors, most notably the design of the mRNA, to maximize protein expression and the efficient delivery of mRNA to the target cells. Specifically, for circulating mRNA vaccines delivery presents a challenge, as the mRNA is injected directly into the patient, requiring the transport to the intended target side and efficient release into the cytoplasm to be translated (Fig. 1.7). In contrast, delivery for an *ex vivo* vaccine is less challenging, as cells are transfected *in vitro* (Fig. 1.8). Consequently, we chose to focus on mRNA design to maximize efficacy. Primary target cells for mRNA vaccines are DCs. In the case of an *ex vivo* vaccine, these are dendritic cells differentiated from monocytes called monocyte-derived dendritic cells (moDCs) as it is challenging to isolate a sufficient amount of of DCs from blood samples. Therefore, we aimed to design an mRNA that would maximize protein expression and epitope presentation in moDCs. Extensively reviewing the published literature, we identified an mRNA design that is commonly used in current mRNA-based vaccines (Fig. 3.1 A upper schematic) (264–266). Our goal was to improve upon this design to enhance vaccine efficacy. Given that epitope processing and presentation is a relatively inefficient process (157), we found that the CDS in mRNA vaccines typically incorporates additional elements besides the antigen to improve this process. This specifically includes an MHC class I section signal (SEC), an MHC class I trafficking signal (MITD), and the Tetanus toxoid CD4+ T cell epitope P2 (160,161). These were incorporated into our mRNA design; those parts were connected by flexible linkers encoding two consecutive GGSGG amino acid stretches (Fig. 3.1 A lower schematic) to improve antigen processing and presentation. Typically, the 3'UTR region of mRNA vaccines is derived from the 3'UTR of beta-globin (*HBB*), often in the form of two repeated sequences of the *HBB* 3'UTR (265,267). However, a recent high-throughput study suggests that for expression in DCs, *HBB* is outperformed by several other 3'UTR sequences (148). In particular, a hybrid sequencing composed of elements from the amino-terminal enhancer of split (AES) and mitochondrially encoded 12S rRNA (mtRNR1) enhanced protein expression in DCs (148). Thus, we incorporated this 3'UTR in our mRNA design (Fig. 3.1A lower schematic). The polyA tail plays a crucial role in mRNA stability and translation, yet it poses a challenge during cloning and amplification in bacteria (268). We found evidence suggesting that introducing a 10-nucleotide-long insert after 30 adenosines, followed by 70 additional adenosines reduces the DNA plasmid recombination, while not compromising translation or

half-life compared to a polyA tail with consecutive adenosines (154). This segmented polyA tail was also incorporated into our mRNA construct (Fig. 3.1 A, lower schematic).

Considering the published literature, we identified the 5'UTR as a critical element influencing protein expression, modulating both ribosome load and stability (143). Consequently, we sought to improve the design of our *ex vivo* vaccine by investigating the impact of various 5'UTRs on protein expression in moDCs, comparing them to the 5'UTR of *HBB* which is typically used in mRNA vaccines (145). We selected five 5'UTRs as potential candidates for the design of our mRNA, with three being previously characterized (143). From this study, we chose the 5'UTR of (i) apolipoprotein A-II *(APOA2*), which maximizes mRNA stability; (ii) terminal oligopyrimidine motif beta-globin (TOP-*HBB*), which had amongst the highest observed ribosomal loads; and (iii) mitochondrial ribosomal protein L18 (*mRpl18*), whose 5'UTR mediates an intermediate ribosome load and mRNA stability. Furthermore, we hypothesized that combining two 5'UTRs, one with optimized ribosomal load and the other with enhanced mRNA stability, may further improve translation and in-cell mRNA stability. Thus, we considered the hybrid *APOA2*-TOP-*HBB* as a possible 5'UTR candidate. We also selected the 5'UTR of alpha-globin (*HBA*), as *HBA* has also gained attention as a possible 5'UTR for mRNA vaccines (146).

To evaluate the influence of these 5'UTRs on protein expression, we inserted each upstream of a reporter encoding Renilla luciferase (RLuc) (Fig. 3.1 A lower schematic). The mRNA was transcribed *in vitro* replacing all uridines with N1-methyl-pseudouridine (m1Ψ), a commonly used approach for mRNA vaccines to maximize protein expression and decrease immunogenicity of mRNA (125,126). As the availability of moDCs, the target cells of an *ex vivo* vaccine is limited, we first performed the optimization experiments in HeLa cells. For this, we transfected HeLa cells with the respective 5'UTR mRNAs. A commercially available Firefly luciferase (FLuc) mRNA was co-transfected for normalization. Thereafter, protein expression was assessed after 24h. All 5'UTRs, except for *APOA2*, improved protein expression compared to *HBB* (Fig. 3.1 B). Notably, *HBA* demonstrated the highest expression with a 1.8-fold increase over that of *HBB* and a significantly higher expression over the second-highest performing 5'UTR from *mRpl18* (Fig. 3.1 B). To confirm that the 5'UTR of *HBA* similarly enhances protein expression in moDCs - the target cells of our mRNA vaccine - monocytes were isolated from peripheral blood mononuclear cells (PBMCs) and differentiated into moDCs before transfection. moDCs were transfected in the same way as HeLa cells and protein expression was determined after 24h. Consistent with the results from HeLa cells, the 5'UTR of *HBA* displayed the highest protein expression among all tested 5'UTRs in moDCs, with a 2.7-fold increase over *HBB* (Fig. 3.1 B). Collectively, these results demonstrate that the 5' UTR of *HBA* outperformed the commonly used 5'UTR of *HBB* in both HeLa cells and moDCs and was therefore included in our optimized mRNA design (Fig. 3.1 A lower schematic) to

maximize protein expression.

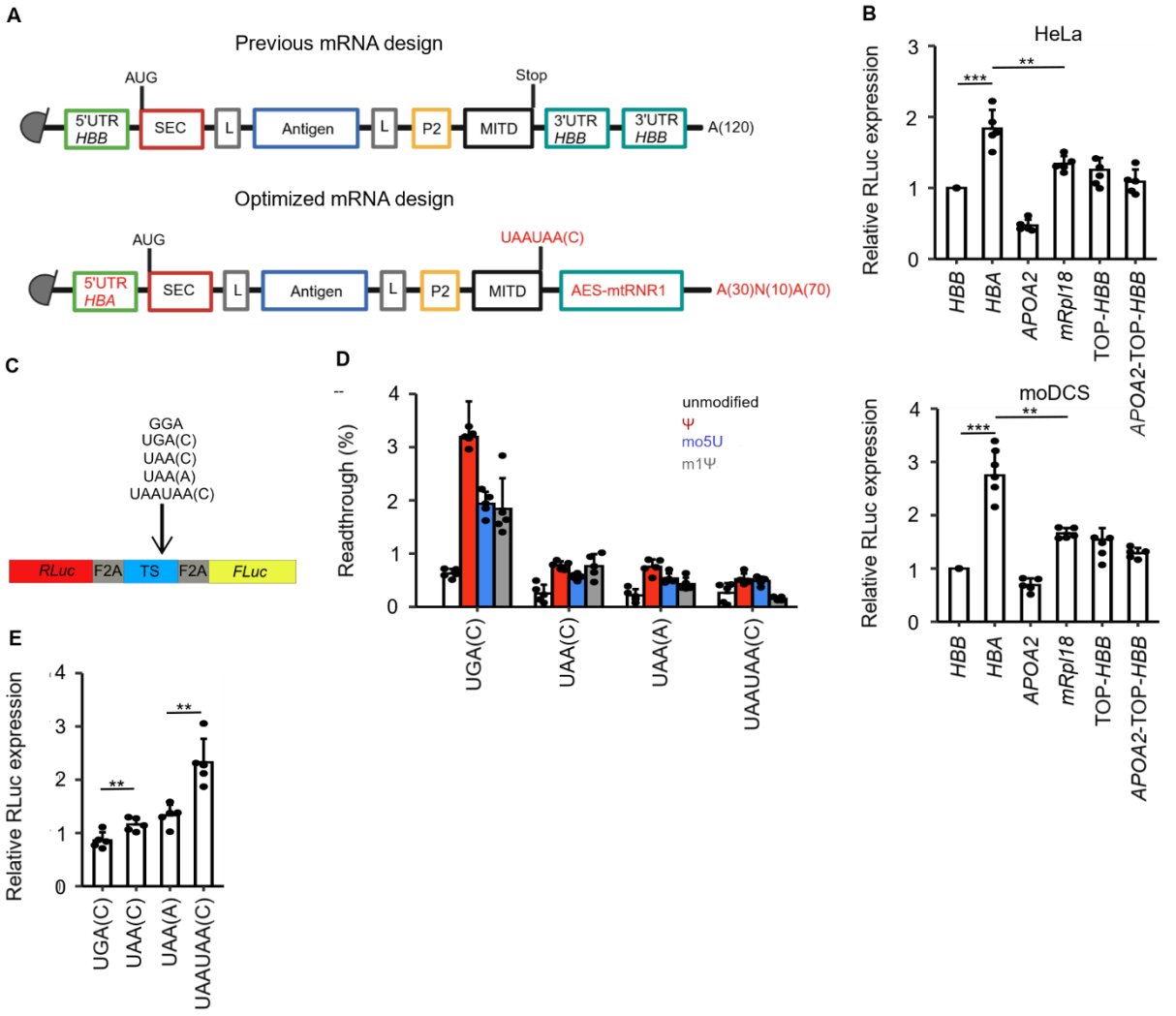


Figure 3.1 mRNA vaccine design is improved by optimizing 5'UTR and stop codon. (**A**) mRNA design for cancer vaccines. The upper schematic represents previously used mRNA designs. The lower schematic represents optimized mRNA design developed and applied within this work. Changes are highlighted in red. *HBB*= Human β-globin, *HBA*= Human α-globin, SEC= MHC class I section signal, P2= Tetanus toxoid CD4+ T cell epitope P2, MITD= MHC class I trafficking signal, L= protein linker, *AES-mtRNR1*= Fusion sequence of Amino-terminal enhancer of split and mitochondrially encoded 12S ribosomal RNA. (**B**) Relative expression of RLuc normalized to FLuc depending on the 5'UTR sequence in HeLa cells and moDCs. (**C**) Reporter mRNA design for assessing stop codon readthrough. Nucleotides in brackets represent the +4 nt. Test sequence insert (TS) consists of 18bp upstream and 3bp downstream flanking the stop codon in the mRNA sequence from (**A**) or GGA as readthrough control. F2A sequences mediate peptide cleavage between individual parts. (**D**) Comparison of stop codon readthrough between reporter mRNAs modified with different nucleotides in moDCs. The percentage was calculated by normalizing the relative protein expression of stop codon-containing mRNAs to that of expression of GGA FLuc/RLuc ratio. (**F**) Relative expression of RLuc normalized to FLuc in moDCs. mRNA contains different stop codons and is fully m1Ψ modified (**A**). For (**B**), (**D**), (**E**), and (**F**) data are mean ± sd (n=5 biological replicates). ** p≤ 0.01,*** p≤ 0.001 by two-tailed unpaired t-test. Some of the data in panel (**D**) was generated by Chris George during his internship.

In addition to the 5'UTR we also identified the stop codon to be a critical component when designing an mRNA. Replacement of the uridines of the stop codon with Ψ has been previously shown to increase the readthrough, depending on stop codon identity, which leads to the generation of unwanted neoepitopes (208,269). However, whether other uridine modifications, such as m1Ψ, similarly affect readthrough is unknown. To address this we determined the impact of the two uridine modifications m1Ψ, commonly used for mRNA vaccines, and 5-methoxyuridine (5moU), which improves protein expression in a similar manner to m1Ψ (270). These modifications were compared to both unmodified and Ψ-modified mRNA. We first tested UGA and UAA, as they have been reported to exhibit the highest and lowest susceptibility to readthrough, respectively (203). To measure stop codon readthrough we utilized a commercially available dual-luciferase reporter mRNA (Fig. 3.1 C). In this reporter, faithful termination leads to no expression of FLuc downstream while RLuc is used as an internal control to quantify readthrough. We inserted a test sequence between RLuc and FLuc consisting of the respective stop codon or GGA encoding glycine as a positive control; the stop codon or GGA was flanked by 33 bp upstream and 3bp downstream corresponding to our mRNA construct (Fig. 3.1 A lower schematic). Since the +4nt in our mRNA construct was a cytosine (UAA(C)), which is reported to enhance readthrough we additionally substituted this position for UAA with an adenine (UAA(A)), which reduces readthrough (204). To determine the readthrough, the reporter mRNAs were transcribed *in vitro*, whereas uridines were completely replaced by the corresponding modified nucleotide and transfected into moDCs for 24h. Readthrough percentage was calculated by normalizing to the protein levels of the GGA-containing reporter. We observed an increase in readthrough when the stop codon was modified irrespective of stop codon identity (Fig. 3.1 D). For UGA, Ψ-modification led to the highest readthrough (3.2%), while m1Ψ and 5moU caused comparable readthrough (Fig. 3.1 D). UAA markedly reduced readthrough and differences amongst the respective modifications were less pronounced with only 5moU showing slightly less readthrough (Fig. 3.1 D). Notably, changing the +4nt reduced only readthrough for m1Ψ-modified mRNAs while Ψ- and 5moU-modified mRNAs were unaffected (Fig. 3.1 D).

Given that UAA showed the least susceptibility to readthrough even modified, we hypothesize that a dual stop codon of UAA might further enhance termination and reduce readthrough. We therefore inserted the dualstop codon UAAUAA into the test sequence of our reporter and transfected the uridine-modified mRNAs into moDCs. 5moU and Ψ- modified mRNA showed comparable readthrough, with Ψ only slightly lowering the readthrough compared to mRNA with a single UAA (Fig. 3.1 D). In contrast, m1Ψ-modified mRNA exhibited markedly reduced readthrough at UAAUAA (Fig. 3.1 D). Notably, a double-stop codon reduced readthrough levels of m1Ψ-modified mRNA below that of unmodified mRNA (Fig. 3.1D). Collectively, these results suggest that a combination of a dual stop codon UAAUAA and the uridine modification

m1Ψ minimizes stop codon readthrough, thus, lowering the likelihood of unwanted neoepitope formation. Stop codon readthrough was reported to also impact the mRNA stability and the susceptibility of the produced protein to lysosomal degradation (209). Increased mRNA and protein degradation lower vaccine efficacy by reducing the amount of available antigens, whichin turn decreases epitope production.

To evaluate protein availability in the context of our *ex vivo* mRNA vaccine, we inserted the stop codons previously tested for readthrough into our mRNA construct encoding RLuc (Fig. 3.1 A lower schematic) and used a commercially available FLuc mRNA for normalization. The fully m1Ψ-modified mRNA was transfected into moDCs and after 24h the luminescence was measured, as an indicator of protein levels. The mRNA with the dual stop codon UAAUAA resulted in a significantly higher RLuc level compared to single stop codons; thereby UAA(C) and UAA(A) terminated mRNAs showed similar levels of RLuc while UGA(C) stop codon resulted in the lowest. This suggests that UAAUAA enhanced protein availability by minimizing the readthrough, thus emphasizing the notion for using double stop codon in our *ex vivo* vaccine.

Considering the results of our 5'UTR and readthrough experiments, we incorporated the 5'UTR of *HBA* and the dual stop codon UAAUAA into our final mRNA construct. This optimized mRNA (Fig. 3.1 A lower schematic) formed the basis for our *ex vivo* vaccine.

3.2 LNPs are not suitable to deliver mRNA in moDCs for *ex vivo* vaccine setup

In recent years LNPs have emerged as a tool for efficient delivery of mRNA vaccines *in vivo* (124). Given this success, we sought to investigate whether LNPs could be utilized for the delivery of mRNA for *ex vivo* vaccines. We first conducted an extensive search of the published literature to identify established LNP formulations for mRNA delivery to antigen-presenting cells (APCs) *in vivo*. We found that an LNP formulation usually consists of the ionizable lipid DLin-MC3-DMA, the phospholipid 1,2-DOPE (1,2-dioleoyl-sn-glycero-3-phosphoethanolamine), cholesterol, and DMG-PEG(2000) (1,2-dimyristoyl-rac-glycerol-polyethylene glycol 2000) (122). It is administered in a N:P ratio of 4:1 (i.e. ratio of ionizable lipid amino groups to phosphate groups of mRNA) (122). The LNP size of 60-200nm demonstrated the best results for transfection APCs in previous research (271). Thus, we encapsulated our fully m1Ψ-modified mRNA (Fig. 3.1 A lower schematic) in LNPs with the above lipid composition and N:P ratio, using laminar flow mixing to first asses both LNP size and encapsulation efficiency. Dynamic light scattering (DLS) measurements revealed that the

LNPs displayed a size ranging from 99 nm to 148 nm, with a median size of 130 nm (Fig. 3.2 A, B).

To evaluate the encapsulation efficiency, we denatured the LNPs with Triton X-100 and measured the amount of released mRNA through fluorescent dye binding. We found that the encapsulation efficiency of our LNP formulation ranged from 78% to 94% with a median of 88% (Fig. 3.2 C). Collectively, this demonstrates that our mRNA-LNPs fall in the optimal size range used for mRNA delivery to APC with a robust encapsulation efficiency, supporting their potential as a vehicle to deliver our *ex vivo* mRNA vaccine.

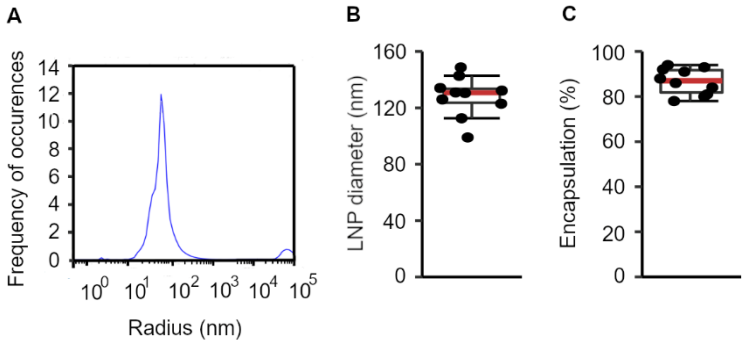


Figure 3.2 Assessment of LNPs properties. (**A**) Representative image of measuring LNP size by DLS. Peak represents mean particle radius determined by 20 individual DLS measurements. (**B**) Statistical analysis of LNP diameter after DLS measurements (n=10). (**C**) Analysis of LNP encapsulation efficiency (n=10). Encapsulation efficiency was determined by the ratio of mRNA amount inside LNP/(mRNA amount inside LNP+unencapsulated amount of mRNA in LNP storage buffer). For (**B**) and (**C**), the boxes represent the 25- to the 75-percentile. The red line denotes the median value. Whiskers represent the remaining data range without exclusion of outliers.

After verifying the selected lipids produce LNPs with suitable characteristics to transfect APCs, we proceeded to test their administration properties. As the cell number of moDCs was limited, we first utilized HeLa cells. We administered LNPs into HeLa cells; the LNPs bear mRNA fully modified with m1Ψ, with optimized sequence (Fig. 3.1 A lower schematic), encoding a reporter GFP. To assess the success of transfection, 24h post transfection we subjected them to fluorescence microscopy using DAPI to stain nuclei. Following LNP administration, HeLa cells displayed robust GFP fluorescence compared to the untransfected control (Fig. 3.3 A, B). We observed a mean fluorescence of 25 (a.u.) compared to 3 (a.u.) in untransfected control (Fig 3.3 B). This indicates that our LNP formulation is capable of delivering mRNA into HeLa cells.

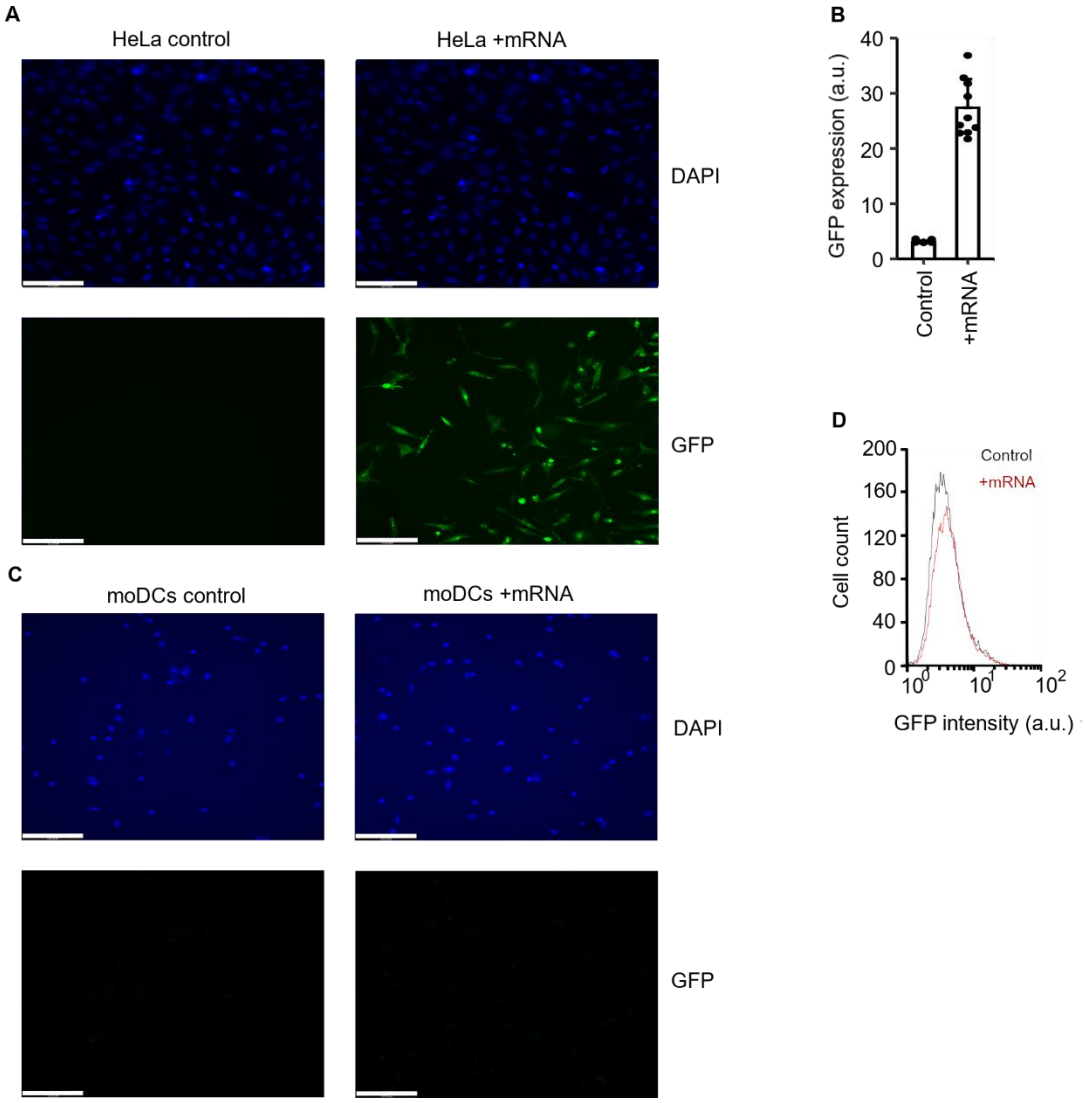


Figure 3.3 LNP administration of mRNA into HeLa cells and immature moDCs. (**A**) Representative fluorescence microscopy images of HeLa cells after delivery of GFP-encoding optimized mRNA by LNPs and untransfected control. (**B**) Statistical analysis of the GFP intensity from fluorescence microscopy images of (**A**). Data are mean ± sd (n=10). (**C**) Representative fluorescence microscopy images of moDCs after delivery of fully m1Ψ-modified mRNA with optimized sequence encoding GFP by LNPs or untransfected control. For (**A**) and (**C**) nuclei were counter-stained with DAPI. Images were taken at 20x. Scale bar: 133 µm. (**D**) Flow cytometry analysis of GFP intensity in moDCs after LNP administration of GFP-encoding optimized mRNA.

Given that moDCs are the target cells for our *ex vivo* vaccine, we next sought to determine the transfection capability of the LNPs for these cells. We transfected immature moDCs with the same mRNA-LNP formulation that we used in HeLa cells and measured the fluorescence after 24h. In contrast to HeLa cells, we did not observe GFP fluorescence in moDCs post-transfection, which were undistinguishable from the untransfected control (Fig. 3.3 C). To

ensure that this was not due to detection limitations of the fluorescence microscopy, we subjected the transfected moDCs to flow cytometry. This technique offers a more quantitative and high-throughput assessment of the fluorescence intensity at single-cell level. Consistent with the microscopy results, no GFP fluorescence was detected 24h post-transfection, i.e. there was no shift in GFP intensity relative to untransfected control (Fig. 3.3 D).
Together, these findings indicate that while our LNP formulation effectively delivers mRNA to HeLa cells, it fails to transfect moDCs, suggesting that this formulation is unsuitable for delivering our *ex vivo* mRNA vaccine to its intended target cells *in vitro*.

3.3 Lipofactamine efficiently delivers of *ex vivo* mRNA vaccine to moDCs

Given that LNPs were unable to deliver mRNA to moDCs *in vitro*, we sought an alternative method to efficiently deliver our *ex vivo* mRNA vaccine to the intended target cells. The most commonly used transfection reagent for cells *in vitro* is lipofectamine, due to its high transfection efficiency. It contains multiple lipids that form liposomes entrapping the payload, e.g. mRNA and delivering it to cells *in vitro* (272). While this approach is highly efficient for laboratory cell lines, transfection of certain primary cells can still pose a challenge with reduced delivery efficiency (273). To assess whether it can be utilized as an efficient tool to deliver our *ex vivo* mRNA vaccine in moDCs, we compared the transfection efficiency of moDCs to that of a well-tranfectable secondary HeLa cell line. We first performed transfection on HeLa cells with our fully m1Ψ-modified mRNA (Fig. 3.1 A lower schematic) encoding GFP. Fluorescence microscopy with DAPI counterstaining was performed to assess successful transfection after 24h. Following mRNA transfection HeLa cells displayed a strong GFP fluorescence compared to mock-transfected control (Fig. 3.4 A, C). We observed a mean fluorescence of 27 (a.u.) compared to 3 (a.u.) in mock-transfected control (Fig. 3.4 A, C). This transfection efficiency was comparable to the previously used LNPs for HeLa cells (Fig. 3.3 B). Next, we transfected immature moDCs with the same mRNA using lipofectamine and subjected cells to fluorescence microscopy after 24h. Post-transfection moDCs displayed a robust GFP expression (Fig. 3.4 B, D). We detected a mean fluorescence of 22 (a.u.), which was lower than that observed for HeLa cells, however, it was still higher and well-distinguishable than the mock-transfected control (Fig. 3.4 D), demonstrating that lipofectamine efficiently delivered mRNA to moDCs.

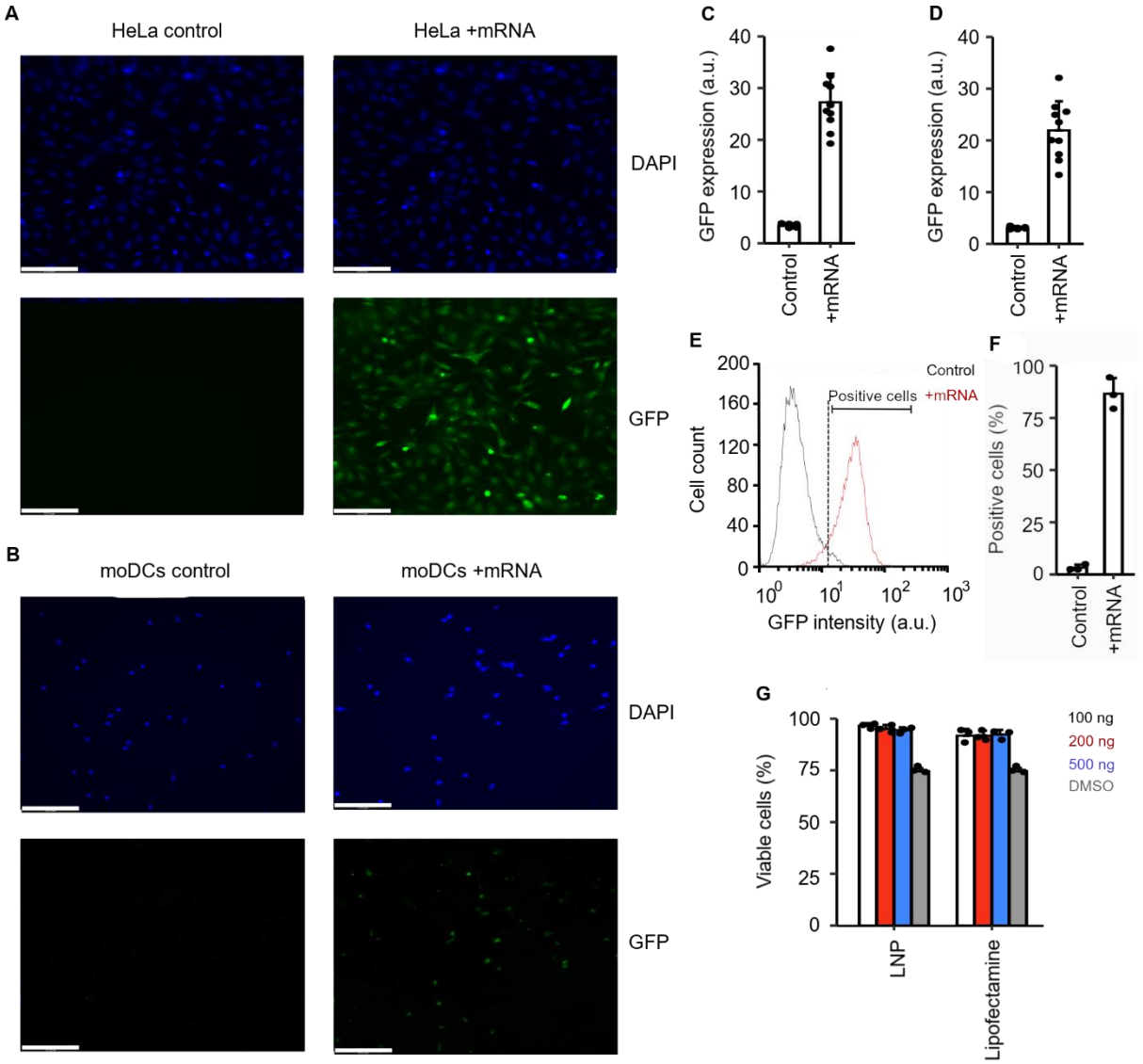


Figure 3.4 Lipofectamine delivers mRNA efficiently to both HeLa cells and moDCs. (**A**) Representative fluorescence microscopy images of HeLa cells after delivery of fully m1Ψ-modfied mRNA with optimized sequence encoding GFP by lipofectamine. (**B**) Representative fluorescence microscopy images of HeLa cells after delivery of fully m1Ψ-modfied mRNA with optimized sequence encoding GFP by LNPs. For (**A**) and (**B**) nuclei were counter-stained with DAPI. Images taken at 20x. Scale bar: 133 µm. (**C**) Statistical analysis of the GFP intensity from fluorescence microscopy images of (**A**). Data are mean ± sd (n=10. (**D**) Statistical analysis of the GFP intensity from fluorescence microscopy images of (**B**). Data are mean ± sd (n=10). (**E**) Representative flow cytometry assessment of GFP-positive moDCs after transfection with fully m1Ψ-modified mRNA with optimized sequence encoding GFP. The dashed line represents the threshold after which cells were classified as GFP-positive. The threshold was determined by the cell distribution of the control sample. (**F**) Statistical analysis of GFP-positive moDCs determined by flow cytometry (**G**) Analysis of Lipofectamine and LNP toxicity in moDCs by assessing cell survival in response to varying amounts of vaccine mRNA. 1% DMSO was used as a positive control for cell death. For (**F**) and (**G**) Data are mean ± sd (n=3 biological replicates).

Given that the success of our *ex vivo* mRNA vaccine is also determined by the proportion of cells transfected, we further analyzed transfection efficiency at single-cell level using flow cytometry. For this moDCs were transfected for 24h with the same mRNA used during fluorescence microscopy, and a threshold for GFP-positive cells was set according to the fluorescence distribution of the mock-transfected control to asses GFP expression. We observed a notable shift in fluorescence of transfected moDCs compared to mock-transfected cells (Fig. 3.4 E). On average, 87% of moDCs were classified as GFP-positive, demonstrating that the majority of moDCs were efficiently transfected by lipofectamine (Fig. 3.4 F). Although lipofectamine is known to efficiently deliver mRNA its possible toxicity which induces cell death in particular to more sensitive primary cells was still a concern (274). To ensure that lipofectamine does not cause extensive cell death, we performed a cell survival assay 5h post-transfection with our fully m1Ψ-modified mRNA (Fig. 3.1 A lower schematic), again encoding GFP. We transfected moDCs to varying amounts of mRNA and compared lipofectamine to transfections with LNPs or 1% DMSO, a known inducer of cell death. While we detected a marginal drop in cell viability with increasing amounts of mRNA for LNPs (96% to 94%), cell survival post-lipofectamine transfection remained constant at around 92% independent of the mRNA amount (Fig. 3.4 G). Lipofectamine only showed marginally higher toxicity than LNPs and by far lower toxicity than the 1% DMSO control, which reduced cell viability to 75% (Fig. 3.4 G).

Collectively these data imply that lipofectamine efficiently delivers mRNA to moDCs with minimal toxicity, thus, making it as a suitable vehicle to deliver the *ex vivo* mRNA vaccine.

3.4 m1Ψ modification differently affects expression yields and maturation of moDCs

Commonly mRNA vaccines utilize modified uridines, such as Ψ or m1Ψ, to enhance protein expression (126,181). However, recently published data suggest that unmodified mRNA might be even beneficial for circulating vaccines; it exhibits higher APCs maturation that increases the likelihood of epitope presentation (235). This raises the question as to whether the unmodified mRNA would also be beneficial for *ex vivo* vaccines by enhancing moDC maturation.

To explore this, we *in vitro* transcribed our mRNA (Fig. 3.1 A lower schematic) encoding RLuc with varying ratios of m1Ψ to uridine nucleotides (i.e. 100% m1Ψ, 50% m1Ψ, and 0% m1Ψ) for transfection of immature moDCs. After 24h we evaluated the maturation of moDCs by flow

cytometry following immunostaining of the two maturation markers CD86 and HLA-DR with fluorophore-coupled antibody. As a benchmark for the maturation of moDCs, we utilized a cocktail consisting of interleukin-1β (IL-1β), interleukinIL-6 (IL-6), tumor necrosis factor α (TNFα), and prostaglandin E2 (PGE2), commonly used for moDC maturation *in vitro* (275). Consequently, only moDCs that displayed comparable levels of CD86 and HLA-DR to cells treated with the maturation cocktail for 24h were classified as mature. Flow cytometry analysis revealed shifts in cell distribution dependent on the m1Ψ content of the mRNA (Fig. 3.5 A-E). Cells that were transfected with unmodified mRNA were predominantly located in the upper right quadrant, representing mature cells (Fig. 3.5 C), whereas moDCs transfected fully m1Ψ-modified mRNA were primarily observed in the lower left quadrant indicating immature cells (Fig. 3.5 E). Statistical analysis of moDC maturation confirmed this trend (Fig. 3.5 F). Fully m1Ψ-modified mRNA transfected moDCs showed the lowest percentage of maturation with only 19%, which was comparable to mock-transfected controls (Fig. 3.5 F). In contrast, partially m1Ψ-modified and unmodified mRNA increased maturation to 55% and 67%, respectively (Fig. 3.5 F). Overall the highest maturation was achieved with the maturation cocktail, with 92% of cells being classified as mature (Fig. 3.5 F). This result suggests that a high proportion of unmodified uridines in the mRNA enhances moDC maturation *in vitro.*

While unmodified mRNA promotes moDC maturation, it may reduce vaccine efficacy by decreasing the protein expression, consequently decreasing the likelihood of epitope processing and presentation. To investigate the impact of unmodified uridines on protein expression in the context of our *ex vivo* mRNA vaccine, we transfected our mRNA (Fig. 3.1 A lower schematic) encoding Rluc, which was transcribed with varying proportions of m1Ψ-modification into immature moDCs. We observed that the level of m1Ψ-modification markedly influences RLuc expression (Fig. 3.5 G). Compared to unmodified mRNA, the fully m1Ψ-modified mRNA displayed a 4.9-fold increase in protein expression, whereby the partially m1Ψ-modified mRNA displayed intermediate protein expression (Fig. 3.5 G) suggesting that m1Ψ-modification enhances expression.

Collectively, these data suggest that while unmodified mRNA enhances the maturation of moDCs, it has much lower expression than fully m1Ψ-modified mRNA. However, higher levels of mature moDCs can be achieved *in vitro* by a maturation cocktail without compromising protein expression. Due to the trade-off between maturation and protein expression, fully modifying mRNA and promoting maturation with specific maturation factors seems to be the more viable strategy for *ex vivo* vaccines.

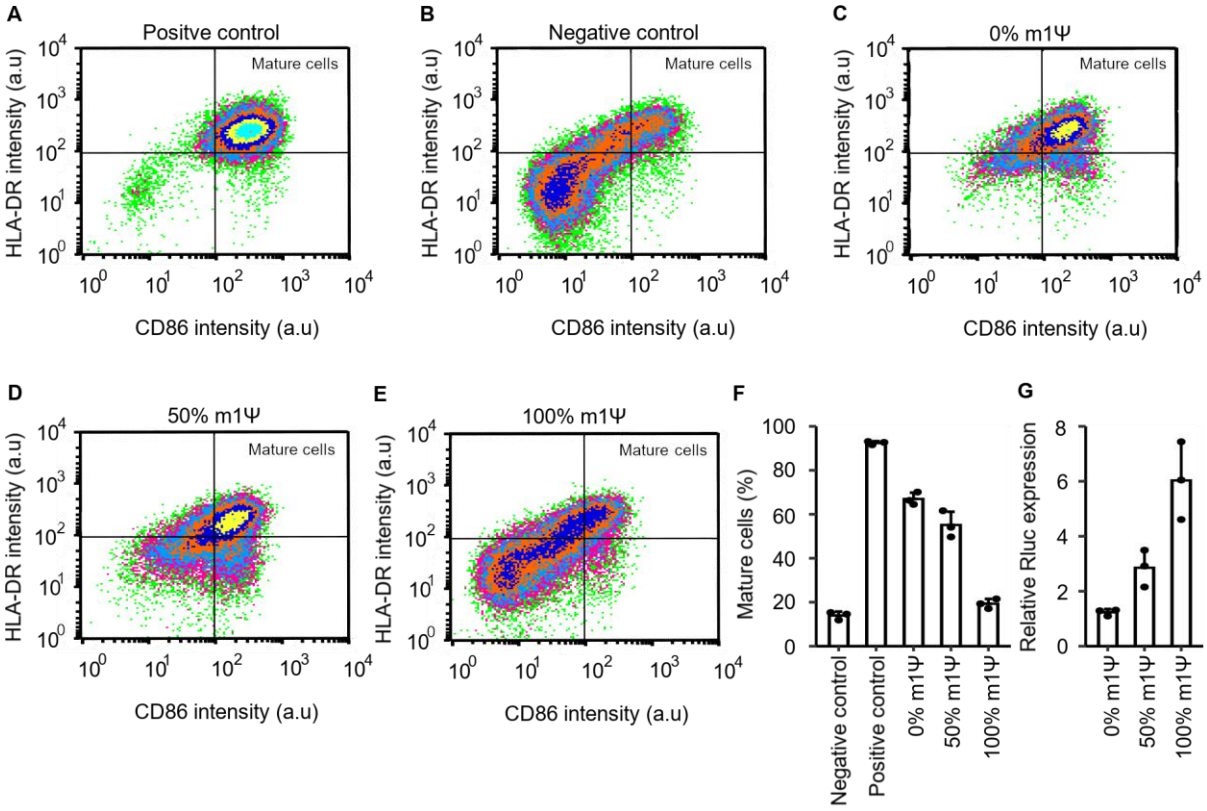


Figure 3.5 m1Ψ modification increases protein expression but reduces maturation of moDCs. (**A-E**) Representative flow cytometry analysis of the moDC maturation markers CD86 and HLA-DR after mRNA transfection with different m1Ψ ratios or treatment with cytokine maturation cocktail as positive control. Thresholds for quadrants were determined according to the distribution of cells in the positive control. Cells in the upper right quadrant were classified as mature cells. (**F**) Statistical analysis of moDC maturation determined by flow cytometry. (**G**) Relative expression of RLuc normalized to FLuc in moDCs after mRNA transfection with different m1Ψ modification ratios. For (**F**) and (**G**) data are mean ± sd (n=3 biological replicates).

3.5 Optimized mRNA vaccine does not provoke innate immunogenicity

The innate immunity plays a crucial role in the recognition of exogenous mRNAs (173). Activation of RLRs such as TLRs triggers the innate immune response, which in turn reduces overall mRNA translation (172). Thus, activation of TLRs by *ex vivo* mRNA vaccines should be avoided as it negatively affects translation and consequently reduces the efficacy. We therefore set out to investigate the innate immunity of our fully m1Ψ-modified mRNA (Fig. 3.1 A lower schematic). We first focused on TLR7 and TLR8 activation as these are specifically activated by ssRNA, consequently reducing overall translation (173). For this, we utilized two

cell lines HEK293XL hTLR7 and HEK293XL hTLR8. These cell lines, which were stably transfected with the human TLR7 or TLR8 genes, respectively, secret IL-8 upon TLR7/8 activation, thus making them a suitable reporter system for testing TLR7/8 activation (125). Protamine, commonly used to test the immunostimulatory effect of RNAs, was utilized to transfect our mRNA (276). Compared to R848, a potent TLR7/8 activator, the mRNA only marginally stimulated TLR7 and TLR8 to levels comparable to mock controls (Fig. 3.6 A ,B), implying that our fully m1Ψ-modified mRNA does not activate TLR7 or TLR8.

To verify that mRNA did not activate other TLRs present in moDCs, which could potentially reduce the efficacy of our vaccine, we transfected our mRNA into immature moDCs and after 24h quantified the release of interferon-alpha (IFN-α) and TNF-α, both of which are synthesized in response TLR activation (277). We additionally compared our mRNA to OD-2216, a potent TLR9 activator, which mimics the activation of TLR9 by unmethylated CpG DNA (278). Interestingly, R848 only led to TNF-α release while OD-2216 only caused IFN-α secretion (Fig. 3.6 C, D). However, in the case of both cytokines, our mRNA only marginally activated the immune response and released comparable levels of TNF-α and IFN-α to that of the mock controls (Fig. 3.6 C, D). Together these data indicate, that our fully m1Ψ optimized mRNA does not trigger a TLR-mediated immune response, emphasizing its potential as an effective *ex vivo* vaccine with high safety that does not trigger immune activation.

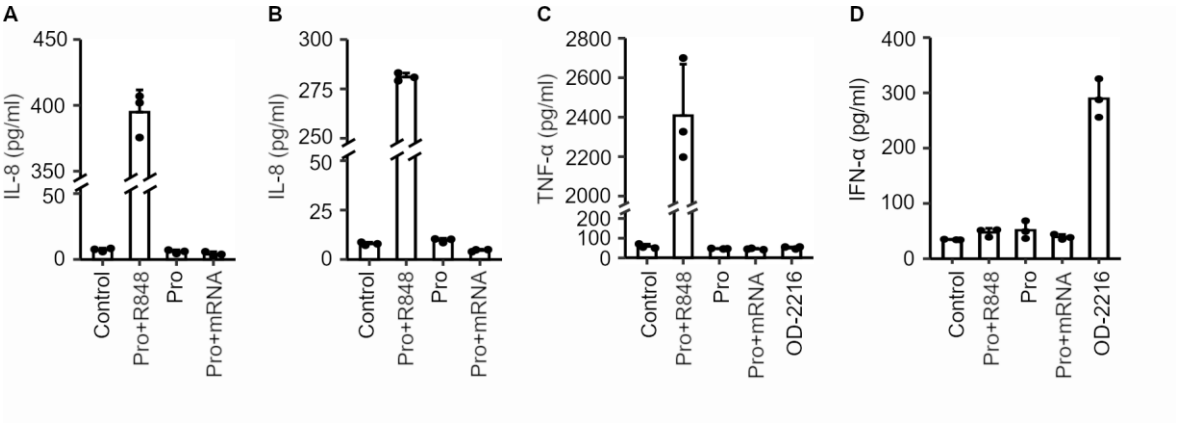


Figure 3.6 Optimized mRNA vaccine does not stimulate innate immunity response. ELISA analysis of TLR7 and TLR8 activation by assessing released IL-8 into the medium of HEK293XL TLR7 (**A**) and TLR8 (**B**) after protamine (Pro)-mediated mRNA transfection or treatment with the R848 activator. (**C**) Assessment of TNF-α levels in cell culture media after protamine-mediated mRNA transfection, treatment with the TLR7/8 activator R848 or the TLR9 activator OD-2216. (**D**) Analysis of IFN-α levels in cell culture media after protamine-mediated mRNA transfection, treatment with the TLR7/8 activator R848 or the TLR9 activator OD-2216. For (**A-D**) Data are mean ± sd (n=3 biological replicates).

3.6 Optimized mRNA vaccine demonstrates moderate in-cell stability

A key parameter of mRNA vaccines is their in-cell stability, which directly impacts their ability to maintain prolonged protein expression and thus, influences the overall vaccine efficacy. To assess the intracellular stability of our fully m1Ψ-modified mRNA (Fig 3.1 A lower schematic), we used HeLa cells which are better transfectable. 3h after transfection, cell culture media was replaced and total RNA was collected up to 24h after media replacement. The mRNA amount of mRNA was quantified using RT-qPCR, normalized to cell number to account for variations at each collection time point. To calculate the decay rate of our mRNA decay, we applied both an exponential decay model and calculated the decay velocity by the difference of mRNA transcript quantity measured at 0 and 24 hours. The results revealed that our fully m1Ψ-modified mRNA with optimized sequence exhibits a half-life ($t_1/_2$) of approximately 9-10 hours, indicating moderate stability (Fig 3.7). These data supports that our optimized mRNA maintains stability comparable to endogenous transcripts with a mean of 9 h (279).

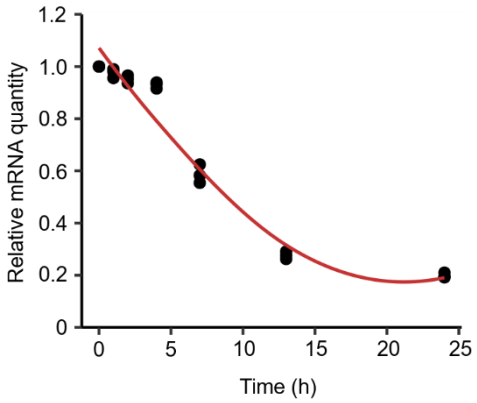


Figure 3.7 Decay kinetics of optimized mRNA vaccine. The stability of the optimized mRNA encoding GFP in HeLa cells was determined by RT-qPCR. 3h after transfection media was replaced and total RNA was first collected. Consecutive time points were normalized to mRNA levels at 0h. The red line represents exponential curve fit (R^2=0.94, exponential decay model). Decay rate for half-life calculations was determined by difference in mRNA transcript quantity at 0 and 24h (k=0.067) or by exponential decay model (k=0.076). Data are mean ± sd (n=3 biological replicates).

3.7 Antigen-encoding mRNA is processed to epitopes presented on the cell surface

While high intracellular antigen expression is crucial for *ex vivo* vaccine efficacy, it is insufficient by itself to trigger an immune response. The efficient antigen processing into

epitopes and their presentation on the cell surface to T-cells is crucial for efficacy. Overall the processing of antigens into epitopes and their binding to MHC receptors is a relatively inefficient process (157). Thus, we next tested the capability of the mRNA vaccine to produce epitopes. Due to the broad diversity of MHC allele combinations amongst human individuals and consequent binding preferences, it is hard to predict which epitopes are bound by a given MHC receptor, thus limiting the ability to directly measure the presence of epitopes on the cell surface. The epitope presentation is commonly assessed using the mouse-derived cell line EL4 (T lymphoblast) in combination with the model protein ovalbumin (OVA). Typically a peptide consisting of the amino acid from position 257-264 of OVA (amino acids SIINFEKL) serves as a model epitope, as it binds to the MHC receptor H-2Kb present in EL4 cells allowing for its detection on the cell surface by fluorescently labeled antibodies (280).

To investigate the capability of the mRNA to produce epitopes we transfected EL4 cells for 24h with our fully m1Ψ-modfied mRNA (Fig. 3.1 A lower schematic) encoding SIINFEKL and compared epitope presentation on the cell surface to mock-transfected controls, using flow cytometry with a fluorophore-coupled antibody. Post transfection, we observed a markable shift in SIINFEKL presence on the cell surface with a mean of 78% of cells classified as SIINFEKL positive (Fig. 3.8 A, B). This suggests, that our optimized mRNA leads to both antigen expression and subsequent processing to epitopes and cell surface presentation, further emphasizing its suitability as an *ex vivo* mRNA vaccine.

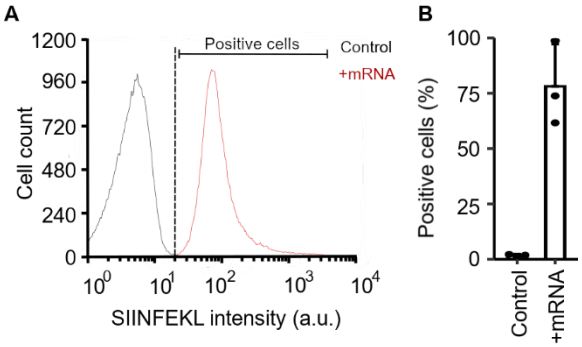


Figure 3.8 Optimized mRNA is capable to present epitope at cell surface. (**A**) Representative flow cytometry analysis of SIINFEKL-positive EL4 cells after transfection of SIINFEKL-encoding optimized vaccine mRNA. The dashed line represents the threshold after which cells were classified as SIINFEKL-positive. The threshold was determined by the fluorescence distribution of the control sample. Percentage of positive cells was determined by the number of SIINFEKL-positive cells/total number of cells. Increased SIINFEKL intensity corresponds to a higher number of epitopes on the cell surface. (**B**) Statistical analysis of SIINFEKL-positive EL4 cells determined by flow cytometry. Data are mean ± sd (n=3 biological replicates)

3.8 Selection of target antigens in endometrial cancer

Given that our optimized mRNA demonstrated to be a suitable approach for an *ex vivo* mRNA vaccine, we next sought to test its applicability as a vaccine in endometrial carcinomas. We first identified unique antigens present in endometrial cancers, which when inserted in our optimized mRNA would induce a robust immune response. For this, we used the data available in the Human protein atlas (https://www.proteinatlas.org/), which provides both RNA sequencing and immunohistochemistry data of collected tissue samples from a variety of tumors, including endometrial cancer. We designed a multi-step process with several criteria to filter for suitable antigen candidates for our *ex vivo* mRNA vaccine (Fig. 3.9).

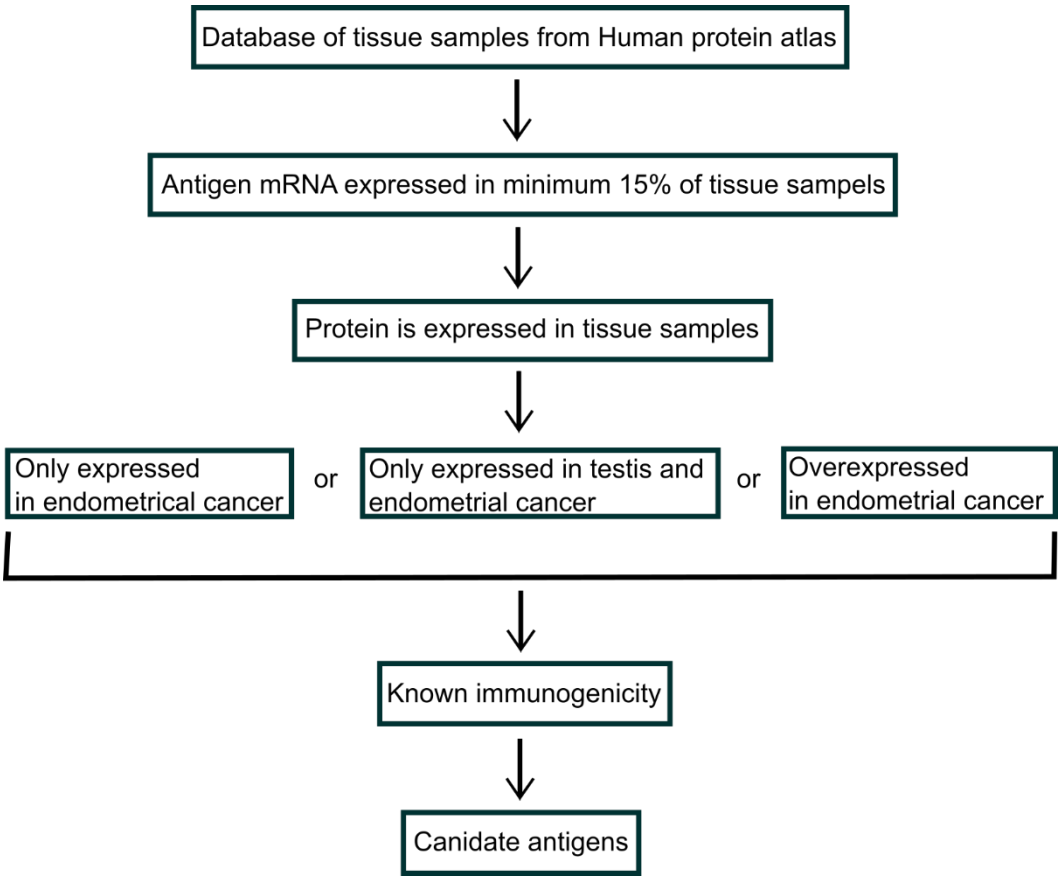


Figure 3.9 Flowchart of the selection process for candidate antigen. Potential antigens annotated in the Human protein atlas databank (https://www.proteinatlas.org/) were filtered by their mRNA and protein expression in endometrial cancers.

In the initial round of filtering, we focused on mRNA expression measured by RNA sequencing in the database. We selected transcripts that were expressed in a minimum of 15% of all

endometrial tumor samples, annotated in the database. This allowed us to eliminate antigens that are lowly expressed in endometrial cancer. Subsequently, we considered the protein expression in the immunohistochemical analysis. The candidate antigens had to be either exclusively expressed in endometrial tumor cells, overexpressed in endometrial cancer compared to adult healthy tissue, or only expressed in endometrial cancer and adult testis tissue, as the tissue is not present in females. At the final step in our selection process, we stratified the antigens using literature data that reports on the immunogenicity of the candidates. Proteins with known immunogenic properties were considered ideal candidates, as they are more likely to generate a strong T cell response.

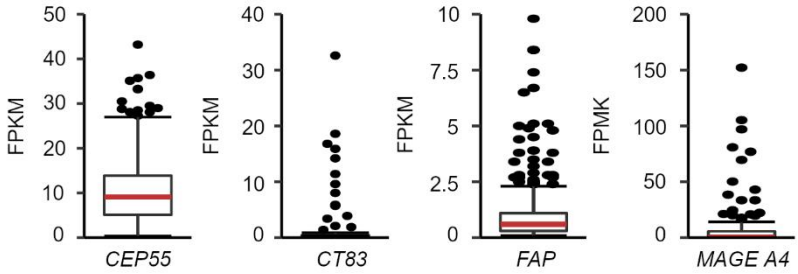
Using our multi-step selection process, we successfully identified four promising candidate antigens for potential use in our ex vivo mRNA vaccine, targeting endometrial cancer: Cancer/testis antigen 83 (*CT83*), melanoma-associated antigen 4 (*MAGE A4*), centrosomal protein 55 (*CEP55*) and fibroblast activation protein (*FAP*). Analysis of RNA sequencing data from the Human protein atlas database revealed that *CEP55* was the most consistently expressed mRNA amongst our selected candidates across all collected endometrial tumor samples (541 out of 541 samples) (Fig. 3.10 A). *FAP* closely followed with expression in 526 of the 541 samples, while M*AGE A4* and *CT83* had lower occurrences, being present in 153 and 95 samples, respectively (Fig. 3.10 A). When comparing fragments per kilobase of transcript per million mapped reads (FPKM) values, *CEP55* additionally displayed the highest median FPKM of 9.1 compared to the other three antigens, namely FPKM of 0.7 (*MAGE A4*), 0.6 (*FAP*), and 0.2 (*CT83*), respectively (Fig. 3.10 A). Overall, the mRNA expression of all candidate antigens varied broadly between individual tumor samples, particularly for *MAGE A4* with an FPKM up to 217-fold higher than its median expression (Fig. 3.10 A).

To assess the protein expression of our selected antigens in endometrial cancer, immunohistochemical images were classified according to the scoring system used in the Human protein atlas, which combines staining intensity and fraction of positive cells to determine the level of protein expression. CEP55 was the only protein detected in all tested samples in the database while FAP and MAGE4 were detected in 4 and 8 out of 12 samples, respectively (Fig. 3.10 B). While CEP55 is expressed in healthy tissue, it is highly overexpressed in endometrial cancer and is known to trigger an immune response in a variety of different tumors, and was therefore chosen as a potential candidate (281,282). MAGE A4 expression is restricted testis together and its high immunogenicity has been demonstrated previously (283,284). Thus, we included it as a potential target antigen. FAP was included as a potential candidate due to its lack of expression in healthy tissue and its known capability to stimulate an immune response when incorporated into a vaccine for cancer immunotherapy (285,286). For *CT83* no immunohistochemical data in endometrial cancer was available, however, given its known immunogenetic potential and restriction to germ cell expression we

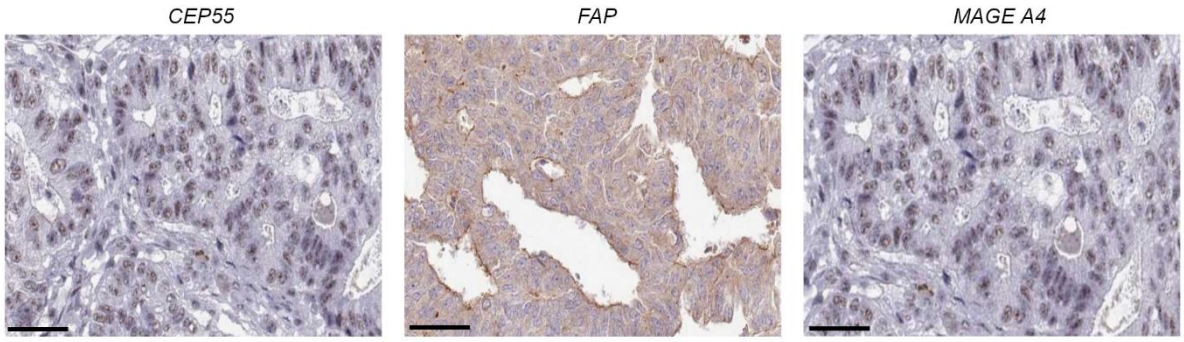
decided to include it as a potential candidate antigen (287,288). Collectively this multiple-step selection process allowed us to identify *CT83*, *CEP55*, *FAP* and *MAGEA4* as potential candidate antigens for our *ex vivo* mRNA vaccine.

A

Antigen	Expression detected	No expression detected
CEP55	541	0
CT83	95	446
FAP	526	15
MAGE A4	153	388



B



Antigen	Not detected	Low	Medium	High
CEP55	0	7	5	0
CT83	N/A	N/A	N/A	N/A
FAP	6	2	2	0
MAGE A4	4	8	0	0

Figure 3.10 Expression profiles of the candidate antigen. (**A**) Summary of tissue samples annotated in the human protein atlas database that express the antigen mRNAs. Boxplots visualize the transcript expression levels of tissue samples positive for *CEP55* (n=541), *CT83* (n=95), *FAP* (n=526), and *MAGE A4* (n=153) measured by RNA sequencing. Box edges represent the 25% to the 75% percentile. The red line denotes the median value. Whiskers include the remaining data without exclusion of outliers. (**B**) Bright-field immunohistochemistry showing candidate antigen expression (blue spots) in endometrial cancer tissue. For *CT83* no immunohistochemistry data was available. Scale bar: 300µm. Table shows the score of immunohistochemical staining of candidate antigens (n=12). Protein expression score was determined by the intensity of staining and the fraction of stained cells. Data in (**A**) and (**B**) are derived from the human protein atlas database (https://www.proteinatlas.org)

3.9 Optimized mRNA encoding candidate antigens activate T cells

For an *ex vivo* mRNA vaccine to elicit a robust immune response, the encoded antigens must successfully activate T cells, in particular CD8+ T cells as these are key mediators of cytotoxic responses (28). Consequently, after identifying *CT83*, *CEP55*, *FAP*, and *MAGEA4* as potential antigen candidates, we focused on testing their immunogenetic potential in the context of our optimized *ex vivo* mRNA vaccine.

To assess their ability to elicit a T cell response, we performed co-culture experiments involving moDCs and CD8+ T cells (Fig. 3.11 A). Immature moDCs were transfected with fully m1Ψ-modified mRNA with optimized sequence (Fig. 3.1 A lower schematic) encoding the respective candidate antigens. To enable epitope presentation, after transfection, the moDCs were matured with maturation cocktails for 24h. To analyze their activation, CD8+ T cells were isolated from PBMCs of the same human donor and co-cultured with transfected mature moDCs at a ratio of 10:1 (T cells to moDcs).

We first chose to test T cell proliferation as a marker for the immunogenetic potential of our candidate antigens, as T cell activation causes clonal expansion of antigen-specific T cells (26). After 5 days, we compared the proliferation of CD8+ T cells of co-culture with antigen mRNA-transfected moDCs to a co-culture with mock-transfected moDCs. To measure proliferation, we performed flow cytometry with the fluorescence cell staining dye carboxyfluorescein succinimidyl ester (CFSE). CFSE allows for monitoring of cell proliferation, as it progressively dilutes during each cycle of cell division. Thus, reduced CFSE intensity is a readout of cell proliferation. Compared to the mock-transfected control, all four antigens displayed an increase in the number of low CFSE intensity T cells, corresponding to proliferating cells (Fig. 3.11 B-E). We detected marginal differences in the number of proliferating cells between the four candidate antigens, namely 17.3% (*FAP*), 16,3% (*CEP55*), 16,4% (*MAGE A4*), and 15.7% (*CT83*) (Fig 3.11 F). This suggests that the four selected antigens possess a similar capability for evoking antigen-specific T-cell proliferation in the context of our *ex vivo* mRNA vaccine.

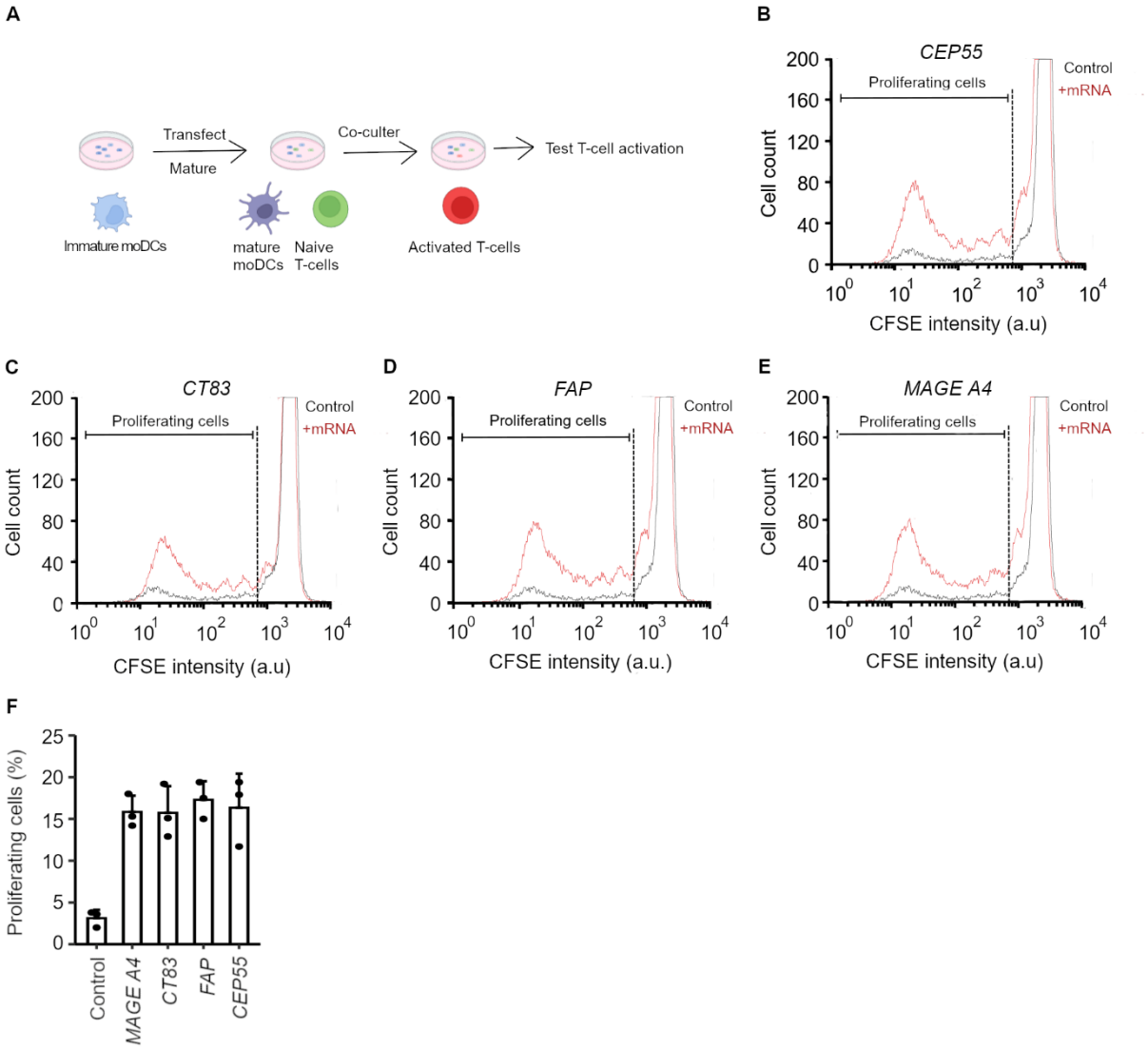


Figure 3.11 mRNAs encoding candidate antigens evoke T-cell proliferation. (**A**) Overview of experimental approach for assessing T-cell activation. (**B-E)** Representative flow cytometry analysis of T-cell proliferation of co-culture with moDC expressing each antigen-encoding mRNA. Co-culture was performed for 5 days. CFSE intensity is reduced with every round of cell division. The dashed line represents the threshold after which cells were classified as proliferating. The threshold was determined by the cell distribution of the control sample. (**F**) Statistical analysis of proliferating T cells determined by flow cytometry. Data are mean ± sd (n=3 biological replicates).

To further validate the immunogenetic potential of the selected antigens, we chose to test for three cytokines that are released upon T-cell activation, i.e. interferone-γ (IFN-γ), interleukin-2 (IL-2), and TNF-α (26). Using ELISA, we analyzed the cytokines in cell supernatants of CD8+ T cells co-cultured with mature antigen mRNA-transfected moDCs for 5 days and compared them to a mock-transfected control. We observed a robust secretion of all three cytokines by T cells when co-cultured moDCs were transfected with antigen-encoding mRNA (Fig. 3.12 A-

C). No cytokines were released in the T cells co-cultured with mock-transfected moDCs (Fig. 3.12 A-C), corroborating the results from the proliferation assay. IFN-γ was the most secreted cytokine, consistent with its pivotal role in T cell mediated immune response (Fig. 3.12 C). *CT83* consistently displayed the highest levels of cytokine release while *MAGE A4* had the lowest among the four antigen candidates (Fig. 3.12 A-C).

Collectively, these data demonstrate the ability of our optimized mRNA to trigger a T-cell response when expressing our candidate antigens further highlighting its potential to be used as an *ex vivo* mRNA vaccine.

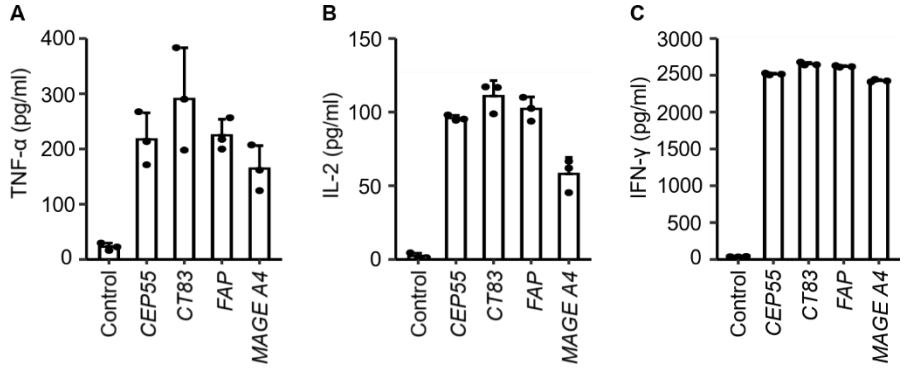


Figure 3.12 mRNA encoding candidate antigens stimulate cytokine release of T cells. ELISA analysis of T-cell activation assessed by TNF-α (**A**), IL-2 (**B**) and IFN-γ (**C**) levels in cell culture media of T-cell and moDCs co-cultured for 5 days. Data are mean ± sd (n=3 biological replicates).

3.10 Validation of antigen candidates in endometrial cancer patients

The presence of the four selected antigen candidates in pathology samples from surgically removed endometrial cancers is currently being analyzed by Prof. Dr. Thomas Kalinski and Martha Dierks (Institute for Pathology, Universitätsklinikum Brandenburg an der Havel, Germany). The tumor tissue from 30-300 patients has been subjected to immunohistochemical staining for *CT83*, *CEP55*, *MAGE A4*, and *FAP*. Current analysis revealed that *MAGE A4* and *FAP* are only expressed at different levels, while *CT83* and *CEP55* are not (personal communication by Prof. Dr. Thomas Kalinski and Martha Dierks; the detailed analysis will be published in the PhD thesis of Martha Dierks). This demonstrates that two of the selected antigens will serve as lead candidates for an mRNA vaccine to combat endometrial cancer.

4. Discussion

The efficient treatment of advanced-stage is still challenging, with conventional therapies, such as chemotherapy and radiotherapy, being the current standard of care. Here, we develop an optimized mRNA-based *ex vivo* vaccine capable of addressing the need for more efficient treatment.

For the development of our mRNA vaccine, we initially focus on optimizing two key elements of the mRNA sequence: the 5'UTR and the stop codon.

We observe that incorporating the 5'UTR of alpha-globin leads to the highest expression in both HeLa cells and moDCs, compared to various other 5'UTRs, including that of beta-globin 5' UTR, which is commonly utilized in mRNA vaccines (145). The analyzed 5'UTRs affect the protein expression across the two cell types to a different extent. However, the relative order of their influence, from highest to lowest expression, remains consistent. This observation aligns with previous reports, that 5'UTRs modulate protein expression across different cell lines in a similar manner (289,290). Alpha-globin is highly expressed in human blood and immune cells, therefore investigating the effects of its UTRs is of particular interest for designing mRNA-based vaccines (291). The exact mechanism detailing how alpha-globin's 5' UTR boosts mRNA expression is not yet fully understood. Data from expression in yeast and mice cell lines suggest that stable secondary structures flanking the start codon reduce the overall polypeptide production by lowering translation efficiency (292,293). Computational prediction of possible secondary structures of the 5'UTR of alpha-globin revealed a comparable low minimal folding energy (294). This low folding energy decreases the probability of secondary structures forming and thus, the absence of secondary structures potentially plays a role in the efficient translation of alpha-globin. It is important to note, that mRNA variants used in our study were fully m1Ψ-modified, to increase protein yield (125,126). Although, data for the effect of m1Ψ on the secondary structure of mRNA is limited, multiple studies have investigated the influence of Ψ modification on secondary structure formation, which may exhibit similar effects to its analog m1Ψ. Ψ modification has been reported to impact secondary structure formation, as it stabilizes RNA duplexes by enhancing its binding strength to all four RNA nucleobases, compared to unmodified U, promoting dsRNA formation (295,296). Whether m1Ψ similarly promotes secondary structure formation still needs to be investigated, however, a recent molecular dynamics study has revealed that m1Ψ displays stronger base pairing and stacking interaction than Ψ, which could potentially promote and stabilize secondary structures (297). However, the potential for an increased propensity of secondary structure formation, due to uridine modification, might be reduced by alpha-globin having a relatively short 5'UTR, only 37nt compared to a median 5'UTR length of

approximately 210nt in humans (298). This short 5'UTR reduces the likelihood of secondary structures forming. Consistent with the hypothesis, that the length of the 5'UTR impacts the potential of secondary structure formation and thus, influences polypeptide production, we observed the highest protein expression, when the 5'UTR of alpha-globin was incorporated into our mRNA, which was the shortest amongst all 5'UTR compared in this work. We found that the half-life of our optimized mRNA is 9-10h. This is comparable to the reported median half-life of 9h for endogenous mammalian mRNA, which has been previously determined using mouse fibroblasts (279). Other mRNA vaccines have demonstrated half-lives spanning from 28h-36h (299,300). Since the mRNA sequences of these vaccines are not publicly disclosed, it is not feasible to assess which specific modifications in their structural elements might enhance mRNA stability. Furthermore, it is important to note that these mRNAs were tested under *in vivo* conditions, making a direct comparison is challenging, as other factors such as tissue context or immune response-mediated RNA cleavage could influence mRNA stability (299,301). For instance, in a study investigating an mRNA vaccine targeting H10N8 influenza viruses in mice, the half-life of the mRNA showed significant variability across different tissues, with values ranging from 3.5 hours in heart tissue to 28 hours in distal lymph nodes (299). Additionally, *in vivo* mRNA vaccines are commonly delivered by LNPs, which are internalized by receptor-mediated endocytosis. mRNA release from endosomes is usually inefficient, thus the measured mRNA level includes mRNAs that are trapped in endosomes and are not actively translated (227,302). Given that ribosome loading on the mRNA affects its stability, this could skew stability measurements (143). The steady-state protein levels are proportional to the mRNA abundance, and would imply that increased half-life will boost protein expression (303). However, recent data also indicates that stability inversely correlates to ribosome load, which in turn argues that high stability does not necessarily lead to the highest protein yield (146,147). This trade-off needs to be considered when optimizing the mRNA sequence and prioritization is dependent on the vaccine strategy. For a circulating mRNA vaccine extended mRNA stability is essential, as the mRNA first needs to be delivered to its intended target cells before translation can occur. Degradation of mRNA during this process can potentially lead to an insufficient immune response. Additionally, high mRNA stability allows for prolonged antigen production and sustained epitope presentation by APCs. Since APCs need to migrate to lymph nodes to interact with T cells—a process that can take up to 3 days—prolonged stability is crucial to achieve a sufficient activation of T cells (304). In contrast, for *ex vivo* vaccines, mRNA transfer into cells and interaction between APCs and T cells can be more precisely controlled and modulated. For this approach, the priority should be on achieving a high protein yield within a short time frame to maximize epitope presentation. This increases the likelihood for activating a sufficient number of T cells, as mRNA is directly transferred into cells, and T cells are co-cultured with APCs approximately 24h post mRNA transfection.

Our study further shows that modified uridines, commonly used as stabilizing nucleotides, markedly increase stop codon readthrough in a stop codon identity-dependent manner. Overall the stop codon ΨGA(C) exhibits the highest, as opposed to m1ΨAAm1ΨAA(C) with the lowest levels of readthrough. This finding corroborates previously reported data, that indicate that ΨGA is generally the most susceptible to readthrough (207). Thus we propose that a tandem-stop codon m1ΨAAm1ΨAA should be used in mRNA vaccines to avoid any readthrough and subsequent formation of unwanted neoepitopes (269). We show that the inclusion of a purine as the first nucleobase downstream of the stop codon (+4 nt) increases termination efficiency when stop codons are modified with m1Ψ, but not with 5moU or Ψ. Consistent with our findings, Ψ-mediated readthrough has been reported to be independent of the +4nt (207). Hence, while Ψ, 5moU, and m1Ψ increase susceptibility of the stop codon to readthrough, they show clear differences. Although there is a lack of data for 5moU, discrepancies between Ψ and m1Ψ in RNA duplex stability and bond formation, attributed to the additional methyl group, have been reported previously and could serve as a potential explanation for the observed differences in termination efficiency (297,305). m1Ψ is predicted to have stronger base pairing and stacking interaction compared to Ψ, stabilizing duplex structures (297). Additionally, unlike Ψ, m1Ψ is predicted not to form non-canonical base pairs (305). For Ψ it is suggested that non-canonical base pairing could allow translation to proceed (169,306). The crystal structure of the bacterial 30s ribosomal subunit bound to ΨAG revealed a formation of two purine-purine base pairs following the Ψ-A base pair (169). This in turn can stabilize the codon-anticodon interaction to favor readthrough over termination. Additionally, due to the increased base rotation allowing N1 and N3 amino protons to become hydrogen donors, Ψ itself can engage in non-canonical base pairing (295). This further strengthens the notion that the enhanced binding capability of near-cognate tRNA facilitates readthrough. However, as mentioned before, due to the additional methyl group, m1Ψ loses the ability to form a hydrogen bond at the N1 position (305). This is predicted to eliminate the universal base pairing ability observed for Ψ, instead forming the classic Watson-Crick base pairing (305). Thus, it remains unclear whether m1Ψ would also enhance the binding strength to near cognate tRNA, albeit not by direct bond formation with non-canonical bases but by unusual base pairing following the m1Ψ. Other factors such as increased dwelling time of the ribosome at the stop codon, e.g. by the formation of secondary structures could also serve as an explanation for the observed decrease in termination efficiency, however, the precise mechanism by which m1Ψ facilitates readthrough remains elusive (307,308).

In this study, we demonstrated that LNPs should not be used for *ex vivo* mRNA vaccines. LNPs have been used effectively for circulating mRNA vaccines (124). However, they have limited efficacy in *in vitro* systems (e.g. isolated cells), and efficiency largely varies among cell types (309). The release from the endosome is a limiting factor for LNP delivery efficiency and

is reported to depend on the changes that the ionizable lipid is subjected to due to the endosomal environment (221). Thus, cell-to-cell variations in endosomal properties could serve as an explanation for differences amongst cell lines. Such variations in endosomal properties, particularly pH, which can range from 5.4 to 6.2, have been reported previously (310–312). Moreover, LNPs are internalized through different endocytic mechanisms, dependent on the cell type, which in turn affects the endosomal properties (302). Corroborating previously reported cell-to-cell differences, we observed an efficient delivery of LNP-encapsulated mRNA to HeLa cells, however, LNPs had limited efficiency for delivering mRNA to moDCs. The key advantages for LNPs *in vivo* are their ability to target specific tissues, which is essential for ensuring that the mRNA reaches its target cells, and their role in reducing adverse immune effects (313,314). However, in *ex vivo* vaccine applications, mRNA is directly introduced into APCs *in vitro* eliminating the need for targeted tissue delivery. Since the cells are outside the body, potential adverse immune effects are also not a concern. Therefore and in light of our results, we instead propose the use of lipofectamine as a delivery tool for *ex vivo* vaccines, which showed efficient delivery to moDCs in our study. However, it is important to note that when scaling up an *ex vivo* vaccine, i.e. to an industrial scale, lipofectamine becomes impracticable, due to the large quantity required. Thus, for industrial scale, LNPs may still serve as a viable delivery option provided further optimization is achieved to enhance delivery efficiency.

Unmodified mRNA is beneficial for circulating mRNA vaccines, as it leads to higher APCs maturation, increasing the likelihood of epitope presentation (235). However, we propose for an *ex vivo* vaccine to use fully m1Ψ-modified mRNA. Our analysis on the effect of m1Ψ modification on protein expression in moDCs revealed a marked drop in expression, when unmodified uridines were used in the IVT of mRNA. This aligns with previously reported data, further demonstrating the importance of uridine modification on the translation of exogenous mRNAs and thus, further supporting the notion of using fully m1Ψ-modified mRNAs (125,126,179,180,270). Uridine modifications prevent TLR-mediated suppression of translation by inhibiting PKR activation and subsequent eiF2α phosphorylation, thereby reducing the innate immunogenicity of exogenous mRNAs (125,180). Corroborating previous reports, we also did not observe any TLR activation in moDCs when administering fully m1Ψ-modified mRNA. However, high expression alone might not be sufficient to activate T cells, due to a low yield of APC maturation. Indeed, when we compared mRNAs with different levels of uridine modification m1Ψ markedly reduced moDC maturation. However, because of manipulations performed *ex vivo*, this can be circumvented by using a cocktail of maturation factors to boost APC maturation. This supports the idea that unmodified mRNA, which engages PRRs, might be beneficial for circulating vaccines, while for the *ex vivo* approach, APC maturation can be modulated *in vitro*, and thus, maximizing protein expression

should be prioritized.

Currently, immunotherapy in endometrial cancer has predominantly focused on Wilms tumor protein encoded by *WT1* as a possible target antigen (315). This is due to its overexpression in up to 79% of endometrial carcinomas, making it a promising candidate for therapeutic intervention (316). Utilizing a multi-step selection process and data from the Human protein atlas we selected four new antigens as possible targets for an mRNA-based vaccine: *CT83*, *MAGE A4*, *CEP55*, and *FAP*. Two of them namely, *CT83* and *MAGE A4*, are classified CTAs which is particularly interesting for gynecological tumors in general, as they are restricted to testis expression, subsequently reducing the risk of off-target effects. *MAGE A4* is part of the melanoma-associated antigen A (MAGE A) family (*MAGE A1*, *A2*, *A2B*, *A3*, *A4*, *A5P*, *A6*, *A8*, *A9*, *A10*, *A11*, *A12*). Expression of MAGE A proteins is associated with poor survival, resistance to chemotherapy, and metastasis, thus making them an interesting target for immunotherapy (317–320). Indeed, several ongoing clinical trials for cancer treatment, such as melanoma and neuroblastoma utilize MAGE A proteins as targets (321–324). However, these clinical trials mainly investigate the potential of *MAGE A1* and *MAGE A3* in combating tumors. For example, *MAGE A1* and *MAGE A3* have been investigated as potential antigen targets in a phase I trial for patients suffering from neuroblastoma, Ewing's sarcoma, osteosarcoma, or rhabdomyosarcoma, as part of a combinational peptide vaccine (321). Immunotherapy targeting *MAGE A4* has, to date, only garnered limited attention and focused primarily on adoptive cell therapy for solid tumors, such as lung, ovarian, and urothelial tumors (325,326). For example, in a phase I trial *MAGE A4* has been investigated as a potential CAR-T cell target for patients suffering from solid tumors, including ovarian, head, and neck cancer (325). This limited attention is surprising given that *MAGE A4* has been observed to be aberrantly expressed in various cancers, such as breast and lung cancer (327–329). Notably, *MAGE A4* has been associated with poor prognosis, e.g. in non-small cell lung cancer MAGE A4 expression correlates with reduced overall survival (328). In endometrial cancer, expression of MAGE A4 correlates with reduced disease-free and overall survival for patients with high-grade tumors (330).

in a variety of malignancies, *FAP* is not exclusively expressed in the tumor cells, but also identified predominantly in CAFs (331–333). CAFs play an essential role in immune evasion by impairing lymphocyte infiltration to the tumor site (77,78). Targeting CAFs in the TME would boost vaccine efficacy by counteracting the immunosuppressive activity of CAFs. Consistent with this idea, several studies in murine cancer models demonstrate that targeting FAP, and consequent depletion of CAFs, enhances anti-tumor activity and lymphocyte infiltration (334–337). For instance, a DNA vaccine targeting FAP significantly improved the overall survival of mice bearing colon cancer, highlighting its potential as a viable therapeutic target (337). The selection of a suitable antigen i.e. *MAGE A4* or *FAP*, for our mRNA-based vaccine,

depends on the patient's specific expression profile. If only one of the antigens is identified in the patient's tumor cells or CAFs, that antigen should be encoded by our mRNA vaccine. However, if both *MAGE A4* and *FAP* are expressed we propose a combinational therapy using a mixture of mRNAs encoding either *FAP* or *MAGE A4*. This approach will allow us to target both the TME and tumor cells simultaneously, potentially enhancing T cell infiltration, and thereby, improving the overall efficacy of the vaccine.

Encoding of either of the four antigens by our optimized mRNA, enabled transfected moDCs to activate CD8+ T cells. This activation was reflected by a clonal expansion of T cells, with proliferation ranging from 15-17%, and cytokine secretion. The marginal differences observed in T cell proliferation between the respective antigens suggest, that they have a similar capacity to elicit an immune response, reflecting their potential as possible candidate antigens. However, given that the MHC gene locus is highly polymorphic, the observed activation efficiencies would vary from individual to individual. Hence, the ability of a respective antigen to activate T cells will not be uniform across individuals – a variability that should be considered in the therapeutic application. *In vivo* patient-specific experiments could be useful for determining the T cell activation in each individual. The T-cell proliferation we observed of 15-17% is comparable to levels reported for other mRNA-based vaccines, ranging from 20-35% (341–343). Infiltration of a sufficient quantity of T cells into the TME is critical for vaccine efficacy, thus, increasing the number of antigen-specific T cells will enhance the likelihood of successful tumor clearance and should be a key focus in the anticancer vaccine development. The level of T cell activation and the amount of transfected mRNA into APCs have been shown previously to correlate with each other, thus suggesting that higher mRNA transfection yields in the moDCs would potentially enhance the fraction of proliferating cells (341). An additional expansion of antigen-specific T cells in vitro following sorting of the activated ones may further help to achieve a sufficient number of T cells, required for eliminating tumor cells.

Collectively, this work provides evidence that by optimizing the mRNA designs higher protein expression can be achieved and readthrough reduced. Incorporating modified nucleotides and utilizing a maturation cocktail enables the optimal activation of moDCs, which are then capable of inducing subsequent T cell activation. Thus, our work provides the foundation for the development of an mRNA-based *ex vivo* vaccine to target endometrial cancer.

5. Conclusion

Besides surgery, efficient treatment of endometrial cancer, particularly at advanced stages, poses a significant problem with rising mortality rates. This work provides the groundwork for combating endometrial cancer with an mRNA-based *ex vivo* vaccine. Identifying pivotal mRNA regions for vaccine development allowed for the design of an optimized mRNA sequence. Particularly, elucidating the impact of the 5'UTR and stop codon on protein expression and readthrough, respectively, gave an insight into how they influence vaccine efficacy. The incorporation of uridine modifications was observed to be pivotal for an mRNA-based *ex vivo* vaccine highlighting a key difference between an *ex vivo* vs. a circulating mRNA vaccine that needs to be considered when designing an mRNA-based vaccine. We further uncover four possible antigens present in endometrial cancer, of which *FAP* also allows for the potential to target the TME. This harbors the possibility of increased vaccine efficacy by enhancing T cell infiltration. While this work is limited by the lack of *in vivo* data it demonstrated the effectiveness of our designed mRNA of activating T cells, essential for an *ex vivo* vaccine and thus, provides the foundation for an *ex vivo* vaccine.

6. Material and Methods

RNA isolation and RT-PCR

Cell culture media was removed and cells were washed with 1x PBS. RNA was extracted with TRIzol reagent (Invitrogen, Germany), according to manufacturer protocol. In short 1ml of TRIzol reagent was added directly on to the cell culture dish and cells were harvested with a cell scraper. Lysed cells in TRIzol reagent were mixed with 0.2ml chloroform/isoamyl alcohol 24:1 (Invitrogen, USA). After centrifugation, the aquatic phase was transferred into a fresh microcentrifuge tube. RNA was precipitated by adding 1µl glycogen (Thermo Fisher Scientific), 0.1 Vol. 3M NaOAc and 100% isopropanol and incubation at -80°C for 30min. The precipitated RNA was washed with 80% ethanol and resuspended in DEPC-H_2O. Quality and quantity of total RNA was assessed on the DS-11+ Spectrophotometer (DeNovix, USA).
For cDNA synthesis 1µg of total RNA was subjected to DNAse I (Thermo Fisher Scientific, Germany) treatment, according to the manufacturer's protocol. Half of the reaction volume was then processed for RT-PCR using the oligo(dt)18 primer (Thermo Fisher Scientific, Germany) and RevertAid H Minus reverse transcriptase (Thermo Fisher Scientific, Germany) according to the manufacturer protocol

Quantitative RT-PCR

mRNA levels were analyzed by quantitative RT-PCR (q-RT-PCR) using the SensiMix SYBR Hi-ROX Kit (Bioline, USA), according to manufacturer protocol. Briefly, cDNA was mixed with the corresponding q-RT-PCR primers and the SensiMix SYBR Hi-ROX mix. q-RT-PCR was then conducted on the T Professional thermocycler (Biometra, Germany) with a maximum of 40 cycles. Technical duplicates of each biological replicate reaction were carried out for each sample.

Overlap PCR

For connecting two DNA fragments the overlap PCR method was applied. To join two DNA fragments complementary overhangs of 17-19 bp were added to the 5’ and 3’ ends, respectively, by PCR. 0.2 pmol of each fragment were then mixed for overlap PCR. Before primers were added 18 cycles of PCR allowed for hybridization and amplification of the joined DNA fragment. PCR products were subsequently purified by agarose gel electrophoresis.

mRNA design and cloning

To optimize the mRNA for protein expression and epitope presentation experimental data from previous literature was summarized and an optimal mRNA sequence was determined which will be referred to as optimized mRNA. To generate a DNA template for *in vitro* transcription the polyA tail, linkers and 5'UTRs were purchased as oligonucleotides (Microsynth, Switzerland). The remaining parts of the mRNA were amplified from the total RNA of either Hela cells or PBMCs. Individual parts of the DNA template were connected by overlap PCR and the T7 promotor sequence 5' TAATACGACTCACTATAAG 3' was added via PCR at the 5' end. The final DNA template sequences were cloned in the commercially available vector pGL4.51[luc2 CMV Neo] (Promega, Germany) for *in vitro* transcription. If not stated otherwise all DNA templates harbored a UAAUAA stop codon.
To assess the effect of stop codon identity on readthrough oligonucleotides were purchased. These oligonucleotides consisted of either the stop codons UGA(C), UAA(C), UAA(A), UAAUAA(C) or a GGA codon flanked by 33 bp upstream and 3 bp downstream of the optimized mRNA sequence. Oligonucleotides were amplified by PCR and cloned into the pSGDlucV 3.0 vector (338) (Addgen, USA) for *in vitro* transcription. The resulting sequences will be referred to as readthrough reporter mRNA.
All DNA template sequences for *in vitro* transcription are listed under the section 8.

In vitro transcription of mRNA and quality assessment

DNA template plasmids for optimized mRNA were digested with SapI (New England Biolabs, Germany) for 15 min at 37 °C. Linearized template plasmids were purified with Monarch PCR&DNA clean-up kit (New England Biolabs, Germany).
For *in vitro* transcription of optimized mRNA, the HiScribe T7 mRNA Kit with CleanCap Reagent AG (New England Biolabs, Germany) was used allowing for co-transcriptional capping with CleanCap. *In vitro* transcription was conducted according to the manufacture protocol for 4h with 1µg of linearized plasmid as a template input. If not stated otherwise all uridines were replaced by m1Ψ (Jena Bioscience, Germany). *In vitro* transcribed mRNA was purified and eluted in 30 µl using the Monarch RNA Cleanup Kit (New England Biolabs, Germany).
DNA template plasmids for readthrough reporter mRNA were digested with XbaI (Thermo Fisher Scientific, Germany) for 15 min at 37 °C. Linearized template plasmids were purified with Monarch PCR&DNA clean-up kit (New England Biolabs, Germany).
For *in vitro* transcription of readthrough mRNA, the HighYield T7 ARCA mRNA Synthesis Kit (Jena Bioscience, Germany) was used allowing for co-transcriptional capping with ARCA. *In*

vitro transcription was conducted according to the manufacture protocol for 4h with 1 µg of linearized plasmid as a template input. For respetive mRNAs uridines were replaced by m1Ψ, Ψ or 5moU (Jena Bioscience, Germany). *In vitro* transcribed mRNA was purified and eluted in 30µl using the Monarch RNA Cleanup Kit (New England Biolabs, Germany).
The quantity and quality of the mRNA were assessed using the Agilent RNA 6000 nano kit on the Agilent 2100 Bioanalyzer system according to manufactures instructions.

LNP formulation and characterization

Dlin-MC3-DMA, 1,2-Dimyristoyl-sn-glycero-3-methoxypolyethylene glycol (DMG-PEG 2000), and 1,2-dioleoyl-sn-glycero-3-phosphoethanolamine were purchased from Biomol (Germany). Cholesterol was purchased from Sigma Aldrich. Lipids were eluted in 100% Ethanol to a stock concentration of 20mg/ml. For LNP formulation the NanoAssemblr Spark (Precision Nano Systems, Canada) was used. 22 µg of mRNA in DEPC H_2O were eluted in 200 mM Citrate buffer pH=4 to a total volume of 40 µl with a buffer strength of 66.5 mM. The required amount of for Dlin-MC3-DMA was calculated for an N:P ratio of 4:1 and lipids were accordingly mixed to a 50:38.5:10:1.5 molar ratio (Dlin-MC3-DMA:Cholesterol:DOPE:DMG-PEG 200) in a total volume of 20 µl. Lipids and mRNA were mixed with the NanoAssemblr Spark using setting 3 and diluted with 180 µl 1x PBS.
20 µl of LNPs in 1x PBS were subjected to DLS measurements using the SpectroSize 300 (Molecular Dimensions, UK). 20 individual measurements were used to determine LNP radius.
To evaluate encapsulation efficiency of LNPs 1 µl of LNPs in 1xPBS were diluted in 9 µl of 1% Triton and heated for 10 min at 37°C to break open LNPs. Subsequently, the mRNA concentration after LNP denaturation was determined by fluorescence measurement using the Quibit RNA assay kit (Thermo Fisher Scientific, Germany) according to manufacturer protocol. Total amount of mRNA after release from LNPs was compared to unencapsulated mRNA in the LNP PBS mixture to determine encapsulation efficiency.

Cell lines and growth conditions

HeLa cells (CCL-2) and EL4 cells (TIB-3) were acquired from ATTC. HeLa cells were cultured in Dulbecco´s Modified Essential Medium (DMEM, Pan Biotech, Germany) with 10% fetal bovine serum (FBS, Pan Biotech, Germany) at 37°C, 5% CO_2. EL4 cells were cultured in RPMI 1640 (Pan Biotech, Germany), 10% FBS, and 2mM L-glutamine (Thermo Fisher Scientific, Germany) at 37°C, 5% CO2. HEK293XL hTLR7/hTLR8 cell lines were purchased from InvivoGen and cultured in DMEM, 10%FBS and 2mM L-glutamine at 37°C, 5% CO_2.

PBMC isolation

Buffy coats for PBMC isolation were kindly provided by Dr. Maria Geffken from the department of transfusion medicine, UKE, Hamburg, Germany. PBMCs were isolated using the Ficoll-Paque PLUS density gradient method. Briefly, buffy coats were diluted with equal amounts of 1x PBS and layered on top of Ficoll-Paque PLUS density gradient media (Cytiva, USA). After 20 min of centrifugation at 760 xg the PBMC layer was transferred into a new conical tube and washed four times with 1x PBS. After isolation, PBMCs were counted and frozen in 10% heat-inactivated FBS, 10% DMSO (Sigma Aldrich, Germany) until further use.

Monocyte isolation and differentiation to immature moDCs

Monocytes were isolated from PBMCs utilizing human CD14 MicroBeads (Miltenyi Biotec, Germany) following the manufacture protocol for magnetic separation. After separation, monocytes were cultured in RPMI 1640 supplemented with 10% heat-inactivated FBS and 2 mM L-glutamine at 37 °C, 5% CO_2. For differentiation into immature moDCs IL-4 (250 U/ml, Miltenyi Biotec, Germany) and GM-CSF (1000 U/ml, Miltenyi Biotec, Germany) were added directly into the cell culture media. After 48h cells were restimulated by repeated addition of IL-4 and GM-CSF. On day 5 immature moDCs were harvested for downstream experiments.

CD8+ T cell isolation and expansion

CD8+ T cells were isolated from PBMCs utilizing the human CD8+ T cell Isolation Kit (Miltenyi Biotec, Germany) following the manufacturing protocol for magnetic separation. After separation, T cells were cultured in ImmunoCult- XF T cell Expansion Medium (STEMCELL Technologies, France) with 10% heat-inactivated FBS at 37 °C, 5% CO_2. Expansion of T cells was achieved by supplementing the cell culture overnight with 5 ng/ml of human recombinant IL-7 (STEMCELL Technologies, France). On the next day CD8+ T cells were harvested for downstream experiments.

ELISA assay

All cell culture media supernatants were stored at -80 °C until analysis. Levels of cytokines were measured utilizing ELISA Flex kits (Mabtech, Sweden) following manufacturer instructions. Briefly, high-binding 96-well microplates were incubated with capture mAb diluted in 1x PBS overnight. Cell culture media supernatants were diluted 3:1 with incubation buffer.

96-well plates were washed and blocked for 1h. After a subsequent wash diluted samples and standards were added onto the plate for 2h at room temperature in duplicates allowing for antigen capturing. Plates were further washed and the detection mAB was added. After 1h plates were washed and Streptdavin-ALP was added for another hour. Following the last wash plates were incubated with pNPP substrate. After 60 min optical density was measured at a wavelength of 405 nm on the Spark microplate reader (Tecan, Switzerland). Standard curve values were used to determine cytokine levels.

Flow cytometry analysis

Cells were harvested washed and resuspended in 4°C 1xPBS. Samples were subjected to flow cytometry on the FACS Calibur (Becton Dickinson, USA). At least 100,000 events per sample were recorded. Data was analyzed using Flowing Software version 2 .5.1.

Dual-Luciferase assay

For the dual luciferase (DLR) assay cells were grown in 96-well cell culture plates according to the required experimental set-up. Cell culture media was removed and cells were washed with 1x PBS. The Dual-Luciferase reporter assay system (Promega, Germany) was then used to analyze expression levels. Briefly, 100 µl/well 1x passive lysis buffer was added directly onto the cells and incubated for 15 min at room temperature with gentle shaking. The lysed cells were transferred into a white 96-well PCR plate. First FLuc then RLuc activity was measured by adding 50 µl/ well of the corresponding assay reagent with the Spark microplate reader (Tecan, Switzerland).

Stop codon readthrough

Immature moDCs ($5x10^4$ cells/well) were seeded in alcian blue-coated 96-well cell culture plates. On the the next, day cells were transfected with readthrough reporter mRNA (100 ng/well) with coresponding uridine modifications using Lipofectamine MessengerMax harboring either a UGA(C), UAA(C), UAA(A) or UAAUAA(C) stop or GGA codon according to the manufacturer protocol. After 24h cells were lysed and fluorescence was determined with the DLR assay system on the Spark microplate reader as described previously. Protein expression levels were determined by the ratio of RLuc/Fluc. Percentage of readthrough was calculated by the ratio of stop codon/GGA codon protein expression.

Transfection cell toxicity assay

To assess cell toxicity of LNPs and Lipofetamine MessengerMax (Thermo Fisher Scientific, Germany) moDCs ($4x10^4$ cells/well) were seeded in 96-well cell culture plates. After 24h were transfected with 100,200 or 500 ng of optimized UGA mRNA encoding GFP encapsulated in LNPs or mixed with corresponding Lipofectamine MessengerMax according to manufacturer protocol. 1%DMSO was used as control for cell death After 5h cell viability was assessed using the CellTiter-Glo Luminescent Cell Viability Assay (Promega, USA) according to manufacturer protocol.

mRNA immunogenicity assessment

HEK293XL hTLR7 and hTLR8 cells or immature moDCs ($5x10^4$ cells/well) were seeded in 96-well cell culture plates. On the next day, cells were transfected with RLuc-encoding optimized mRNA using protamine. Resiquimod (R848, InvivoGen, France) a TLR7/8 or OD-2216 (InvivoGen) a TLR9 antagonist served as a positive control for TLRactivation (339). R848, OD-2216 and the mRNA were diluted to 0.5 µg/µl and incubated with equal amounts of protamine for 10 min at room temperature. Subsequently, 5 µg/ml of the RNA and 1 µg/ml of R848 or OD-2216 mixed with protamine were added directly to the cells. After 1h the cell culture media was replaced. 7h after media renewal cell culture media supernatants were collected and IL-8 levels, TNF-α or IFN-γ representing TLR activation were analyzed using ELISA as described previously.

mRNA stability test

HeLa cells were transfected with GFP-encoding optimized mRNA (2.5 µg/well) with a UAAUAA stop codon using Lipofectamine MessengerMax (Thermo Fisher Scientific, Germany) according to the manufacturer protocol. Cell culture media was replaced with fresh media after 3h. To analyze the stability of the mRNA over time cells were harvested at 6 separate time points after media change: 0h, 1h, 2h, 4h, 8h, 13h, 24h. For each timepoint the cell number was determined to account for variation between timepoints. Total RNA was extracted and reverse-transcribed into cDNA as described previously. The following q-RT-PCR was performed as mentioned before by amplifying the 3'UTR region of the optimized mRNA with the following primer pair: forward: 5'- AGCTTGACTGGTACTGCATGCAC- 3' and reverse 5'-GCGTGCTTGGGAGGTGTCT-3'. Actin-β was used as a housekeeping gene and amplified with: 5'- CCCCAAAGTTCACAATGTG -3' and reverse 5'-

AGCAATGCTATCACCTCC -3' mRNA levels at each time point were determined by calculating the expression with $2^{\Delta CT(GFP-ACTB)}$ and multiplying it with the increase in cell number compared to the 0h time point.

Protein expression analysis

To verify uptake and mRNA translation HeLa cells and immature moDCs were seeded on a glass coverslip at $3x10^5$ cells/well in a 6-well plate. In the case of moDCs were coated with alcian blue (Sigma Aldrich, Germany). On the next day cells were transfected with GFP-encoding optimized mRNA (2.5 µg/well) using Lipofectamine MessengerMax according to the manufacture protocol or by directly adding LNPs in the cell culture media. After 24h cell culture media was removed, cells were washed with 1x PBS and fixed with 4% PFA in 1x PBS for 10 min at room temperature. Fixed cells were subsequently mounted using mounting media (1x PBS, 0,5% N-propyl gallate, 90% glycerol) supplemented with 20 ng/ml DAPI. Expression of GFP and DAPI staining was visualized with Leica DMi 8 fluorescence microscope. To analyze the percentage of positive cells after mRNA transfection moDCs ($1x10^6$ cells/well) were seeded in a 6-well plate and transfected for 24h with GFP-encoding mRNA (2.5 µg/well) by Lipofectamine MessengerMax or by directly adding LNPs in cell culture media and subsequently subjected to flow cytometry as described previously.

For the effect of the 5'UTR sequence on protein expression levels, immature moDCs ($5x10^4$ cells/well) or HeLa cells ($2x10^4$ cells/well) were seeded in 96-well cell culture plates. For moDCs plates were coated with alcain blue. On the next day, moDCs and HeLa cells were transfected with RLuc-encoding mRNA (100 ng/wells) with the different 5'UTRs and 10 ng/well of commercial Cleancap FLuc-encoding mRNA (TriLink, USA) for normalization. After 24h cells were lysed and Fluorescence was determined with the DLR assay system on the on the Spark microplate reader as described previously. Protein expression levels were determined by the ratio of RLuc/Fluc.

For the effect of stop codon identity on protein expression levels immature moDCs ($5x10^4$ cells/well) were seeded on alcian blue-coated 96-well cell culture plates. On the next day moDCs were transfected with RLuc-encoding optimized mRNA (100 ng/well) using Lipofectamine MessengerMax harboring either a UGA(C), UAA(C), UAA(A) or UAAUAA(C) stop codon according to the manufacturer protocol. For normalization cells were co-transfected with 10 ng/well of commercial CleanCap FLuc-encoding (TriLink). After 24h cells were lysed and Fluorescence was determined with the DLR assay system on the on the Spark microplate reader as described previously. Protein expression levels were determined by the ratio of RLuc/Fluc.

moDCs maturation analysis

Immature moDCs were seeded in a 6-well plate ($1x10^6$ cells/well) and transfected with either unmodified, 50% m1Ψ or 100% m1Ψ modified RLuc-encoding optimized mRNA (2.5 µg/well) using Lipofectamine MessengerMax according to the manufacturer's protocol. As a positive control immature moDCs were treated with a maturation cocktail consisting of IL-1β (13.2 ng/ml, Sigma Aldrich, Germany), IL-6 (150 ng/ml, Sigma Aldrich, Germany), TNFα (10 ng/ml, Biomol, Germany) and Prostaglandin E2 (1 µg/ml, Biomol, Germany). 24h later cells were stained for flow cytometry with APC conjugated anti-human HLA-DR and FITC conjugated anti-human CD86 antibodies (Miltenyi Biotech, Germany) following the manufacturer standard protocol. Stained cells were subsequently subjected to flow cytometry as described previously

Antigen-presentation assay

Levels of epitope presentation were measured by seeding EL4 cells in a T-25 flask ($3x10^5$ cells/well) and transfecting cells with SIINFEKL-encoding optimized mRNA (2.5 µg/flask) using Lipofectamine MessengerMax according to the manufacturer's protocol. After 24h cells were stained for flow cytometry with APC conjugated anti-mouse H-2Kb/SIINFEKL antibody (Miltenyi Biotech, Germany) following the manufacturer standard protocol. Stained cells were subsequently subjected to flow cytometry as described previously.

T cell activation and proliferation

T cell activation and proliferation was analyzed by seeding and transfecting immature moDCs ($1x10^6$ cells/well) with the corresponding candidate optimized mRNA (2.5 µg/well) in a 6-well plate using Lipofectamine MessengerMax according to manufacturer protocol. 1h after transfection the ImmunoCult Dendritic Cell Maturation Supplement (STEMCELL Technologies) was added to the transfected moDCs according to manufacturer instructions. After 24h mature moDCs were harvested and resuspended in ImmunoCult- XF T cell Expansion Medium.

Expanded CD8+ T cells were stained with CFSE. In short, T cells were resuspended in 1x PBS supplemented with 5% heat-inactivated FBS. T cells were then labeled by incubation with 50 µM of CFSE for 5 min at room temperature. Labeled CD8+ T cells were washed with 1x PBS, 5% heat-inactivated FBS, resuspended in ImmunoCult- XF T cell Expansion Medium and co-cultured with mature moDCS at a ratio of 10:1 in 96 well u bottom plates (Greiner Bio-One, Austria) to monitor proliferation and activation.

On day 6 of co-culture T cell activation was analyzed by measuring IL-2, TNFα and IFNγ levels

in the cell culture media supernatant by ELISA as described previously. On the same day, proliferation was assessed by subjecting T cells to flow cytometry as described previously measuring CFSE fluorescence.

Statistical analysis

All statistical analysis was conducted in RStudio Version 1.4.1106

7.References

1. Turvey SE, Broide DH. Innate immunity. *The Journal of allergy and clinical immunology*. 2010;125(2 Suppl 2):S24-32. doi:10.1016/j.jaci.2009.07.016.
2. Cooper MD, Alder MN. The evolution of adaptive immune systems. *Cell*. 2006;124(4):815-822. doi:10.1016/j.cell.2006.02.001.
3. Bonilla FA, Oettgen HC. Adaptive immunity. *The Journal of allergy and clinical immunology*. 2010;125(2 Suppl 2):S33-40. doi:10.1016/j.jaci.2009.09.017.
4. Oettinger MA. Activation of V(D)J recombination by RAG1 and RAG2. *Trends in genetics : TIG*. 1992;8(12):413-416. doi:10.1016/0168-9525(92)90323-V.
5. Kantor AB, Herzenberg LA. Origin of murine B cell lineages. *Annual review of immunology*. 1993;11:501-538. doi:10.1146/annurev.iy.11.040193.002441.
6. Jackson KJL, Kidd MJ, Wang Y, Collins AM. The shape of the lymphocyte receptor repertoire: lessons from the B cell receptor. *Frontiers in immunology*. 2013;4:263. doi:10.3389/fimmu.2013.00263.
7. Mårtensson I-L, Almqvist N, Grimsholm O, Bernardi AI. The pre-B cell receptor checkpoint. *FEBS letters*. 2010;584(12):2572-2579. doi:10.1016/j.febslet.2010.04.057.
8. LeBien TW, Tedder TF. B lymphocytes: how they develop and function. *Blood*. 2008;112(5):1570-1580. doi:10.1182/blood-2008-02-078071.
9. Loder F, et al. B cell development in the spleen takes place in discrete steps and is determined by the quality of B cell receptor-derived signals. *The Journal of experimental medicine*. 1999;190(1):75-89. doi:10.1084/jem.190.1.75.
10. Haan JMM den, Arens R, van Zelm MC. The activation of the adaptive immune system: cross-talk between antigen-presenting cells, T cells and B cells. *Immunology letters*. 2014;162(2 Pt B):103-112. doi:10.1016/j.imlet.2014.10.011.
11. Crotty S. A brief history of T cell help to B cells. *Nature reviews. Immunology*. 2015;15(3):185-189. doi:10.1038/nri3803.
12. Sun L, Su Y, Jiao A, Wang X, Zhang B. T cells in health and disease. *Signal transduction and targeted therapy*. 2023;8(1):235. doi:10.1038/s41392-023-01471-y.
13. *RF738946 Dr Gilles Dupuis - Biochimie*.
14. Takahama Y. Journey through the thymus: stromal guides for T-cell development and selection. *Nature reviews. Immunology*. 2006;6(2):127-135. doi:10.1038/nri1781.
15. Klein L, Kyewski B, Allen PM, Hogquist KA. Positive and negative selection of the T cell repertoire: what thymocytes see (and don't see). *Nature reviews. Immunology*. 2014;14(6):377-391. doi:10.1038/nri3667.

16. Roche PA, Furuta K. The ins and outs of MHC class II-mediated antigen processing and presentation. *Nature reviews. Immunology*. 2015;15(4):203-216. doi:10.1038/nri3818.
17. Pishesha N, Harmand TJ, Ploegh HL. A guide to antigen processing and presentation. *Nature reviews. Immunology*. 2022;22(12):751-764. doi:10.1038/s41577-022-00707-2.
18. Harding CV, Geuze HJ. Class II MHC molecules are present in macrophage lysosomes and phagolysosomes that function in the phagocytic processing of Listeria monocytogenes for presentation to T cells. *The Journal of cell biology*. 1992;119(3):531-542. doi:10.1083/jcb.119.3.531.
19. Kleijmeer MJ, Oorschot VM, Geuze HJ. Human resident langerhans cells display a lysosomal compartment enriched in MHC class II. *The Journal of investigative dermatology*. 1994;103(4):516-523. doi:10.1111/1523-1747.ep12395666.
20. Chow A, Toomre D, Garrett W, Mellman I. Dendritic cell maturation triggers retrograde MHC class II transport from lysosomes to the plasma membrane. *Nature*. 2002;418(6901):988-994. doi:10.1038/nature01006.
21. Kleijmeer MJ, et al. MHC class II compartments and the kinetics of antigen presentation in activated mouse spleen dendritic cells. *Journal of immunology (Baltimore, Md. : 1950)*. 1995;154(11):5715-5724. doi:10.4049/jimmunol.154.11.5715.
22. Mouriès J, Moron G, Schlecht G, Escriou N, Dadaglio G, Leclerc C. Plasmacytoid dendritic cells efficiently cross-prime naive T cells in vivo after TLR activation. *Blood*. 2008;112(9):3713-3722. doi:10.1182/blood-2008-03-146290.
23. Rock KL, Goldberg AL. Degradation of cell proteins and the generation of MHC class I-presented peptides. *Annual review of immunology*. 1999;17:739-779. doi:10.1146/annurev.immunol.17.1.739.
24. Jensen PE. Recent advances in antigen processing and presentation. *Nature immunology*. 2007;8(10):1041-1048. doi:10.1038/ni1516.
25. Faith Mokobi. MHC Class I, Class II, Antigen Processing, And Presentation. https://microbenotes.com/mhc-antigen-processing-presentation/.
26. Dustin ML. The cellular context of T cell signaling. *Immunity*. 2009;30(4):482-492. doi:10.1016/j.immuni.2009.03.010.
27. Luckheeram RV, Zhou R, Verma AD, Xia B. $CD4^+$T cells: differentiation and functions. *Clinical & developmental immunology*. 2012;2012:925135. doi:10.1155/2012/925135.
28. Koh C-H, Lee S, Kwak M, Kim B-S, Chung Y. CD8 T-cell subsets: heterogeneity, functions, and therapeutic potential. *Experimental & molecular medicine*. 2023;55(11):2287-2299. doi:10.1038/s12276-023-01105-x.
29. Vesely MD, Kershaw MH, Schreiber RD, Smyth MJ. Natural innate and adaptive immunity to cancer. *Annual review of immunology*. 2011;29:235-271. doi:10.1146/annurev-immunol-031210-101324.

30. Sim MJW, Sun PD. T Cell Recognition of Tumor Neoantigens and Insights Into T Cell Immunotherapy. *Frontiers in immunology*. 2022;13:833017. doi:10.3389/fimmu.2022.833017.
31. Shankaran V, et al. IFNgamma and lymphocytes prevent primary tumour development and shape tumour immunogenicity. *Nature*. 2001;410(6832):1107-1111. doi:10.1038/35074122.
32. Kaplan DH, et al. Demonstration of an interferon gamma-dependent tumor surveillance system in immunocompetent mice. *Proceedings of the National Academy of Sciences of the United States of America*. 1998;95(13):7556-7561. doi:10.1073/pnas.95.13.7556.
33. Dighe AS, Richards E, Old LJ, Schreiber RD. Enhanced in vivo growth and resistance to rejection of tumor cells expressing dominant negative IFN gamma receptors. *Immunity*. 1994;1(6):447-456. doi:10.1016/1074-7613(94)90087-6.
34. Dunn GP, Old LJ, Schreiber RD. The three Es of cancer immunoediting. *Annual review of immunology*. 2004;22:329-360. doi:10.1146/annurev.immunol.22.012703.104803.
35. Koebel CM, et al. Adaptive immunity maintains occult cancer in an equilibrium state. *Nature*. 2007;450(7171):903-907. doi:10.1038/nature06309.
36. Riaz N, et al. Tumor and Microenvironment Evolution during Immunotherapy with Nivolumab. *Cell*. 2017;171(4):934-949.e16. doi:10.1016/j.cell.2017.09.028.
37. Chang C-C, et al. Multiple structural and epigenetic defects in the human leukocyte antigen class I antigen presentation pathway in a recurrent metastatic melanoma following immunotherapy. *The Journal of biological chemistry*. 2015;290(44):26562-26575. doi:10.1074/jbc.M115.676130.
38. Mandai M, Hamanishi J, Abiko K, Matsumura N, Baba T, Konishi I. Dual Faces of IFNγ in Cancer Progression: A Role of PD-L1 Induction in the Determination of Pro- and Antitumor Immunity. *Clinical cancer research : an official journal of the American Association for Cancer Research*. 2016;22(10):2329-2334. doi:10.1158/1078-0432.CCR-16-0224.
39. Takeda K, et al. IFN-γ is required for cytotoxic T cell-dependent cancer genome immunoediting. *Nature communications*. 2017;8:14607. doi:10.1038/ncomms14607.
40. Swann JB, Smyth MJ. Immune surveillance of tumors. *The Journal of clinical investigation*. 2007;117(5):1137-1146. doi:10.1172/JCI31405.
41. Mei Z, Huang J, Qiao B, Lam AK-Y. Immune checkpoint pathways in immunotherapy for head and neck squamous cell carcinoma. *International journal of oral science*. 2020;12(1):16. doi:10.1038/s41368-020-0084-8.
42. Rohaan MW, Wilgenhof S, Haanen JBAG. Adoptive cellular therapies: the current landscape. *Virchows Archiv : an international journal of pathology*. 2019;474(4):449-461. doi:10.1007/s00428-018-2484-0.

43. Zhang M, et al. miRNA-5119 regulates immune checkpoints in dendritic cells to enhance breast cancer immunotherapy. *Cancer immunology, immunotherapy : CII*. 2020;69(6):951-967. doi:10.1007/s00262-020-02507-w.
44. O'Donnell JS, Teng MWL, Smyth MJ. Cancer immunoediting and resistance to T cell-based immunotherapy. *Nature reviews. Clinical oncology*. 2019;16(3):151-167. doi:10.1038/s41571-018-0142-8.
45. Mattiuzzi C, Lippi G. Current Cancer Epidemiology. *Journal of epidemiology and global health*. 2019;9(4):217-222. doi:10.2991/jegh.k.191008.001.
46. Queirolo P, Boutros A, Tanda E, Spagnolo F, Quaglino P. Immune-checkpoint inhibitors for the treatment of metastatic melanoma: a model of cancer immunotherapy. *Seminars in cancer biology*. 2019;59:290-297. doi:10.1016/j.semcancer.2019.08.001.
47. Mamdani H, Matosevic S, Khalid AB, Durm G, Jalal SI. Immunotherapy in Lung Cancer: Current Landscape and Future Directions. *Frontiers in immunology*. 2022;13:823618. doi:10.3389/fimmu.2022.823618.
48. Wołącewicz M, et al. Immunotherapy in Bladder Cancer: Current Methods and Future Perspectives. *Cancers*. 2020;12(5). doi:10.3390/cancers12051181.
49. Waldman AD, Fritz JM, Lenardo MJ. A guide to cancer immunotherapy: from T cell basic science to clinical practice. *Nature reviews. Immunology*. 2020;20(11):651-668. doi:10.1038/s41577-020-0306-5.
50. Farkona S, Diamandis EP, Blasutig IM. Cancer immunotherapy: the beginning of the end of cancer? *BMC medicine*. 2016;14:73. doi:10.1186/s12916-016-0623-5.
51. Garber K. Beyond ipilimumab: new approaches target the immunological synapse. *Journal of the National Cancer Institute*. 2011;103(14):1079-1082. doi:10.1093/jnci/djr281.
52. Algarra I, García-Lora A, Cabrera T, Ruiz-Cabello F, Garrido F. The selection of tumor variants with altered expression of classical and nonclassical MHC class I molecules: implications for tumor immune escape. *Cancer immunology, immunotherapy : CII*. 2004;53(10):904-910. doi:10.1007/s00262-004-0517-9.
53. Restifo NP. Not so Fas: Re-evaluating the mechanisms of immune privilege and tumor escape. *Nature medicine*. 2000;6(5):493-495. doi:10.1038/74955.
54. Todaro M, et al. Apoptosis resistance in epithelial tumors is mediated by tumor-cell-derived interleukin-4. *Cell death and differentiation*. 2008;15(4):762-772. doi:10.1038/sj.cdd.4402305.
55. Hersey P, Zhang XD. How melanoma cells evade trail-induced apoptosis. *Nature reviews. Cancer*. 2001;1(2):142-150. doi:10.1038/35101078.

56. Ben-Baruch A. Inflammation-associated immune suppression in cancer: the roles played by cytokines, chemokines and additional mediators. *Seminars in cancer biology*. 2006;16(1):38-52. doi:10.1016/j.semcancer.2005.07.006.
57. Salazar-Onfray F, López MN, Mendoza-Naranjo A. Paradoxical effects of cytokines in tumor immune surveillance and tumor immune escape. *Cytokine & growth factor reviews*. 2007;18(1-2):171-182. doi:10.1016/j.cytogfr.2007.01.015.
58. Simsek H, Klotzsch E. The solid tumor microenvironment-Breaking the barrier for T cells: How the solid tumor microenvironment influences T cells: How the solid tumor microenvironment influences T cells. *BioEssays : news and reviews in molecular, cellular and developmental biology*. 2022;44(6):e2100285. doi:10.1002/bies.202100285.
59. Anderson NM, Simon MC. The tumor microenvironment. *Current biology : CB*. 2020;30(16):R921-R925. doi:10.1016/j.cub.2020.06.081.
60. Yuan Y, Jiang Y-C, Sun C-K, Chen Q-M. Role of the tumor microenvironment in tumor progression and the clinical applications (Review). *Oncology reports*. 2016;35(5):2499-2515. doi:10.3892/or.2016.4660.
61. Sica A. Role of tumour-associated macrophages in cancer-related inflammation. *Experimental oncology*. 2010;32(3):153-158.
62. Lee KY. M1 and M2 polarization of macrophages: a mini-review. *Med Biol Sci Eng*. 2019;2(1):1-5. doi:10.30579/mbse.2019.2.1.1.
63. Mills CD, Ley K. M1 and M2 macrophages: the chicken and the egg of immunity. *Journal of innate immunity*. 2014;6(6):716-726. doi:10.1159/000364945.
64. Sica A, et al. Macrophage polarization in tumour progression. *Seminars in cancer biology*. 2008;18(5):349-355. doi:10.1016/j.semcancer.2008.03.004.
65. Gajewski TF. The Next Hurdle in Cancer Immunotherapy: Overcoming the Non-T-Cell-Inflamed Tumor Microenvironment. *Seminars in oncology*. 2015;42(4):663-671. doi:10.1053/j.seminoncol.2015.05.011.
66. Lim SA, et al. Lipid signalling enforces functional specialization of Treg cells in tumours. *Nature*. 2021;591(7849):306-311. doi:10.1038/s41586-021-03235-6.
67. Knochelmann HM, et al. When worlds collide: Th17 and Treg cells in cancer and autoimmunity. *Cellular & molecular immunology*. 2018;15(5):458-469. doi:10.1038/s41423-018-0004-4.
68. Zheng L, et al. Pan-cancer single-cell landscape of tumor-infiltrating T cells. *Science (New York, N.Y.)*. 2021;374(6574):abe6474. doi:10.1126/science.abe6474.
69. Thorsson V, et al. The Immune Landscape of Cancer. *Immunity*. 2018;48(4):812-830.e14. doi:10.1016/j.immuni.2018.03.023.
70. Scheper W, et al. Low and variable tumor reactivity of the intratumoral TCR repertoire in human cancers. *Nature medicine*. 2019;25(1):89-94. doi:10.1038/s41591-018-0266-5.

71. Oliveira G, et al. Phenotype, specificity and avidity of antitumour CD8+ T cells in melanoma. *Nature*. 2021;596(7870):119-125. doi:10.1038/s41586-021-03704-y.
72. Nagarsheth N, Wicha MS, Zou W. Chemokines in the cancer microenvironment and their relevance in cancer immunotherapy. *Nature reviews. Immunology*. 2017;17(9):559-572. doi:10.1038/nri.2017.49.
73. Peng D, et al. Epigenetic silencing of TH1-type chemokines shapes tumour immunity and immunotherapy. *Nature*. 2015;527(7577):249-253. doi:10.1038/nature15520.
74. Liao W, et al. KRAS-IRF2 Axis Drives Immune Suppression and Immune Therapy Resistance in Colorectal Cancer. *Cancer cell*. 2019;35(4):559-572.e7. doi:10.1016/j.ccell.2019.02.008.
75. Piersma B, Hayward M-K, Weaver VM. Fibrosis and cancer: A strained relationship. *Biochimica et biophysica acta. Reviews on cancer*. 2020;1873(2):188356. doi:10.1016/j.bbcan.2020.188356.
76. Dzobo K, Dandara C. Architecture of Cancer-Associated Fibroblasts in Tumor Microenvironment: Mapping Their Origins, Heterogeneity, and Role in Cancer Therapy Resistance. *Omics : a journal of integrative biology*. 2020;24(6):314-339. doi:10.1089/omi.2020.0023.
77. Erdogan B, Webb DJ. Cancer-associated fibroblasts modulate growth factor signaling and extracellular matrix remodeling to regulate tumor metastasis. *Biochemical Society transactions*. 2017;45(1):229-236. doi:10.1042/BST20160387.
78. Vicente CM, Ricci R, Nader HB, Toma L. Syndecan-2 is upregulated in colorectal cancer cells through interactions with extracellular matrix produced by stromal fibroblasts. *BMC cell biology*. 2013;14:25. doi:10.1186/1471-2121-14-25.
79. Peng L, et al. Emerging Role of Cancer-Associated Fibroblasts-Derived Exosomes in Tumorigenesis. *Frontiers in immunology*. 2021;12:795372. doi:10.3389/fimmu.2021.795372.
80. Bainbridge P. Wound healing and the role of fibroblasts. *Journal of wound care*. 2013;22(8):407-8, 410-12. doi:10.12968/jowc.2013.22.8.407.
81. Joshi RS, Kanugula SS, Sudhir S, Pereira MP, Jain S, Aghi MK. The Role of Cancer-Associated Fibroblasts in Tumor Progression. *Cancers*. 2021;13(6). doi:10.3390/cancers13061399.
82. Kubo N, Araki K, Kuwano H, Shirabe K. Cancer-associated fibroblasts in hepatocellular carcinoma. *World Journal of Gastroenterology*. 2016;22(30):6841-6850. doi:10.3748/wjg.v22.i30.6841.
83. Abudukelimu S, Miranda NFCC de, Hawinkels LJAC. Fibroblasts in Orchestrating Colorectal Tumorigenesis and Progression. *Cellular and molecular gastroenterology and hepatology*. 2024;17(5):821-826. doi:10.1016/j.jcmgh.2024.01.013.

84. Sun H, Wang X, Wang X, Xu M, Sheng W. The role of cancer-associated fibroblasts in tumorigenesis of gastric cancer. *Cell death & disease*. 2022;13(10):874. doi:10.1038/s41419-022-05320-8.
85. Zhang T, Zhang P, Li H-X. CAFs-Derived Exosomal miRNA-130a Confers Cisplatin Resistance of NSCLC Cells Through PUM2-Dependent Packaging. *International journal of nanomedicine*. 2021;16:561-577. doi:10.2147/IJN.S271976.
86. Yang F, et al. MiR-210 in exosomes derived from CAFs promotes non-small cell lung cancer migration and invasion through PTEN/PI3K/AKT pathway. *Cellular signalling*. 2020;73:109675. doi:10.1016/j.cellsig.2020.109675.
87. Dou D, et al. Cancer-Associated Fibroblasts-Derived Exosomes Suppress Immune Cell Function in Breast Cancer via the miR-92/PD-L1 Pathway. *Frontiers in immunology*. 2020;11:2026. doi:10.3389/fimmu.2020.02026.
88. Li B-L, Lu W, Qu J-J, Ye L, Du G-Q, Wan X-P. Loss of exosomal miR-148b from cancer-associated fibroblasts promotes endometrial cancer cell invasion and cancer metastasis. *Journal of cellular physiology*. 2019;234(3):2943-2953. doi:10.1002/jcp.27111.
89. Subramaniam KS, et al. Cancer-associated fibroblasts promote endometrial cancer growth via activation of interleukin-6/STAT-3/c-Myc pathway. *American journal of cancer research*. 2016;6(2):200-213.
90. Esfahani K, Roudaia L, Buhlaiga N, Del Rincon SV, Papneja N, Miller WH. A review of cancer immunotherapy: from the past, to the present, to the future. *Current oncology (Toronto, Ont.)*. 2020;27(Suppl 2):S87-S97. doi:10.3747/co.27.5223.
91. Zhu S, et al. Combination strategies to maximize the benefits of cancer immunotherapy. *Journal of hematology & oncology*. 2021;14(1):156. doi:10.1186/s13045-021-01164-5.
92. Pentcheva-Hoang T, Corse E, Allison JP. Negative regulators of T-cell activation: potential targets for therapeutic intervention in cancer, autoimmune disease, and persistent infections. *Immunological reviews*. 2009;229(1):67-87. doi:10.1111/j.1600-065X.2009.00763.x.
93. Li B, Chan HL, Chen P. Immune Checkpoint Inhibitors: Basics and Challenges. *Current medicinal chemistry*. 2019;26(17):3009-3025. doi:10.2174/0929867324666170804143706.
94. Kroemer G, Zitvogel L. Immune checkpoint inhibitors. *The Journal of experimental medicine*. 2021;218(3). doi:10.1084/jem.20201979.
95. Rittmeyer A, et al. Atezolizumab versus docetaxel in patients with previously treated non-small-cell lung cancer (OAK): a phase 3, open-label, multicentre randomised controlled trial. *Lancet (London, England)*. 2017;389(10066):255-265. doi:10.1016/S0140-6736(16)32517-X.

96. Mansh M. Ipilimumab and cancer immunotherapy: a new hope for advanced stage melanoma. *The Yale journal of biology and medicine*. 2011;84(4):381-389.
97. Migden MR, et al. PD-1 Blockade with Cemiplimab in Advanced Cutaneous Squamous-Cell Carcinoma. *The New England journal of medicine*. 2018;379(4):341-351. doi:10.1056/NEJMoa1805131.
98. Shirley M. Avelumab: A Review in Metastatic Merkel Cell Carcinoma. *Targeted oncology*. 2018;13(3):409-416. doi:10.1007/s11523-018-0571-4.
99. Pakish JB, et al. Immune Microenvironment in Microsatellite-Instable Endometrial Cancers: Hereditary or Sporadic Origin Matters. *Clinical cancer research : an official journal of the American Association for Cancer Research*. 2017;23(15):4473-4481. doi:10.1158/1078-0432.CCR-16-2655.
100. Howitt BE, et al. Association of Polymerase e-Mutated and Microsatellite-Instable Endometrial Cancers With Neoantigen Load, Number of Tumor-Infiltrating Lymphocytes, and Expression of PD-1 and PD-L1. *JAMA oncology*. 2015;1(9):1319-1323. doi:10.1001/jamaoncol.2015.2151.
101. Zhan L, Liu X, Zhang J, Cao Y, Wei B. Immune disorder in endometrial cancer: Immunosuppressive microenvironment, mechanisms of immune evasion and immunotherapy. *Oncology letters*. 2020;20(3):2075-2090. doi:10.3892/ol.2020.11774.
102. Crosbie EJ, Kitson SJ, McAlpine JN, Mukhopadhyay A, Powell ME, Singh N. Endometrial cancer. *Lancet (London, England)*. 2022;399(10333):1412-1428. doi:10.1016/S0140-6736(22)00323-3.
103. Jenkins RW, Barbie DA, Flaherty KT. Mechanisms of resistance to immune checkpoint inhibitors. *British journal of cancer*. 2018;118(1):9-16. doi:10.1038/bjc.2017.434.
104. Dobosz P, Stępień M, Golke A, Dzieciątkowski T. Challenges of the Immunotherapy: Perspectives and Limitations of the Immune Checkpoint Inhibitor Treatment. *International journal of molecular sciences*. 2022;23(5). doi:10.3390/ijms23052847.
105. Vormittag P, Gunn R, Ghorashian S, Veraitch FS. A guide to manufacturing CAR T cell therapies. *Current opinion in biotechnology*. 2018;53:164-181. doi:10.1016/j.copbio.2018.01.025.
106. Labanieh L, Majzner RG, Mackall CL. Programming CAR-T cells to kill cancer. *Nature biomedical engineering*. 2018;2(6):377-391. doi:10.1038/s41551-018-0235-9.
107. Han D, Xu Z, Zhuang Y, Ye Z, Qian Q. Current Progress in CAR-T Cell Therapy for Hematological Malignancies. *Journal of Cancer*. 2021;12(2):326-334. doi:10.7150/jca.48976.

108. Albinger N, Hartmann J, Ullrich E. Current status and perspective of CAR-T and CAR-NK cell therapy trials in Germany. *Gene therapy*. 2021;28(9):513-527. doi:10.1038/s41434-021-00246-w.

109. AlDallal SM. Yescarta: A New Era for Non-Hodgkin Lymphoma Patients. *Cureus*. 2020;12(11):e11504. doi:10.7759/cureus.11504.

110. Awasthi R, Maier HJ, Zhang J, Lim S. Kymriah® (tisagenlecleucel) - An overview of the clinical development journey of the first approved CAR-T therapy. *Human vaccines & immunotherapeutics*. 2023;19(1):2210046. doi:10.1080/21645515.2023.2210046.

111. Brudno JN, Kochenderfer JN. Recent advances in CAR T-cell toxicity: Mechanisms, manifestations and management. *Blood reviews*. 2019;34:45-55. doi:10.1016/j.blre.2018.11.002.

112. Drent E, et al. A Rational Strategy for Reducing On-Target Off-Tumor Effects of CD38-Chimeric Antigen Receptors by Affinity Optimization. *Molecular therapy : the journal of the American Society of Gene Therapy*. 2017;25(8):1946-1958. doi:10.1016/j.ymthe.2017.04.024.

113. Singh N, et al. Mechanisms of resistance to CAR T cell therapies. *Seminars in cancer biology*. 2020;65:91-98. doi:10.1016/j.semcancer.2019.12.002.

114. Singh N, Perazzelli J, Grupp SA, Barrett DM. Early memory phenotypes drive T cell proliferation in patients with pediatric malignancies. *Science translational medicine*. 2016;8(320):320ra3. doi:10.1126/scitranslmed.aad5222.

115. Meo SA, Bukhari IA, Akram J, Meo AS, Klonoff DC. COVID-19 vaccines: comparison of biological, pharmacological characteristics and adverse effects of Pfizer/BioNTech and Moderna Vaccines. *European review for medical and pharmacological sciences*. 2021;25(3):1663-1669. doi:10.26355/eurrev_202102_24877.

116. Chaudhary N, Weissman D, Whitehead KA. mRNA vaccines for infectious diseases: principles, delivery and clinical translation. *Nature reviews. Drug discovery*. 2021;20(11):817-838. doi:10.1038/s41573-021-00283-5.

117. Martinon F, et al. Induction of virus-specific cytotoxic T lymphocytes in vivo by liposome-entrapped mRNA. *European journal of immunology*. 1993;23(7):1719-1722. doi:10.1002/eji.1830230749.

118. Pardi N, Hogan MJ, Porter FW, Weissman D. mRNA vaccines - a new era in vaccinology. *Nature reviews. Drug discovery*. 2018;17(4):261-279. doi:10.1038/nrd.2017.243.

119. Muttach F, Muthmann N, Rentmeister A. Synthetic mRNA capping. *Beilstein journal of organic chemistry*. 2017;13:2819-2832. doi:10.3762/bjoc.13.274.

120. Schlake T, Thess A, Fotin-Mleczek M, Kallen K-J. Developing mRNA-vaccine technologies. *RNA biology*. 2012;9(11):1319-1330. doi:10.4161/rna.22269.

121. Karikó K, Muramatsu H, Ludwig J, Weissman D. Generating the optimal mRNA for therapy: HPLC purification eliminates immune activation and improves translation of nucleoside-modified, protein-encoding mRNA. *Nucleic acids research*. 2011;39(21):e142. doi:10.1093/nar/gkr695.

122. Weng Y, et al. The challenge and prospect of mRNA therapeutics landscape. *Biotechnology advances*. 2020;40:107534. doi:10.1016/j.biotechadv.2020.107534.

123. Swetha K, et al. Recent Advances in the Lipid Nanoparticle-Mediated Delivery of mRNA Vaccines. *Vaccines*. 2023;11(3). doi:10.3390/vaccines11030658.

124. Hou X, Zaks T, Langer R, Dong Y. Lipid nanoparticles for mRNA delivery. *Nature reviews. Materials*. 2021;6(12):1078-1094. doi:10.1038/s41578-021-00358-0.

125. Karikó K, Buckstein M, Ni H, Weissman D. Suppression of RNA recognition by Toll-like receptors: the impact of nucleoside modification and the evolutionary origin of RNA. *Immunity*. 2005;23(2):165-175. doi:10.1016/j.immuni.2005.06.008.

126. Svitkin YV, Cheng YM, Chakraborty T, Presnyak V, John M, Sonenberg N. N1-methyl-pseudouridine in mRNA enhances translation through eIF2α-dependent and independent mechanisms by increasing ribosome density. *Nucleic acids research*. 2017;45(10):6023-6036. doi:10.1093/nar/gkx135.

127. Gote V, et al. A Comprehensive Review of mRNA Vaccines. *International journal of molecular sciences*. 2023;24(3). doi:10.3390/ijms24032700.

128. Thess A, et al. Sequence-engineered mRNA Without Chemical Nucleoside Modifications Enables an Effective Protein Therapy in Large Animals. *Molecular therapy : the journal of the American Society of Gene Therapy*. 2015;23(9):1456-1464. doi:10.1038/mt.2015.103.

129. Sevil Domènech VE, Panthel K, Meinel KM, Winter SE, Rüssmann H. Pre-existing anti-Salmonella vector immunity prevents the development of protective antigen-specific CD8 T-cell frequencies against murine listeriosis. *Microbes and infection*. 2007;9(12-13):1447-1453. doi:10.1016/j.micinf.2007.07.010.

130. Pine SO, et al. Pre-existing adenovirus immunity modifies a complex mixed Th1 and Th2 cytokine response to an Ad5/HIV-1 vaccine candidate in humans. *PloS one*. 2011;6(4):e18526. doi:10.1371/journal.pone.0018526.

131. Leong ML, et al. Impact of preexisting vector-specific immunity on vaccine potency: characterization of listeria monocytogenes-specific humoral and cellular immunity in humans and modeling studies using recombinant vaccines in mice. *Infection and immunity*. 2009;77(9):3958-3968. doi:10.1128/iai.01274-08.

132. Buchbinder SP, et al. Efficacy assessment of a cell-mediated immunity HIV-1 vaccine (the Step Study): a double-blind, randomised, placebo-controlled, test-of-concept trial.

Lancet (London, England). 2008;372(9653):1881-1893. doi:10.1016/S0140-6736(08)61591-3.

133. Rosa SS, Prazeres DMF, Azevedo AM, Marques MPC. mRNA vaccines manufacturing: Challenges and bottlenecks. *Vaccine*. 2021;39(16):2190-2200. doi:10.1016/j.vaccine.2021.03.038.

134. Ramanathan A, Robb GB, Chan S-H. mRNA capping: biological functions and applications. *Nucleic acids research*. 2016;44(16):7511-7526. doi:10.1093/nar/gkw551.

135. Bélanger F, Stepinski J, Darzynkiewicz E, Pelletier J. Characterization of hMTr1, a human Cap1 2'-O-ribose methyltransferase. *The Journal of biological chemistry*. 2010;285(43):33037-33044. doi:10.1074/jbc.M110.155283.

136. Leung DW, Amarasinghe GK. When your cap matters: structural insights into self vs non-self recognition of 5' RNA by immunomodulatory host proteins. *Current opinion in structural biology*. 2016;36:133-141. doi:10.1016/j.sbi.2016.02.001.

137. Drazkowska K, et al. 2′-O-Methylation of the second transcribed nucleotide within the mRNA 5′ cap impacts the protein production level in a cell-specific manner and contributes to RNA immune evasion. *Nucleic acids research*. 2022;50(16):9051-9071. doi:10.1093/nar/gkac722.

138. Ziemniak M, Strenkowska M, Kowalska J, Jemielity J. Potential therapeutic applications of RNA cap analogs. *Future medicinal chemistry*. 2013;5(10):1141-1172. doi:10.4155/fmc.13.96.

139. Babendure JR, Babendure JL, Ding J-H, Tsien RY. Control of mammalian translation by mRNA structure near caps. *RNA (New York, N.Y.)*. 2006;12(5):851-861. doi:10.1261/rna.2309906.

140. Chatterjee S, Pal JK. Role of 5'- and 3'-untranslated regions of mRNAs in human diseases. *Biology of the cell*. 2009;101(5):251-262. doi:10.1042/BC20080104.

141. Navarro E, Mallén A, Hueso M. Dynamic Variations of 3'UTR Length Reprogram the mRNA Regulatory Landscape. *Biomedicines*. 2021;9(11). doi:10.3390/biomedicines9111560.

142. Ryczek N, Łyś A, Makałowska I. The Functional Meaning of 5'UTR in Protein-Coding Genes. *International journal of molecular sciences*. 2023;24(3). doi:10.3390/ijms24032976.

143. Leppek K, et al. Combinatorial optimization of mRNA structure, stability, and translation for RNA-based therapeutics. *Nature communications*. 2022;13(1):1536. doi:10.1038/s41467-022-28776-w.

144. Bicknell AA, et al. Attenuating ribosome load improves protein output from mRNA by limiting translation-dependent mRNA decay. *Cell reports*. 2024;43(4):114098. doi:10.1016/j.celrep.2024.114098.

145. Kirshina A, et al. Effects of Combinations of Untranslated-Region Sequences on Translation of mRNA. *Biomolecules*. 2023;13(11). doi:10.3390/biom13111677.

146. Trepotec Z, Aneja MK, Geiger J, Hasenpusch G, Plank C, Rudolph C. Maximizing the Translational Yield of mRNA Therapeutics by Minimizing 5'-UTRs. *Tissue engineering. Part A*. 2019;25(1-2):69-79. doi:10.1089/ten.TEA.2017.0485.

147. Carralot J-P, et al. Polarization of immunity induced by direct injection of naked sequence-stabilized mRNA vaccines. *Cellular and molecular life sciences : CMLS*. 2004;61(18):2418-2424. doi:10.1007/s00018-004-4255-0.

148. Orlandini von Niessen AG, et al. Improving mRNA-Based Therapeutic Gene Delivery by Expression-Augmenting 3' UTRs Identified by Cellular Library Screening. *Molecular therapy : the journal of the American Society of Gene Therapy*. 2019;27(4):824-836. doi:10.1016/j.ymthe.2018.12.011.

149. Eckmann CR, Rammelt C, Wahle E. Control of poly(A) tail length. *Wiley interdisciplinary reviews. RNA*. 2011;2(3):348-361. doi:10.1002/wrna.56.

150. Schwartz DC, Parker R. mRNA decapping in yeast requires dissociation of the cap binding protein, eukaryotic translation initiation factor 4E. *Molecular and cellular biology*. 2000;20(21):7933-7942. doi:10.1128/MCB.20.21.7933-7942.2000.

151. Wilson T, Treisman R. Removal of poly(A) and consequent degradation of c-fos mRNA facilitated by 3' AU-rich sequences. *Nature*. 1988;336(6197):396-399. doi:10.1038/336396a0.

152. Zhang J, et al. Recent Advances and Innovations in the Preparation and Purification of In Vitro-Transcribed-mRNA-Based Molecules. *Pharmaceutics*. 2023;15(9). doi:10.3390/pharmaceutics15092182.

153. Godiska R, et al. Linear plasmid vector for cloning of repetitive or unstable sequences in Escherichia coli. *Nucleic acids research*. 2010;38(6):e88. doi:10.1093/nar/gkp1181.

154. Trepotec Z, Geiger J, Plank C, Aneja MK, Rudolph C. Segmented poly(A) tails significantly reduce recombination of plasmid DNA without affecting mRNA translation efficiency or half-life. *RNA (New York, N.Y.)*. 2019;25(4):507-518. doi:10.1261/rna.069286.118.

155. Fu H, et al. Codon optimization with deep learning to enhance protein expression. *Scientific reports*. 2020;10(1):17617. doi:10.1038/s41598-020-74091-z.

156. Zhang H, et al. Algorithm for optimized mRNA design improves stability and immunogenicity. *Nature*. 2023;621(7978):396-403. doi:10.1038/s41586-023-06127-z.

157. Lehner PJ, Cresswell P. Recent developments in MHC-class-I-mediated antigen presentation. *Current opinion in immunology*. 2004;16(1):82-89. doi:10.1016/j.coi.2003.11.012.

158. Princiotta MF, et al. Quantitating protein synthesis, degradation, and endogenous antigen processing. *Immunity*. 2003;18(3):343-354. doi:10.1016/s1074-7613(03)00051-7.

159. Yewdell JW, Reits E, Neefjes J. Making sense of mass destruction: quantitating MHC class I antigen presentation. *Nature reviews. Immunology*. 2003;3(12):952-961. doi:10.1038/nri1250.

160. Wen X, et al. Inclusion of a universal tetanus toxoid CD4(+) T cell epitope P2 significantly enhanced the immunogenicity of recombinant rotavirus ΔVP8* subunit parenteral vaccines. *Vaccine*. 2014;32(35):4420-4427. doi:10.1016/j.vaccine.2014.06.060.

161. Kreiter S, et al. Increased antigen presentation efficiency by coupling antigens to MHC class I trafficking signals. *Journal of immunology (Baltimore, Md. : 1950)*. 2008;180(1):309-318. doi:10.4049/jimmunol.180.1.309.

162. Sobhani N, et al. Therapeutic cancer vaccines: From biological mechanisms and engineering to ongoing clinical trials. *Cancer treatment reviews*. 2022;109:102429. doi:10.1016/j.ctrv.2022.102429.

163. Haen SP, Löffler MW, Rammensee H-G, Brossart P. Towards new horizons: characterization, classification and implications of the tumour antigenic repertoire. *Nature reviews. Clinical oncology*. 2020;17(10):595-610. doi:10.1038/s41571-020-0387-x.

164. Yao R, Xie C, Xia X. Recent progress in mRNA cancer vaccines. *Human vaccines & immunotherapeutics*. 2024;20(1):2307187. doi:10.1080/21645515.2024.2307187.

165. Khattak A, et al. Distant metastasis-free survival results from the randomized, phase 2 mRNA-4157-P201/KEYNOTE-942 trial. *JCO*. 2023;41(17_suppl):LBA9503-LBA9503. doi:10.1200/JCO.2023.41.17_suppl.LBA9503.

166. Alatrash G, Crain AK, Molldrem JJ. Tumor-Associated Antigens. In: *Immune Biology of Allogeneic Hematopoietic Stem Cell Transplantation*: Elsevier; 2019:107-125.

167. Nin DS, Deng L-W. Biology of Cancer-Testis Antigens and Their Therapeutic Implications in Cancer. *Cells*. 2023;12(6). doi:10.3390/cells12060926.

168. Boccaletto P, et al. MODOMICS: a database of RNA modification pathways. 2017 update. *Nucleic acids research*. 2018;46(D1):D303-D307. doi:10.1093/nar/gkx1030.

169. Fernández IS, Ng CL, Kelley AC, Wu G, Yu Y-T, Ramakrishnan V. Unusual base pairing during the decoding of a stop codon by the ribosome. *Nature*. 2013;500(7460):107-110. doi:10.1038/nature12302.

170. Batista PJ, et al. m(6)A RNA modification controls cell fate transition in mammalian embryonic stem cells. *Cell stem cell*. 2014;15(6):707-719. doi:10.1016/j.stem.2014.09.019.

171. Lin S, Choe J, Du P, Triboulet R, Gregory RI. The m(6)A Methyltransferase METTL3 Promotes Translation in Human Cancer Cells. *Molecular cell*. 2016;62(3):335-345. doi:10.1016/j.molcel.2016.03.021.

172. Li D, Wu M. Pattern recognition receptors in health and diseases. *Signal transduction and targeted therapy*. 2021;6(1):291. doi:10.1038/s41392-021-00687-0.

173. Heil F, et al. Species-specific recognition of single-stranded RNA via toll-like receptor 7 and 8. *Science (New York, N.Y.)*. 2004;303(5663):1526-1529. doi:10.1126/science.1093620.

174. Alexopoulou L, Holt AC, Medzhitov R, Flavell RA. Recognition of double-stranded RNA and activation of NF-kappaB by Toll-like receptor 3. *Nature*. 2001;413(6857):732-738. doi:10.1038/35099560.

175. Kumagai Y, Takeuchi O, Akira S. TLR9 as a key receptor for the recognition of DNA. *Advanced drug delivery reviews*. 2008;60(7):795-804. doi:10.1016/j.addr.2007.12.004.

176. Karikó K, Ni H, Capodici J, Lamphier M, Weissman D. mRNA is an endogenous ligand for Toll-like receptor 3. *The Journal of biological chemistry*. 2004;279(13):12542-12550. doi:10.1074/jbc.M310175200.

177. Mu X, Hur S. Immunogenicity of In Vitro-Transcribed RNA. *Accounts of chemical research*. 2021;54(21):4012-4023. doi:10.1021/acs.accounts.1c00521.

178. Hornung V, et al. 5'-Triphosphate RNA is the ligand for RIG-I. *Science (New York, N.Y.)*. 2006;314(5801):994-997. doi:10.1126/science.1132505.

179. Karikó K, et al. Incorporation of pseudouridine into mRNA yields superior nonimmunogenic vector with increased translational capacity and biological stability. *Molecular therapy : the journal of the American Society of Gene Therapy*. 2008;16(11):1833-1840. doi:10.1038/mt.2008.200.

180. Anderson BR, et al. Incorporation of pseudouridine into mRNA enhances translation by diminishing PKR activation. *Nucleic acids research*. 2010;38(17):5884-5892. doi:10.1093/nar/gkq347.

181. Andries O, Mc Cafferty S, Smedt SC de, Weiss R, Sanders NN, Kitada T. N(1)-methylpseudouridine-incorporated mRNA outperforms pseudouridine-incorporated mRNA by providing enhanced protein expression and reduced immunogenicity in mammalian cell lines and mice. *Journal of controlled release : official journal of the Controlled Release Society*. 2015;217:337-344. doi:10.1016/j.jconrel.2015.08.051.

182. Morais P, Adachi H, Yu Y-T. The Critical Contribution of Pseudouridine to mRNA COVID-19 Vaccines. *Frontiers in cell and developmental biology*. 2021;9:789427. doi:10.3389/fcell.2021.789427.

183. Blanchet S, Ranjan N. Translation Phases in Eukaryotes. *Methods in molecular biology (Clifton, N.J.)*. 2022;2533:217-228. doi:10.1007/978-1-0716-2501-9_13.

184. Carvalho MD, Carvalho JF, Merrick WC. Biological characterization of various forms of elongation factor 1 from rabbit reticulocytes. *Archives of biochemistry and biophysics*. 1984;234(2):603-611. doi:10.1016/0003-9861(84)90310-2.

185. Schuller AP, Wu CC-C, Dever TE, Buskirk AR, Green R. eIF5A Functions Globally in Translation Elongation and Termination. *Molecular cell*. 2017;66(2):194-205.e5. doi:10.1016/j.molcel.2017.03.003.

186. Taylor DJ, Nilsson J, Merrill AR, Andersen GR, Nissen P, Frank J. Structures of modified eEF2 80S ribosome complexes reveal the role of GTP hydrolysis in translocation. *The EMBO journal*. 2007;26(9):2421-2431. doi:10.1038/sj.emboj.7601677.

187. Hudson BH, Zaher HS. O6-Methylguanosine leads to position-dependent effects on ribosome speed and fidelity. *RNA (New York, N.Y.)*. 2015;21(9):1648-1659. doi:10.1261/rna.052464.115.

188. You C, Dai X, Wang Y. Position-dependent effects of regioisomeric methylated adenine and guanine ribonucleosides on translation. *Nucleic acids research*. 2017;45(15):9059-9067. doi:10.1093/nar/gkx515.

189. Licht K, Hartl M, Amman F, Anrather D, Janisiw MP, Jantsch MF. Inosine induces context-dependent recoding and translational stalling. *Nucleic acids research*. 2019;47(1):3-14. doi:10.1093/nar/gky1163.

190. Eyler DE, et al. Pseudouridinylation of mRNA coding sequences alters translation. *Proceedings of the National Academy of Sciences of the United States of America*. 2019;116(46):23068-23074. doi:10.1073/pnas.1821754116.

191. Svitkin YV, Gingras A-C, Sonenberg N. Membrane-dependent relief of translation elongation arrest on pseudouridine- and N1-methyl-pseudouridine-modified mRNAs. *Nucleic acids research*. 2022;50(13):7202-7215. doi:10.1093/nar/gkab1241.

192. Swart EC, Serra V, Petroni G, Nowacki M. Genetic Codes with No Dedicated Stop Codon: Context-Dependent Translation Termination. *Cell*. 2016;166(3):691-702. doi:10.1016/j.cell.2016.06.020.

193. Bertram G, Bell HA, Ritchie DW, Fullerton G, Stansfield I. Terminating eukaryote translation: domain 1 of release factor eRF1 functions in stop codon recognition. *RNA (New York, N.Y.)*. 2000;6(9):1236-1247. doi:10.1017/S1355838200000777.

194. Salas-Marco J, Bedwell DM. GTP hydrolysis by eRF3 facilitates stop codon decoding during eukaryotic translation termination. *Molecular and cellular biology*. 2004;24(17):7769-7778. doi:10.1128/MCB.24.17.7769-7778.2004.

195. Alkalaeva EZ, Pisarev AV, Frolova LY, Kisselev LL, Pestova TV. In vitro reconstitution of eukaryotic translation reveals cooperativity between release factors eRF1 and eRF3. *Cell*. 2006;125(6):1125-1136. doi:10.1016/j.cell.2006.04.035.

196. Zhouravleva G, et al. Termination of translation in eukaryotes is governed by two interacting polypeptide chain release factors, eRF1 and eRF3. *The EMBO journal*. 1995;14(16):4065-4072. doi:10.1002/j.1460-2075.1995.tb00078.x.

197. Pisarev AV, et al. The role of ABCE1 in eukaryotic posttermination ribosomal recycling. *Molecular cell*. 2010;37(2):196-210. doi:10.1016/j.molcel.2009.12.034.

198. Lawson MR, et al. Mechanisms that ensure speed and fidelity in eukaryotic translation termination. *Science (New York, N.Y.)*. 2021;373(6557):876-882. doi:10.1126/science.abi7801.

199. Dabrowski M, Bukowy-Bieryllo Z, Zietkiewicz E. Translational readthrough potential of natural termination codons in eucaryotes--The impact of RNA sequence. *RNA biology*. 2015;12(9):950-958. doi:10.1080/15476286.2015.1068497.

200. Rodnina MV, et al. Translational recoding: canonical translation mechanisms reinterpreted. *Nucleic acids research*. 2020;48(3):1056-1067. doi:10.1093/nar/gkz783.

201. Anzalone AV, Zairis S, Lin AJ, Rabadan R, Cornish VW. Interrogation of Eukaryotic Stop Codon Readthrough Signals by in Vitro RNA Selection. *Biochemistry*. 2019;58(8):1167-1178. doi:10.1021/acs.biochem.8b01280.

202. Wangen JR, Green R. Stop codon context influences genome-wide stimulation of termination codon readthrough by aminoglycosides. *eLife*. 2020;9. doi:10.7554/eLife.52611.

203. Albers S, et al. Engineered tRNAs suppress nonsense mutations in cells and in vivo. *Nature*. 2023;618(7966):842-848. doi:10.1038/s41586-023-06133-1.

204. Brown A, Shao S, Murray J, Hegde RS, Ramakrishnan V. Structural basis for stop codon recognition in eukaryotes. *Nature*. 2015;524(7566):493-496. doi:10.1038/nature14896.

205. Manuvakhova M, Keeling K, Bedwell DM. Aminoglycoside antibiotics mediate context-dependent suppression of termination codons in a mammalian translation system. *RNA (New York, N.Y.)*. 2000;6(7):1044-1055. doi:10.1017/s1355838200000716.

206. Karijolich J, Yu Y-T. Converting nonsense codons into sense codons by targeted pseudouridylation. *Nature*. 2011;474(7351):395-398. doi:10.1038/nature10165.

207. Adachi H, Yu Y-T. Pseudouridine-mediated stop codon readthrough in S. cerevisiae is sequence context-independent. *RNA (New York, N.Y.)*. 2020;26(9):1247-1256. doi:10.1261/rna.076042.120.

208. Song J, et al. CRISPR-free, programmable RNA pseudouridylation to suppress premature termination codons. *Molecular cell*. 2023;83(1):139-155.e9. doi:10.1016/j.molcel.2022.11.011.

209. Kramarski L, Arbely E. Translational read-through promotes aggregation and shapes stop codon identity. *Nucleic acids research*. 2020;48(7):3747-3760. doi:10.1093/nar/gkaa136.

210. Mulroney TE, et al. N1-methylpseudouridylation of mRNA causes +1 ribosomal frameshifting. *Nature*. 2024;625(7993):189-194. doi:10.1038/s41586-023-06800-3.

211. Bounds CE, et al. An immunoinformatics-derived DNA vaccine encoding human class II T cell epitopes of Ebola virus, Sudan virus, and Venezuelan equine encephalitis virus is immunogenic in HLA transgenic mice. *Human vaccines & immunotherapeutics*. 2017;13(12):2824-2836. doi:10.1080/21645515.2017.1329788.

212. Guo M, Liu X, Chen X, Li Q. Insights into new-onset autoimmune diseases after COVID-19 vaccination. *Autoimmunity reviews*. 2023;22(7):103340. doi:10.1016/j.autrev.2023.103340.

213. Houseley J, Tollervey D. The many pathways of RNA degradation. *Cell*. 2009;136(4):763-776. doi:10.1016/j.cell.2009.01.019.

214. Sahin U, Karikó K, Türeci Ö. mRNA-based therapeutics--developing a new class of drugs. *Nature reviews. Drug discovery*. 2014;13(10):759-780. doi:10.1038/nrd4278.

215. Wolff JA, et al. Direct gene transfer into mouse muscle in vivo. *Science (New York, N.Y.)*. 1990;247(4949 Pt 1):1465-1468. doi:10.1126/science.1690918.

216. Da Sun, Lu Z-R. Structure and Function of Cationic and Ionizable Lipids for Nucleic Acid Delivery. *Pharmaceutical research*. 2023;40(1):27-46. doi:10.1007/s11095-022-03460-2.

217. Semple SC, et al. Efficient encapsulation of antisense oligonucleotides in lipid vesicles using ionizable aminolipids: formation of novel small multilamellar vesicle structures. *Biochimica et biophysica acta*. 2001;1510(1-2):152-166. doi:10.1016/S0005-2736(00)00343-6.

218. Álvarez-Benedicto E, et al. Optimization of phospholipid chemistry for improved lipid nanoparticle (LNP) delivery of messenger RNA (mRNA). *Biomaterials science*. 2022;10(2):549-559. doi:10.1039/d1bm01454d.

219. Samaridou E, Heyes J, Lutwyche P. Lipid nanoparticles for nucleic acid delivery: Current perspectives. *Advanced drug delivery reviews*. 2020;154-155:37-63. doi:10.1016/j.addr.2020.06.002.

220. Cheng X, Lee RJ. The role of helper lipids in lipid nanoparticles (LNPs) designed for oligonucleotide delivery. *Advanced drug delivery reviews*. 2016;99(Pt A):129-137. doi:10.1016/j.addr.2016.01.022.

221. Akinc A, et al. Targeted delivery of RNAi therapeutics with endogenous and exogenous ligand-based mechanisms. *Molecular therapy : the journal of the American Society of Gene Therapy*. 2010;18(7):1357-1364. doi:10.1038/mt.2010.85.

222. Hald Albertsen C, Kulkarni JA, Witzigmann D, Lind M, Petersson K, Simonsen JB. The role of lipid components in lipid nanoparticles for vaccines and gene therapy. *Advanced drug delivery reviews*. 2022;188:114416. doi:10.1016/j.addr.2022.114416.

223. Nakamura T, Kawai M, Sato Y, Maeki M, Tokeshi M, Harashima H. The Effect of Size and Charge of Lipid Nanoparticles Prepared by Microfluidic Mixing on Their Lymph Node Transitivity and Distribution. *Molecular pharmaceutics*. 2020;17(3):944-953. doi:10.1021/acs.molpharmaceut.9b01182.

224. Jürgens DC, et al. Lab-scale siRNA and mRNA LNP manufacturing by various microfluidic mixing techniques – an evaluation of particle properties and efficiency. *OpenNano*. 2023;12:100161. doi:10.1016/j.onano.2023.100161.

225. Carrasco MJ, et al. Ionization and structural properties of mRNA lipid nanoparticles influence expression in intramuscular and intravascular administration. *Communications biology*. 2021;4(1):956. doi:10.1038/s42003-021-02441-2.

226. Li S, et al. Payload distribution and capacity of mRNA lipid nanoparticles. *Nature communications*. 2022;13(1):5561. doi:10.1038/s41467-022-33157-4.

227. Liu H, Chen MZ, Payne T, Porter CJ, Pouton CW, Johnston AP. Beyond the Endosomal Bottleneck: Understanding the Efficiency of mRNA/LNP Delivery. *Adv Funct Materials*. 2024. doi:10.1002/adfm.202404510.

228. Lee Y, Jeong M, Park J, Jung H, Lee H. Immunogenicity of lipid nanoparticles and its impact on the efficacy of mRNA vaccines and therapeutics. *Experimental & molecular medicine*. 2023;55(10):2085-2096. doi:10.1038/s12276-023-01086-x.

229. Jeong M, Lee Y, Park J, Jung H, Lee H. Lipid nanoparticles (LNPs) for in vivo RNA delivery and their breakthrough technology for future applications. *Advanced drug delivery reviews*. 2023;200:114990. doi:10.1016/j.addr.2023.114990.

230. Thomas A, et al. Microfluidic Production and Application of Lipid Nanoparticles for Nucleic Acid Transfection. *Methods in molecular biology (Clifton, N.J.)*. 2018;1792:193-203. doi:10.1007/978-1-4939-7865-6_14.

231. Baden LR, et al. Efficacy and Safety of the mRNA-1273 SARS-CoV-2 Vaccine. *The New England journal of medicine*. 2021;384(5):403-416. doi:10.1056/NEJMoa2035389.

232. Iavarone C, O'hagan DT, Yu D, Delahaye NF, Ulmer JB. Mechanism of action of mRNA-based vaccines. *Expert review of vaccines*. 2017;16(9):871-881. doi:10.1080/14760584.2017.1355245.

233. Ramachandran S, Satapathy SR, Dutta T. Delivery Strategies for mRNA Vaccines. *Pharmaceutical medicine*. 2022;36(1):11-20. doi:10.1007/s40290-021-00417-5.

234. Sayers EJ, et al. Endocytic Profiling of Cancer Cell Models Reveals Critical Factors Influencing LNP-Mediated mRNA Delivery and Protein Expression. *Molecular therapy :*

the journal of the American Society of Gene Therapy. 2019;27(11):1950-1962. doi:10.1016/j.ymthe.2019.07.018.

235. Rojas LA, et al. Personalized RNA neoantigen vaccines stimulate T cells in pancreatic cancer. *Nature*. 2023;618(7963):144-150. doi:10.1038/s41586-023-06063-y.

236. Nelson J, et al. Impact of mRNA chemistry and manufacturing process on innate immune activation. *Science advances*. 2020;6(26):eaaz6893. doi:10.1126/sciadv.aaz6893.

237. Dörrie J, Schaft N, Schuler G, Schuler-Thurner B. Therapeutic Cancer Vaccination with Ex Vivo RNA-Transfected Dendritic Cells-An Update. *Pharmaceutics*. 2020;12(2). doi:10.3390/pharmaceutics12020092.

238. Liu L, et al. Differential trends in rising endometrial cancer incidence by age, race, and ethnicity. *JNCI cancer spectrum*. 2023;7(1). doi:10.1093/jncics/pkad001.

239. Ferlay J, et al. Cancer incidence and mortality worldwide: sources, methods and major patterns in GLOBOCAN 2012. *International journal of cancer*. 2015;136(5):E359-86. doi:10.1002/ijc.29210.

240. Sung H, et al. Global Cancer Statistics 2020: GLOBOCAN Estimates of Incidence and Mortality Worldwide for 36 Cancers in 185 Countries. *CA: a cancer journal for clinicians*. 2021;71(3):209-249. doi:10.3322/caac.21660.

241. Gu B, et al. Variations in incidence and mortality rates of endometrial cancer at the global, regional, and national levels, 1990-2019. *Gynecologic oncology*. 2021;161(2):573-580. doi:10.1016/j.ygyno.2021.01.036.

242. Aune D, et al. Anthropometric factors and endometrial cancer risk: a systematic review and dose-response meta-analysis of prospective studies. *Annals of oncology : official journal of the European Society for Medical Oncology*. 2015;26(8):1635-1648. doi:10.1093/annonc/mdv142.

243. Wu Y, Sun W, Liu H, Zhang D. Age at Menopause and Risk of Developing Endometrial Cancer: A Meta-Analysis. *BioMed research international*. 2019;2019:8584130. doi:10.1155/2019/8584130.

244. Kaaks R, Lukanova A, Kurzer MS. Obesity, endogenous hormones, and endometrial cancer risk: a synthetic review. *Cancer epidemiology, biomarkers & prevention : a publication of the American Association for Cancer Research, cosponsored by the American Society of Preventive Oncology*. 2002;11(12):1531-1543.

245. Potischman N, et al. Case-control study of endogenous steroid hormones and endometrial cancer. *Journal of the National Cancer Institute*. 1996;88(16):1127-1135. doi:10.1093/jnci/88.16.1127.

246. Wilczyński M, Danielska J, Wilczyński J. An update of the classical Bokhman's dualistic model of endometrial cancer. *Przegląd Menopauzalny = Menopause Review*. 2016;15(2):63-68. doi:10.5114/pm.2016.61186.

247. Morice P, Leary A, Creutzberg C, Abu-Rustum N, Darai E. Endometrial cancer. *Lancet (London, England)*. 2016;387(10023):1094-1108. doi:10.1016/S0140-6736(15)00130-0.

248. Höhn AK, Brambs CE, Hiller GGR, May D, Schmoeckel E, Horn L-C. 2020 WHO Classification of Female Genital Tumors. *Geburtshilfe und Frauenheilkunde*. 2021;81(10):1145-1153. doi:10.1055/a-1545-4279.

249. Berek JS, et al. FIGO staging of endometrial cancer: 2023. *International journal of gynaecology and obstetrics: the official organ of the International Federation of Gynaecology and Obstetrics*. 2023;162(2):383-394. doi:10.1002/ijgo.14923.

250. Bokhman JV. Two pathogenetic types of endometrial carcinoma. *Gynecologic oncology*. 1983;15(1):10-17. doi:10.1016/0090-8258(83)90111-7.

251. Paleari L, et al. New Insights into Endometrial Cancer. *Cancers*. 2021;13(7). doi:10.3390/cancers13071496.

252. Kandoth C, et al. Integrated genomic characterization of endometrial carcinoma. *Nature*. 2013;497(7447):67-73. doi:10.1038/nature12113.

253. Yao X, Feng M, Wang W. The Clinical and Pathological Characteristics of POLE-Mutated Endometrial Cancer: A Comprehensive Review. *Cancer Management and Research*. 2024;16:117-125. doi:10.2147/CMAR.S445055.

254. Loukovaara M, Pasanen A, Bützow R. Mismatch Repair Deficiency as a Predictive and Prognostic Biomarker in Molecularly Classified Endometrial Carcinoma. *Cancers*. 2021;13(13). doi:10.3390/cancers13133124.

255. Freitas D de, et al. Clinicopathological characteristics of endometrial carcinomas according to DNA mismatch repair protein status. *Heliyon*. 2023;9(6). doi:10.1016/j.heliyon.2023.e17495.

256. Momeni-Boroujeni A, et al. Genomic landscape of endometrial carcinomas of no specific molecular profile. *Modern pathology : an official journal of the United States and Canadian Academy of Pathology, Inc*. 2022;35(9):1269-1278. doi:10.1038/s41379-022-01066-y.

257. Momeni-Boroujeni A, et al. Clinicopathologic and Genomic Analysis of TP53-Mutated Endometrial Carcinomas. *Clinical cancer research : an official journal of the American Association for Cancer Research*. 2021;27(9):2613-2623. doi:10.1158/1078-0432.CCR-20-4436.

258. Trojano G, Olivieri C, Tinelli R, Damiani GR, Pellegrino A, Cicinelli E. Conservative treatment in early stage endometrial cancer: a review. *Acta Bio Medica : Atenei Parmensis*. 2019;90(4):405-410. doi:10.23750/abm.v90i4.7800.

259. Sonoda Y. Surgical treatment for apparent early stage endometrial cancer. *Obstetrics & gynecology science*. 2014;57(1):1-10. doi:10.5468/ogs.2014.57.1.1.

260. Colombo N, et al. ESMO-ESGO-ESTRO Consensus Conference on Endometrial Cancer: diagnosis, treatment and follow-up. *Annals of oncology : official journal of the European Society for Medical Oncology*. 2016;27(1):16-41. doi:10.1093/annonc/mdv484.

261. Harkenrider MM, et al. Radiation Therapy for Endometrial Cancer: An American Society for Radiation Oncology Clinical Practice Guideline. *Practical radiation oncology*. 2023;13(1):41-65. doi:10.1016/j.prro.2022.09.002.

262. Miller DS, et al. Carboplatin and Paclitaxel for Advanced Endometrial Cancer: Final Overall Survival and Adverse Event Analysis of a Phase III Trial (NRG Oncology/GOG0209). *JCO*. 2020;38(33):3841-3850. doi:10.1200/JCO.20.01076.

263. Lupini L, et al. Molecular biomarkers predicting early development of endometrial carcinoma: A pilot study. *European journal of cancer care*. 2019;28(6):e13137. doi:10.1111/ecc.13137.

264. Huang X, Kong N, Zhang X, Cao Y, Langer R, Tao W. The landscape of mRNA nanomedicine. *Nature medicine*. 2022;28(11):2273-2287. doi:10.1038/s41591-022-02061-1.

265. Holtkamp S, et al. Modification of antigen-encoding RNA increases stability, translational efficacy, and T-cell stimulatory capacity of dendritic cells. *Blood*. 2006;108(13):4009-4017. doi:10.1182/blood-2006-04-015024.

266. Perenkov AD, Sergeeva AD, Vedunova MV, Krysko DV. In Vitro Transcribed RNA-Based Platform Vaccines: Past, Present, and Future. *Vaccines*. 2023;11(10). doi:10.3390/vaccines11101600.

267. Peixeiro I, Silva AL, Romão L. Control of human beta-globin mRNA stability and its impact on beta-thalassemia phenotype. *Haematologica*. 2011;96(6):905-913. doi:10.3324/haematol.2010.039206.

268. Grier AE, et al. pEVL: A Linear Plasmid for Generating mRNA IVT Templates With Extended Encoded Poly(A) Sequences. *Molecular therapy. Nucleic acids*. 2016;5(4):e306. doi:10.1038/mtna.2016.21.

269. Goodenough E, et al. Cryptic MHC class I-binding peptides are revealed by aminoglycoside-induced stop codon read-through into the 3' UTR. *Proceedings of the National Academy of Sciences of the United States of America*. 2014;111(15):5670-5675. doi:10.1073/pnas.1402670111.

270. Moradian H, Roch T, Anthofer L, Lendlein A, Gossen M. Chemical modification of uridine modulates mRNA-mediated proinflammatory and antiviral response in primary human macrophages. *Molecular therapy. Nucleic acids*. 2022;27:854-869. doi:10.1016/j.omtn.2022.01.004.

271. Hassett KJ, et al. Impact of lipid nanoparticle size on mRNA vaccine immunogenicity. *Journal of controlled release : official journal of the Controlled Release Society*. 2021;335:237-246. doi:10.1016/j.jconrel.2021.05.021.

272. Cardarelli F, et al. The intracellular trafficking mechanism of Lipofectamine-based transfection reagents and its implication for gene delivery. *Scientific reports*. 2016;6:25879. doi:10.1038/srep25879.

273. Dalby B, et al. Advanced transfection with Lipofectamine 2000 reagent: primary neurons, siRNA, and high-throughput applications. *Methods (San Diego, Calif.)*. 2004;33(2):95-103. doi:10.1016/j.ymeth.2003.11.023.

274. Wang T, Larcher LM, Ma L, Veedu RN. Systematic Screening of Commonly Used Commercial Transfection Reagents towards Efficient Transfection of Single-Stranded Oligonucleotides. *Molecules (Basel, Switzerland)*. 2018;23(10). doi:10.3390/molecules23102564.

275. Cunningham S, Hackstein H. Rapid generation of monocyte-derived antigen-presenting cells with dendritic cell-like properties. *Transfusion*. 2021;61(6):1845-1855. doi:10.1111/trf.16385.

276. Sköld AE, et al. Protamine-stabilized RNA as an ex vivo stimulant of primary human dendritic cell subsets. *Cancer immunology, immunotherapy : CII*. 2015;64(11):1461-1473. doi:10.1007/s00262-015-1746-9.

277. Duan T, Du Y, Xing C, Wang HY, Wang R-F. Toll-Like Receptor Signaling and Its Role in Cell-Mediated Immunity. *Frontiers in immunology*. 2022;13:812774. doi:10.3389/fimmu.2022.812774.

278. Huang X, Yang Y. Targeting the TLR9-MyD88 pathway in the regulation of adaptive immune responses. *Expert opinion on therapeutic targets*. 2010;14(8):787-796. doi:10.1517/14728222.2010.501333.

279. Schwanhäusser B, et al. Global quantification of mammalian gene expression control. *Nature*. 2011;473(7347):337-342. doi:10.1038/nature10098.

280. Dersh D, Yewdell JW, Wei J. A SIINFEKL-Based System to Measure MHC Class I Antigen Presentation Efficiency and Kinetics. *Methods in molecular biology (Clifton, N.J.)*. 2019;1988:109-122. doi:10.1007/978-1-4939-9450-2_9.

281. Zhang X, Xu Q, Li E, Shi T, Chen H. CEP55 predicts the poor prognosis and promotes tumorigenesis in endometrial cancer by regulating the Foxo1 signaling.

Molecular and cellular biochemistry. 2023;478(7):1561-1571. doi:10.1007/s11010-022-04607-w.

282. Wang G, Chen B, Su Y, Qu N, Zhou D, Zhou W. CEP55 as a Promising Immune Intervention Marker to Regulate Tumor Progression: A Pan-Cancer Analysis with Experimental Verification. *Cells*. 2023;12(20). doi:10.3390/cells12202457.
283. Cen L, et al. Efficacy of MAGE-A4 long peptide as a universal immunoprevention cancer vaccine. *Cancer cell international*. 2024;24(1):232. doi:10.1186/s12935-024-03421-2.
284. Aubry F, et al. MAGE-A4, a germ cell specific marker, is expressed differentially in testicular tumors. *Cancer*. 2001;92(11):2778-2785. doi:10.1002/1097-0142(20011201)92:11<2778:aid-cncr10125>3.0.co;2-s.
285. Brennen WN, Isaacs JT, Denmeade SR. Rationale behind targeting fibroblast activation protein-expressing carcinoma-associated fibroblasts as a novel chemotherapeutic strategy. *Molecular cancer therapeutics*. 2012;11(2):257-266. doi:10.1158/1535-7163.MCT-11-0340.
286. Zhang F-F, et al. Epitope-based minigene vaccine targeting fibroblast activation protein α induces specific immune responses and anti-tumor effects in 4 T1 murine breast cancer model. *International immunopharmacology*. 2022;112:109237. doi:10.1016/j.intimp.2022.109237.
287. Li Q, Hu W, Liao B, Song C, Li L. Natural high-avidity T-cell receptor efficiently mediates regression of cancer/testis antigen 83 positive common solid cancers. *Journal for immunotherapy of cancer*. 2022;10(7). doi:10.1136/jitc-2022-004713.
288. Marcinkowski B, et al. Cancer targeting by TCR gene-engineered T cells directed against Kita-Kyushu Lung Cancer Antigen-1. *Journal for immunotherapy of cancer*. 2019;7(1):229. doi:10.1186/s40425-019-0678-x.
289. Blair JD, Hockemeyer D, Doudna JA, Bateup HS, Floor SN. Widespread Translational Remodeling during Human Neuronal Differentiation. *Cell reports*. 2017;21(7):2005-2016. doi:10.1016/j.celrep.2017.10.095.
290. Floor SN, Doudna JA. Tunable protein synthesis by transcript isoforms in human cells. *eLife*. 2016;5. doi:10.7554/eLife.10921.
291. Voon HPJ, Vadolas J. Controlling alpha-globin: a review of alpha-globin expression and its impact on beta-thalassemia. *Haematologica*. 2008;93(12):1868-1876. doi:10.3324/haematol.13490.
292. Pelletier J, Sonenberg N. Insertion mutagenesis to increase secondary structure within the 5' noncoding region of a eukaryotic mRNA reduces translational efficiency. *Cell*. 1985;40(3):515-526. doi:10.1016/0092-8674(85)90200-4.

293. Dvir S, et al. Deciphering the rules by which 5'-UTR sequences affect protein expression in yeast. *Proceedings of the National Academy of Sciences of the United States of America*. 2013;110(30):E2792-801. doi:10.1073/pnas.1222534110.

294. Xia X. Detailed Dissection and Critical Evaluation of the Pfizer/BioNTech and Moderna mRNA Vaccines. *Vaccines*. 2021;9(7). doi:10.3390/vaccines9070734.

295. Kierzek E, Malgowska M, Lisowiec J, Turner DH, Gdaniec Z, Kierzek R. The contribution of pseudouridine to stabilities and structure of RNAs. *Nucleic acids research*. 2014;42(5):3492-3501. doi:10.1093/nar/gkt1330.

296. Deb I, et al. Computational and NMR studies of RNA duplexes with an internal pseudouridine-adenosine base pair. *Scientific reports*. 2019;9(1):16278. doi:10.1038/s41598-019-52637-0.

297. Dutta N, Sarzynska J, Deb I, Lahiri A. Predicting nearest neighbor free energies of modified RNA with LIE: results for pseudouridine and N1-methylpseudouridine within RNA duplexes. *Physical chemistry chemical physics : PCCP*. 2024;26(2):992-999. doi:10.1039/d3cp02442c.

298. Mignone F, Gissi C, Liuni S, Pesole G. Untranslated regions of mRNAs. *Genome biology*. 2002;3(3):REVIEWS0004. doi:10.1186/gb-2002-3-3-reviews0004.

299. Bahl K, et al. Preclinical and Clinical Demonstration of Immunogenicity by mRNA Vaccines against H10N8 and H7N9 Influenza Viruses. *Molecular therapy : the journal of the American Society of Gene Therapy*. 2017;25(6):1316-1327. doi:10.1016/j.ymthe.2017.03.035.

300. Hassett KJ, et al. mRNA vaccine trafficking and resulting protein expression after intramuscular administration. *Molecular therapy. Nucleic acids*. 2024;35(1):102083. doi:10.1016/j.omtn.2023.102083.

301. Anderson BR, Muramatsu H, Jha BK, Silverman RH, Weissman D, Karikó K. Nucleoside modifications in RNA limit activation of 2'-5'-oligoadenylate synthetase and increase resistance to cleavage by RNase L. *Nucleic acids research*. 2011;39(21):9329-9338. doi:10.1093/nar/gkr586.

302. Gilleron J, et al. Image-based analysis of lipid nanoparticle-mediated siRNA delivery, intracellular trafficking and endosomal escape. *Nature biotechnology*. 2013;31(7):638-646. doi:10.1038/nbt.2612.

303. Liu Y, Beyer A, Aebersold R. On the Dependency of Cellular Protein Levels on mRNA Abundance. *Cell*. 2016;165(3):535-550. doi:10.1016/j.cell.2016.03.014.

304. Tomura M, et al. Tracking and quantification of dendritic cell migration and antigen trafficking between the skin and lymph nodes. *Scientific reports*. 2014;4:6030. doi:10.1038/srep06030.

305. Ho LLY, Schiess GHA, Miranda P, Weber G, Astakhova K. Pseudouridine and N1-methylpseudouridine as potent nucleotide analogues for RNA therapy and vaccine development. *RSC chemical biology*. 2024;5(5):418-425. doi:10.1039/d4cb00022f.

306. Monajemi H, M. Zain S. How stop codon pseudouridylation induces nonsense suppression. *Computational and Theoretical Chemistry*. 2021;1204:113414. doi:10.1016/j.comptc.2021.113414.

307. Hudson AM, Szabo NL, Loughran G, Wills NM, Atkins JF, Cooley L. Tissue-specific dynamic codon redefinition in Drosophila. *Proceedings of the National Academy of Sciences of the United States of America*. 2021;118(5). doi:10.1073/pnas.2012793118.

308. Seidman JS, Janssen BD, Hayes CS. Alternative fates of paused ribosomes during translation termination. *The Journal of biological chemistry*. 2011;286(36):31105-31112. doi:10.1074/jbc.M111.268201.

309. Zhang J, Shrivastava S, Cleveland RO, Rabbitts TH. Lipid-mRNA Nanoparticle Designed to Enhance Intracellular Delivery Mediated by Shock Waves. *ACS applied materials & interfaces*. 2019;11(11):10481-10491. doi:10.1021/acsami.8b21398.

310. Weigert R. Imaging the dynamics of endocytosis in live mammalian tissues. *Cold Spring Harbor perspectives in biology*. 2014;6(4):a017012. doi:10.1101/cshperspect.a017012.

311. Chen P, Cabral H. Enhancing Targeted Drug Delivery through Cell-Specific Endosomal Escape. *ChemMedChem*. 2024;19(18):e202400274. doi:10.1002/cmdc.202400274.

312. Rybak SL, Murphy RF. Primary cell cultures from murine kidney and heart differ in endosomal pH. *Journal of cellular physiology*. 1998;176(1):216-222. doi:10.1002/(SICI)1097-4652(199807)176:1<216:AID-JCP23>3.0.CO;2-3.

313. Kularatne RN, Crist RM, Stern ST. The Future of Tissue-Targeted Lipid Nanoparticle-Mediated Nucleic Acid Delivery. *Pharmaceuticals (Basel, Switzerland)*. 2022;15(7). doi:10.3390/ph15070897.

314. Wan C, Allen TM, Cullis PR. Lipid nanoparticle delivery systems for siRNA-based therapeutics. *Drug Deliv. and Transl. Res.* 2014;4(1):74-83. doi:10.1007/s13346-013-0161-z.

315. an Coosemans, et al. Wilms' Tumor Gene 1 (WT1)--loaded dendritic cell immunotherapy in patients with uterine tumors: a phase I/II clinical trial. *Anticancer research*. 2013;33(12):5495-5500.

316. an Coosemans, et al. Wilms' tumor gene 1 (WT1) in endometrial carcinoma. *Gynecologic oncology*. 2008;111(3):502-508. doi:10.1016/j.ygyno.2008.08.032.

317. Gure AO, et al. Cancer-testis genes are coordinately expressed and are markers of poor outcome in non-small cell lung cancer. *Clinical cancer research : an official journal*

of the American Association for Cancer Research. 2005;11(22):8055-8062. doi:10.1158/1078-0432.CCR-05-1203.

318. Cho HJ, et al. MAGE-a Mediate Resistance to Chemotherapy in Multiple Myeloma through Regulation of Bcl-2 Proteins. *Blood*. 2016;128(22):3277. doi:10.1182/blood.V128.22.3277.3277.
319. Zhang S, et al. High expression of MAGE-A9 in tumor and stromal cells of non-small cell lung cancer was correlated with patient poor survival. *International journal of clinical and experimental pathology*. 2015;8(1):541-550.
320. Mendonça BDS, Agostini M, Aquino IG, Dias WB, Bastos DC, Rumjanek FD. Suppression of MAGE-A10 alters the metastatic phenotype of tongue squamous cell carcinoma cells. *Biochemistry and biophysics reports*. 2017;10:267-275. doi:10.1016/j.bbrep.2017.04.009.
321. Krishnadas DK, et al. A phase I trial combining decitabine/dendritic cell vaccine targeting MAGE-A1, MAGE-A3 and NY-ESO-1 for children with relapsed or therapy-refractory neuroblastoma and sarcoma. *Cancer immunology, immunotherapy : CII*. 2015;64(10):1251-1260. doi:10.1007/s00262-015-1731-3.
322. Kruit WHJ, et al. Selection of immunostimulant AS15 for active immunization with MAGE-A3 protein: results of a randomized phase II study of the European Organisation for Research and Treatment of Cancer Melanoma Group in Metastatic Melanoma. *JCO*. 2013;31(19):2413-2420. doi:10.1200/JCO.2012.43.7111.
323. Lin L, Wei J, Chen Y, Huang A, Li KK-W, Zhang W. Induction of antigen-specific immune responses by dendritic cells transduced with a recombinant lentiviral vector encoding MAGE-A3 gene. *Journal of cancer research and clinical oncology*. 2014;140(2):281-289. doi:10.1007/s00432-013-1552-8.
324. Keersmaecker B de, et al. TriMix and tumor antigen mRNA electroporated dendritic cell vaccination plus ipilimumab: link between T-cell activation and clinical responses in advanced melanoma. *Journal for immunotherapy of cancer*. 2020;8(1). doi:10.1136/jitc-2019-000329.
325. Hong DS, et al. Autologous T cell therapy for MAGE-A4+ solid cancers in HLA-A*02+ patients: a phase 1 trial. *Nature medicine*. 2023;29(1):104-114. doi:10.1038/s41591-022-02128-z.
326. Wang T, et al. Identifying MAGE-A4-positive tumors for TCR T cell therapies in HLA-A∗02-eligible patients. *Molecular therapy. Methods & clinical development*. 2024;32(2):101265. doi:10.1016/j.omtm.2024.101265.
327. Cabezón T, et al. Proteomic profiling of triple-negative breast carcinomas in combination with a three-tier orthogonal technology approach identifies Mage-A4 as

potential therapeutic target in estrogen receptor negative breast cancer. *Molecular & cellular proteomics : MCP*. 2013;12(2):381-394. doi:10.1074/mcp.M112.019786.

328. Fujiwara-Kuroda A, et al. Prognostic value of MAGEA4 in primary lung cancer depends on subcellular localization and p53 status. *International journal of oncology*. 2018;53(2):713-724. doi:10.3892/ijo.2018.4425.
329. Otte M, et al. MAGE-A gene expression pattern in primary breast cancer. *Cancer research*. 2001;61(18):6682-6687.
330. Srdelić S, Kuzmić-Prusac I, Spagnoli GC, Juretić A, Čapkun V. MAGE-A4 and MAGE-A1 Immunohistochemical Expression in High-grade Endometrial Cancer. *International journal of gynecological pathology : official journal of the International Society of Gynecological Pathologists*. 2019;38(1):59-65. doi:10.1097/PGP.0000000000000470.
331. Goodman JD, Rozypal TL, Kelly T. Seprase, a membrane-bound protease, alleviates the serum growth requirement of human breast cancer cells. *Clinical & experimental metastasis*. 2003;20(5):459-470. doi:10.1023/a:1025493605850.
332. Iwasa S, Jin X, Okada K, Mitsumata M, Ooi A. Increased expression of seprase, a membrane-type serine protease, is associated with lymph node metastasis in human colorectal cancer. *Cancer letters*. 2003;199(1):91-98. doi:10.1016/s0304-3835(03)00315-x.
333. Shi M, et al. Expression of fibroblast activation protein in human pancreatic adenocarcinoma and its clinicopathological significance. *World Journal of Gastroenterology*. 2012;18(8):840-846. doi:10.3748/wjg.v18.i8.840.
334. Chen M, et al. A whole-cell tumor vaccine modified to express fibroblast activation protein induces antitumor immunity against both tumor cells and cancer-associated fibroblasts. *Scientific reports*. 2015;5:14421. doi:10.1038/srep14421.
335. Kakarla S, et al. Antitumor effects of chimeric receptor engineered human T cells directed to tumor stroma. *Molecular therapy : the journal of the American Society of Gene Therapy*. 2013;21(8):1611-1620. doi:10.1038/mt.2013.110.
336. Loeffler M, Krüger JA, Niethammer AG, Reisfeld RA. Targeting tumor-associated fibroblasts improves cancer chemotherapy by increasing intratumoral drug uptake. *The Journal of clinical investigation*. 2006;116(7):1955-1962. doi:10.1172/JCI26532.
337. Wen Y, et al. Immunotherapy targeting fibroblast activation protein inhibits tumor growth and increases survival in a murine colon cancer model. *Cancer science*. 2010;101(11):2325-2332. doi:10.1111/j.1349-7006.2010.01695.x.
338. Loughran G, Fedorova AD, Khan YA, Atkins JF, Baranov PV. Lack of evidence for ribosomal frameshifting in ATP7B mRNA decoding. *Molecular cell*. 2022;82(19):3745-3749.e2. doi:10.1016/j.molcel.2022.08.024.

339. Jurk M, et al. Human TLR7 or TLR8 independently confer responsiveness to the antiviral compound R-848. *Nature immunology*. 2002;3(6):499. doi:10.1038/ni0602-499.

8. Supplementary Information

8.1 DNA template sequences

Table 8.1 Sequences of DNA templates used in this study for *in vitro* transcription. 5'UTR (red), CDS(green), 3'UTR(orange) and Poly A tail (blue) are color-coded in the optimized mRNA sequences. For the readthrough reporter mRNA only the test sequence inserts are shown with stop codons underlined.

Template name	Nucleotide sequence
GFP optimized mRNA	5'ACTCTTCTGGTCCCCACAGACTCAGAGAGAACCCACCATGCTGGTCATGGCGCCCCGAACCGTCCTCCTGCTGCTCTCGGCGGCCCTGGCCC TGACCGAGACCTGGGCCGGCTCCGGTGGTGGCGGTTCAGGCGGAGGTGGCTCTATGGTGAGCAAGGGCGAGGAGCTGTTCACCGGGGTGGT GCCCATCCTGGTCGAGCTGGACGGCGACGTAAACGGCCACAAGTTCAGCGTGTCCGGCGAGGGCGAGGGCGATGCCACCTACGGCAAGCTG ACCCTGAAGTTCATCTGCACCACCGGCAAGCTGCCCGTGCCCTGGCCCACCCTCGTGACCACCCTGACCTACGGCGTGCAGTGCTTCAGCCGC TACCCCGACCACATGAAGCAGCACGACTTCTTCAAGTCCGCCATGCCCGAAGGCTACGTCCAGGAGCGCACCATCTTCTTCAAGGACGACGGC AACTACAAGACCCGCGCCGAGGTGAAGTTCGAGGGCGACACCCTGGTGAACCGCATCGAGCTGAAGGGCATCGACTTCAAGGAGGACGGCAA CATCCTGGGGCACAAGCTGGAGTACAACTACAACAGCCACAACGTCTATATCATGGCCGACAAGCAGAAGAACGGCATCAAGGTGAACTTCAAG ATCCGCCACAACATCGAGGACGGCAGCGTGCAGCTCGCCGACCACTACCAGCAGAACACCCCCATCGGCGACGGCCCCGTGCTGCTGCCCGA CAACCACTACCTGAGCACCCAGTCCGCCCTGAGCAAAGACCCCAACGAGAAGCGCGATCACATGGTCCTGCTGGAGTTCGTGACCGCCGCCG GGATCACTCTCGGCATGGACGAGCTGTACAAGGGATCCGCTGGCTCCGCTGCTGGCTCTGGCGAGTTCCAGTATATAAAAGCAAATTCTAAATT TATAGGTATAACTGAACTAGGTGGTTCAGGCGGTGGCGGATCTGGTGGCATCGTGGGCATTGTTGCTGGCCTGGCTGTCCTAGCAGTTGTGGT CATCGGAGCTGTGGTCGCTGCTGTGATGTGTAGGAGGAAGAGTTCAGGTGGAAAAGGAGGGAGCTACTCTCAGGCTGCGTGCAGCGACAGTG CCCAGGGCTCTGATGTGTCTCTCACAGCTTAATAACTGGTACTGCATGCACGCAATGCTAGCTGCCCCTTTCCCGTCCTGGGCACCCCGAGTCT CCCCCGACCCCGGGTCCCAGGTATGCTCCCACCTCCACCTGCCCCACTCACCACCTCTGCTAGTTCCAGACACCTCCCAAGCACGCAGCAATG CAGCTCAAAACGCTTAGCCTAGCCACACCCCCACGGGAAACAGCAGTGATTAACCTTTAGCAATAAACGAAAGTTTAACTAAGCTATACTAACCC CAGGGTTGGTCAATTTCGTGCCAGCCACACCAAAAAAAAAAAAAAAAAAAAAAAAAAAAAAAAAAAAAAAAAAAAAAAAAAAAAAAAAAAAAA AAAAAAAAAAAAAAAAAAAA

	GGCCTTCTGATAATCGTCCTGGGCACAATTGCAATGGAGGGCGACAGCGCCTCTGAGGAGGAAATCTGGGAGGAGCTGGGTGTGATGGGGGT GTATGATGGGAGGGAGCACACTGTCTATGGGGAGCCCAGGAAACTGCTCACCCAAGATTGGGTGCAGGAAAACTACCTGGAGTACCGGCAGGT ACCCGGCAGTAATCCTGCGCGCTATGAGTTCCTGTGGGGTCCAAGGGCTCTGGCTGAAACCAGCTATGTGAAAGTCCTGGAGCATGTGGTCAG GGTCAATGCAAGAGTTCGCATTGCCTACCCATCCCTGCGTGAAGCAGCTTTGTTAGAGGAGGAAGAGGGAGTCTGAGGATCCGCTGGCTCCGC TGCTGGCTCTGGCGAGTTCCAGTATATAAAAGCAAATTCTAAATTTATAGGTATAACTGAACTAGGTGGTTCAGGCGGTGGCGGATCTGGTGGCA TCGTGGGCATTGTTGCTGGCCTGGCTGTCCTAGCAGTTGTGGTCATCGGAGCTGTGGTCGCTGCTGTGATGTGTAGGAGGAAGAGTTCAGGTG GAAAAGGAGGGAGCTACTCTCAGGCTGCGTGCAGCGACAGTGCCCAGGGCTCTGATGTGTCTCTCACAGCTTAATAACTGGTACTGCATGCAC GCAATGCTAGCTGCCCCTTTCCCGTCCTGGGCACCCCGAGTCTCCCCCGACCCCGGGTCCCAGGTATGCTCCCACCTCCACCTGCCCCACTCA CCACCTCTGCTAGTTCCAGACACCTCCCAAGCACGCAGCAATGCAGCTCAAAACGCTTAGCCTAGCCACACCCCCACGGGAAACAGCAGTGATT AACCTTTAGCAATAAACGAAAGTTTAACTAAGCTATACTAACCCCAGGGTTGGTCAATTTCGTGCCAGCCACACCAAAAAAAAAAAAAAAAAAA AAAAAAAAATGCATGCACGAAAAAAAAAAAAAAAAAA

	TAACCCCAGGGTTGGTCAATTTCGTGCCAGCCACACCAAAAAAAAAAAAAAAAAAAAAAAAAAAAAAAAAATGCATGCACGAAAAAAAAAAAAAAAAAAA

9. List of the hazardous substances used by GHS (hazard symbols,H&P statements)

Substances	Pictogram	Signal word	Hazard statements	Precautionary statements
Acetone		Danger	225, 319, 336	304+340, 305+351+338, 308+310
Acrylamide/Bis-acrylamide		Danger	302+332, 315, 317, 319, 340, 350, 361f, 372	201, 305+351+338, 370+378, 403+235 201, 261, 280, 304+340+312, 305+351+338, 308+313
Agarose	Not dangerous according to GHS			
Alcian Blue	Not dangerous according to GHS			
Ammonium persulfate		Danger	272, 302, 315, 317, 319, 334, 335	220, 261, 280, 305+351+338, 342+311
Ampicillin		Danger	315, 317, 319, 334, 335	261, 280, 305+351+338, 342+311
Bovine Serum Albumin	Not dangerous according to GHS			
Bromophenol blue	Not dangerous according to GHS			
Chloroform		Danger	302, 331, 315, 319, 351, 361d, 336, 372	
Citric Acid		Warning	319,335	261,264,271,280,304+340+312,305+351+338
Cycloheximide		Danger	300,341,360D ,411	273,280,301+310,308+313,391
Diethanolamine		Danger	302,315,318,373, 412	273,280,302+352,305+351+338,314
Dimethyl sulfoxide	Not dangerous according to GHS			
Dithiothreitol		Warning	302, 315, 319, 335	261, 305+351+338

Ethanol		Danger	225, 319	210, 240, 305+351+338, 403+233
Ethylenediamine-tetraacetic acid		Warning	319, 332, 373	280, 304+340, 312, 305+351+338, 337+313
Formamide		Danger	315, 360D, 373	201, 314
Glycerol	Not dangerous according to GHS			
Glycin	Not dangerous according to GHS			
Hydrogen peroxide (30%)		Danger	302, 318	280, 305+351+338,310
Isopropyl alcohol		Danger	225, 319, 336	210,233,305,351,338
LB-Agar	Not dangerous according to GHS			
LB-Medium	Not dangerous according to GHS			
Luminol	Not dangerous according to GHS			
Magnesium chloride	Not dangerous according to GHS			
Methanol		Dangerous	225,301+311+331,370	210,233,280,301+310,303+361+353,304+340+311
p-Coumaric acid		Warning	315, 319, 335	261, 305+351+338
Phenol		Danger	301+311+331,314, 341, 373, 411	260, 280, 301+330+331+310, 303+361+353, 304+340+310, 305+351+338
Potassium chloride	Not dangerous according to GHS			
Potassium dihydrogen phosphate	Not dangerous according to GHS			
Potassium Phosphate Monobasic		Warning	315,319	264,280,305+351+338,321,332+313,337+313
Pursept(TM)-A disinfectant		Warning	226,319	210,233,240,241,242,305+351+338

RedSafe	Not dangerous according to GHS			
Sodium acetate	Not dangerous according to GHS			
Sodium chloride	Not dangerous according to GHS			
Sodium dodecyl sulfate		Danger	315, 318, 335, 412	301+312+330, 305+351+338+310, 370+378
Sodium hydrogen phosphate	Not dangerous according to GHS			
Sodium Phosphate Dibasic	Not dangerous according to GHS			
SYBR Gold		Warning	227	210, 280, 370+378
Tetramethyl-ethylenediamine		Danger	225, 332, 302, 314	210, 280, 305+351+338, 310
TRIS acetate	Not dangerous according to GHS			
TRIzol		Danger	314, 335, 341, 373, 412	302+352, 303+361+353, 304+340, 305+351+338

10. Acknowledgments

First and foremost, I want to deeply thank Prof. Zoya Ignatova for giving me the opportunity to work on this fascinating project, for her scientific guidance and trust in me which allowed me to freely pursue my scientific curiosity, and ideas helping me to grow as a scientist.
I am very thankful to Dr. Maria Geffken for supplying us with PBMCs, Prof Thomas Kalinski and Martha Dierks for the immunohistological analysis of patient samples, and Prof. Daniel Wilson for taking the time to review my thesis.
I want to deeply thank my wife Vroni Freyberg. She moved with me to Hamburg away from our families and friends at a time were a pandemic shut down the world which I will always be deeply thankful for. Without your unconditional love and moral support, I could have not completed my PhD.
I am deeply thankful to my family, especially my Parents Maria and Hans Freyberg who always supported me unconditionally throughout my life, allowing me to pursue my interests. Without them, I would not be where I am right now.
I want to thank my dear friends Ivan Simpson-Kent and Luca Göbel for their moral support and stimulating discussions.
I would like to express my deep gratitude to all current and former members of the Ignatova Lab who made it a great environment to purse my PhD. Especially to Bjarne Klopprogge, Jose Antonio Herrera Gavilan, and Chris George which I had the pleasure to supervise and contributed significantly to the Project. Special thanks to Dr. Nikhil Bharti and Dr. Robin Thompson for the stimulating scientific discussion, advice, help in the lab, and friendship.
Lastly, I want to dedicate this thesis to my late grandfather Alfred Remiger who was always so proud of me for pursuing a PhD in science, but unfortunately passed away before I could complete it.

EIDESSTATTLICHE VERSICHERUNG

Hiermit versichere ich an Eides statt, die vorliegende Dissertationsschrift selbst verfasst und keine anderen als die angegebenen Quellen und Hilfsmittel benutzt zu haben. Sofern im Zuge der Erstellung der vorliegenden Dissertationsschrift generative Künstliche Intelligenz (gKI) basierte elektronische Hilfsmittel verwendet wurden, versichere ich, dass meine eigene Leistung im Vordergrund stand und dass eine vollständige Dokumentation aller verwendeten Hilfsmittel gemäß der Guten wissenschaftlichen Praxis vorliegt. Ich trage die Verantwortung für eventuell durch die gKI generierte fehlerhafte oder verzerrte Inhalte, fehlerhafte Referenzen, Verstöße gegen das Datenschutz- und Urheberrecht oder Plagiate.

Hamburg, den 18.10.24

MFreyberg

Moritz Freyberg